CTIPS Center for Transformative Infrastructure Preservation and Sustainability

USDOT Region 8 University Transportation Center

CTIPS-26-005

Y. Song
R. Freyre
Z. Soe

IMPROVING COMPATIBILITY OF TRUCK PLATOONING WITH EXISTING INFRASTRUCTURE VIA DEVELOPMENT OF DYNAMIC OPERATIONAL RULES ON HIGHWAY NETWORKS

A University Transportation Center sponsored by the U.S. Department of Transportation serving the Center for Transformative Infrastructure Preservation and Sustainability members:

Colorado State University
Fort Lewis College
North Dakota State University
South Dakota State University
United Tribes Technical College
University of Colorado Denver
University of Denver
University of North Dakota
University of Utah
University of Wyoming
Utah State University

Technical Report Documentation Page

1. Report No.	2. Government Accession No.	3. Recipient's Catalog No.
CTIPS-26-005		

4. Title and Subtitle	5. Report Date
Improving Compatibility of Truck Platooning with Existing Infrastructure via Development of Dynamic Operational Rules on Highway Networks	July 2026
	6. Performing Organization Code CTIPS
7. Author(s) ▪ Yu (Fred) Song https://orcid.org/0000-0003-2309-716X ▪ Raul Freyre https://orcid.org/0009-0008-8328-477X ▪ Zaw Than Soe https://orcid.org/0009-0001-9273-4954	8. Performing Organization Report No. CTIPS-26-005
9. Performing Organization Name and Address Center for Transformative Infrastructure Preservation and Sustainability North Dakota State University PO Box 6050 Fargo, ND 58108	10. Work Unit No.
	11. Contract or Grant No. 69A3552348308
12. Sponsoring Agency Name and Address Department of Transportation Research and Innovative Technology Administration 400 7th Street, SW Washington, DC 20590	13. Type of Report and Period Covered Final Report
	14. Sponsoring Agency Code

15. Supplementary Notes

Conducted in cooperation with the U.S. Department of Transportation, Federal Highway Administration.

16. Abstract

Truck platooning, a technology where connected and automated trucks travel in closely linked convoys, promises significant reductions in fuel consumption and emissions. However, these long convoys present a major safety hazard on existing roadways, particularly on rural two-lane undivided highways. On these roads, human drivers must use the oncoming traffic lane to overtake, and a long truck platoon acts as a dangerous and extended barrier. To address this problem, we established a comprehensive framework to safely integrate platoons into mixed traffic. The research progressed through four steps. First, we modeled the precise time and distance required for a human driver to safely pass a platoon. Second, we developed a dynamic algorithm that determines safe platooning limits, such as the maximum number of trucks allowed, based on real-time road geometry and oncoming traffic. Third, we tested these rules using advanced traffic simulations. Finally, we designed an active gap opening control system, allowing automated trucks to proactively split apart and provide a safe harbor for passing vehicles. Our findings demonstrate that while long platoons operate safely on multilane highways, they require strict, dynamic limitations on two-lane roads. This research provides transportation policymakers with a clear, data-driven blueprint. By shifting from rigid rules to context-aware operational rules and utilizing cooperative gap opening technologies, agencies can preserve the economic benefits of truck platooning while rigorously protecting the safety of everyday drivers.

17. Key Words	18. Distribution Statement
Automated Truck Platooning; Highway Infrastructure Compatibility; Two-lane Highways; Rural Highways; Dynamic Operational Rules; Cooperative Gap-Opening Control	No restrictions. This document is available through the National Technical Information Service, Springfield, VA 22161.

19. Security Classif. (of this report)	20. Security Classif. (of this page)	21. No. of Pages	22. Price
Unclassified	Unclassified	137	n/a

Form DOT F 1700.7 (8-72) Reproduction of completed page authorized

Improving Compatibility of Truck Platooning with Existing Infrastructure via Development of Dynamic Operational Rules on Highway Networks

Principal Investigator: Yu (Fred) Song, Ph.D.

Department of Civil and Architectural Engineering and Construction Management

University of Wyoming

Authors

Yu (Fred) Song, Raul Freyre, Zaw Than Soe

A report from

University of Wyoming

Department of Civil and Architectural Engineering
and Construction Management

1000 E University Ave. Dept. 3295

Laramie, WY 82071

Phone: (307) 766-2390

Website: https://www.uwyo.edu/civil/index.html

July 2026

About the Center for Transformative Infrastructure Preservation and Sustainability

The Center for Transformative Infrastructure Preservation and Sustainability (CTIPS) is the US DOT Region 8 University Transportation Center (UTC) located at North Dakota State University. CTIPS will focus on "Preserving the Existing Transportation System," along with consortia members Colorado State University, Fort Lewis College, Fort Lewis College, South Dakota State University, United Tribes Technical College, University of Colorado Denver, University of Denver, University of North Dakota, University of Utah, University of Wyoming and Utah State University.

U.S. Department of Transportation (US DOT) Disclaimer

ABSTRACT

Truck platooning, a technology where connected and automated trucks travel in closely linked convoys, promises significant reductions in fuel consumption and emissions. However, these long convoys present a major safety hazard on existing roadways, particularly on rural two-lane undivided highways. On these roads, human drivers must use the oncoming traffic lane to overtake, and a long truck platoon acts as a dangerous and extended barrier. To address this problem, we established a comprehensive framework to safely integrate platoons into mixed traffic. The research progressed through four steps. First, we modeled the precise time and distance required for a human driver to safely pass a platoon. Second, we developed a dynamic algorithm that determines safe platooning limits, such as the maximum number of trucks allowed, based on real-time road geometry and oncoming traffic. Third, we tested these rules using advanced traffic simulations. Finally, we designed an active gap opening control system, allowing automated trucks to proactively split apart and provide a safe harbor for passing vehicles. Our findings demonstrate that while long platoons operate safely on multilane highways, they require strict, dynamic limitations on two-lane roads. This research provides transportation policymakers with a clear, data-driven blueprint. By shifting from rigid rules to context-aware operational rules and utilizing cooperative gap opening technologies, agencies can preserve the economic benefits of truck platooning while rigorously protecting the safety of everyday drivers.

CONTENTS

LIST OF FIGURES

LIST OF TABLES

LIST OF KEY TERMS

AADT: Annual Average Daily Traffic
AASHTO: American Association of State Highway and Transportation Officials
ANOVA: Analysis of Variance
ASD: Available Sight Distance
CACC: Cooperative Adaptive Cruise Control
CAV: Connected and Automated Vehicle
CTIPS: Center for Transformative Infrastructure Preservation and Sustainability
FHWA: Federal Highway Administration
GEH: Geoffrey E. Havers (Traffic Volume Statistic)
HDV: Human-Driven Vehicle
LCV: Longer Combination Vehicle
NHTSA: National Highway Traffic Safety Administration
NRMSE: Normalized Root Mean Squared Error
PET: Post-Encroachment Time
PSD: Passing Sight Distance
RMSE: Root Mean Squared Error
SLSQP: Sequential Least Squares Programming
SQP: Sequential Quadratic Programming
SSAM: Surrogate Safety Assessment Model
SSM: Surrogate Safety Measure
TDTC: Time Difference to Collision
TTC: Time-to-Collision
UAFS: Uniform Acceleration until a Final Speed
USDOT: United States Department of Transportation
V2I: Vehicle-to-Infrastructure
V2V: Vehicle-to-Vehicle
VISSIM: Verkehr In Städten - SIMulationsmodell (Microscopic Traffic Simulation Software)
VSL: Variable Speed Limit
WYDOT: Wyoming Department of Transportation

EXECUTIVE SUMMARY

The freight transportation industry is undergoing a significant transformation with the introduction of connected and automated vehicle (CAV) platooning. While electronically linked truck convoys offer substantial benefits in fuel efficiency, emission reduction, and highway throughput, their deployment on existing infrastructure introduces complex operational challenges. These challenges are most acute in mixed-autonomy traffic environments, particularly on two-lane undivided rural highways where human-driven vehicles (HDVs) must share limited lane space and utilize opposing traffic gaps to safely overtake long platoons. This report establishes a comprehensive, data-driven framework for safely integrating truck platooning into existing mixed-traffic networks by evaluating the precise interactions between roadway geometry, platooning parameters, and mixed-fleet safety.

The research methodology was conducted in four progressive phases:

1. **Overtaking Behavior and Safety Risk Modeling:** An integrated kinematic overtaking model was developed to quantify the passing sight distance (PSD) and collision risks, measured via time difference to collision, inherent in passing a truck platoon. The analytical assessment confirmed that overtaking time, distance, and collision risks increase linearly as platoon length grows, highlighting the severe safety hazards HDVs face on two-lane undivided highways when confronting large platoons.

2. **Dynamic Platooning Rule Development:** Utilizing the safety constraints identified in the overtaking model, a stochastic approximation-based algorithm was engineered to define optimal truck platooning rules for two-lane operations. This algorithm dynamically calculates the maximum safe operating speed, inter-vehicle following gap, and the maximum number of trucks per platoon based on real-time restrictions from opposing traffic flow, horizontal and vertical curves, and uphill grades.

3. **Simulation-Based Rule Evaluation:** The algorithm-generated rules were rigorously evaluated using PTV-VISSIM microsimulation on a 25-mile segment of U.S. Highway 287 in Wyoming, incorporating both multilane divided and two-lane undivided segments. The model was calibrated using real-world traffic volumes and speed distributions, and a surrogate safety assessment model (SSAM) was utilized to measure conflicts. The simulation demonstrated that enforcing the algorithm's stricter rules—which frequently limited platoons to a maximum of two trucks on undivided segments—restored traffic fluidity and significantly reduced severe network delays by up to 150 seconds compared with unregulated eight-truck platoons. However, SSAM evaluation revealed a critical safety trade-off: the increased frequency of platoon boundaries inadvertently elevated localized rear-end and lane-change conflicts among eager HDVs attempting to pass.

4. **Gap-Opening Control Strategy:** To resolve the friction identified in the simulation, an active control strategy was developed utilizing cooperative adaptive cruise control (CACC) frameworks. This strategy enables the CAV platoon to dynamically open an internal gap to safely harbor an overtaking HDV. The control algorithms accurately predict passing vehicle trajectories and calculate the optimal start time, end time, and gap location to safely accommodate the HDV without sacrificing the platoon's string stability.

This project, with the comprehensive approaches, demonstrates that dynamic, context-aware operational rules, coupled with active gap-opening control systems, can preserve the economic benefits of platooning while strictly protecting the safety of all road users. While highly effective at managing truck platoons and mitigating safety risks, these dynamic regulations depend on rigorous geometric and traffic constraints, making them inherently strict and frequently restricting convoys to minimal sizes on two-lane undivided highways. To address this limitation, the exploration of active, CACC-based gap-opening algorithms revealed that flexible platoon control can safely relieve these rigid constraints. By cooperating with macroscopic dynamic rules, flexible gap control presents a holistic pathway to successfully deploy automated truck platoons on two-lane highways while fully maintaining the safety of HDVs. Follow-up studies are necessary to evaluate the optimal strategies for co-implementing dynamic regulatory systems alongside flexible truck platoon controls and to rigorously assess their combined effectiveness in mixed-autonomy environments.

1. INTRODUCTION AND BACKGROUND

In recent years, truck platooning has emerged as one of the most promising technological advancements for the freight transportation industry. By utilizing vehicle-to-vehicle (V2V) communication and cooperative adaptive cruise control (CACC), heavy trucks can travel in closely linked convoys, drastically reducing aerodynamic drag and lowering fuel consumption. However, the deployment of these automated platoons introduces a unique set of challenges within mixed-autonomy traffic, particularly concerning the strategic interactions between CAVs and conventional HDVs.

A truck platoon operates as a highly elongated, train-like physical barrier. On multilane divided freeways, HDVs can generally bypass these convoys using adjacent lanes. Yet, a vast proportion of freight routing relies on two-lane undivided highways, especially in rural states like Wyoming. In these environments, overtaking a heavy truck platoon demands that an HDV driver enter the opposing traffic lane for an extended duration. This radically increases PSD requirements and exposes passing vehicle drivers to elevated head-on collision risks. Current geometric design guidelines and static infrastructure policies are calibrated for single-vehicle overtaking only and would potentially fail to adapt to the dimensions and dynamics of automated truck platoons. Therefore, adjustments in traffic rules are needed for implementing dynamic platoon regulations that adapt to real-time roadway constraints, alongside active platoon control systems designed to proactively accommodate overtaking vehicles.

To bridge the gap between platooning technology and existing highway infrastructure, this project establishes a regulatory control framework to ensure overtaking safety for HDVs without compromising the operational efficiency of the platoons. The scope of this research is structured sequentially across four primary phases:

1. **Modeling Overtaking on Two-Lane Highways:** Modeling the complex overtaking trajectories and safety parameters of human-driven vehicles (HDVs) attempting to pass truck platoons to evaluate the required time, distance, and collision risks.

2. **Developing Algorithmic Rules for Truck Platooning:** Developing dynamic truck platooning rules for two-lane highways by engineering a stochastic algorithm to compute safe operational limits based on immediate geometric and traffic constraints.

3. **Simulation for Evaluating Dynamic Truck Platooning Rules:** Performing a comprehensive simulation-based evaluation to test the operational efficiency and surrogate safety impacts of these rules on rural highway networks.

4. **Explore Active Platoon Control to Assist Overtaking:** Developing and testing a CACC-based control algorithm for truck platoon gap opening to actively assist overtaking vehicles, resolve network turbulence, and facilitate guided, step-by-step overtaking.

This report is organized as follows: Section 2 investigates the theoretical modeling of overtaking behavior and safety risks. Section 3 details the development of algorithm-driven truck platooning rules for two-lane highways. Section 4 provides a simulation-based evaluation of these proposed regulations. Section 5 introduces a cooperative gap-opening control algorithm to accommodate passing vehicles. The report concludes in Section 6 with a summary of findings and strategic recommendations for policy and implementation.

2. MODELING OVERTAKING BEHAVIOR AND SAFETY RISKS ON TWO-LANE HIGHWAYS

This section has been published as the paper “Integrated Overtaking Model and Safety Analysis for Truck Platooning Requirements on Two-lane Undivided Highways” in Transportation Research Record, DOI: 10.1177/03611981231220635. Slight modifications were applied to ensure consistency in this report.

2.1 Introduction

In recent years, truck platooning has emerged as a promising solution for enhancing efficiency and reducing fuel consumption in the freight transportation industry. This concept involves a convoy of semi-automated trucks traveling closely together, utilizing V2V communication and advanced driver assistance systems. However, the unique nature of a truck platoon, resembling a long, train-like moving object on the road, presents challenges for other vehicles attempting to overtake them. Consequently, it is crucial to address potential safety issues associated with overtaking truck platoons as this technology gains momentum.

The objective of this section is to employ an integrated overtaking model and safety analysis to model and analytically assess the safety risks involved in vehicle overtaking of a truck platoon. By evaluating the inherent safety risks in this scenario, this research aims to provide insights that will inform the specification of truck platooning requirements. The proposed overtaking model builds upon classic models by incorporating lane change dynamics. Under assumptions about vehicle dynamics and driver behavior, the model generates vehicle trajectories and kinematic information, offering a more comprehensive understanding of safety risks during the overtaking process. The overall safety assessment considers three aspects: roadway geometry, traffic conditions, and driver behavior, described by measures that include overtaking distance, time, and collision risks.

Through a numerical analysis, we show how different truck platoon configurations interact with the three safety assessment aspects and influence overall safety in the overtaking process. Following the numerical analysis, we discuss the insights we obtained from the analysis and provide recommendations on how truck platooning safety would be ensured from an overtaking perspective. The findings presented in this section have practical implications for policymakers, transportation authorities, and industry stakeholders, enabling them to develop standardized safety guidelines, establish appropriate inter-vehicle distances, and formulate protocols for safe overtaking of truck platoons. Ultimately, this section contributes to the development of effective safety regulations and guidelines for deploying truck platooning onto the existing roadway systems while prioritizing safety.

2.2 Literature Review

2.2.1 Truck Platooning and Its Operational Safety Challenges

Truck platooning technology has advanced in recent years and has proven to be effective in improving operational efficiency and reducing fuel consumption (*1–10*). Challenges, however, still exist and need to be addressed for this technology to be widely deployed. Some of the most critical obstacles to overcome are truck platooning's compatibility with available infrastructure, safety in critical situations, and safety effects on other road users (*6*). Prior studies on the effects of general vehicle platooning have shown that platooning can reduce shockwave in traffic flow and also improve throughput (*2*, *11*). However, truck platooning, especially when operating at or near freeway ramp locations and interacting with lane changing traffic, posts maneuvering challenges and safety risks to the adjacent vehicles (*12–15*). Prior driving simulation studies on driver behavior around truck platoons have found preliminary evidence of driver behavior changes in response to the maneuvering challenges when interacting with truck platoons, including increased speeds and reduced following distances (*16*, *17*). It has been noted that platoon length, determined by the number of trucks and internal following gap, should be carefully managed for operational safety considerations (*12*, *14*). Some platoon control strategies have also been suggested to address the impact of platooning on lane changing; these strategies include yielding and providing a gap for lane-changing vehicles to merge into and cut across the platoon, although these may add complexity to the existing issues (*14*, *18*).

Apart from developing solutions on the truck platooning technology side, governments have also started passing laws to promote and regulate truck platooning. Considering platoon operational safety and the technology's compatibility with the existing infrastructure, several U.S. states have passed laws to legally define truck platooning, permit the technology, and require specific operational features. For example, 20 states have passed laws or bills restricting truck platoons' minimum internal following gap, ranging from 250 ft to 500 ft (*19*). Infrastructure owners and operators havemore to consider beyond the general regulations written into laws. The Federal Highway Administration (FHWA) has published requirements for performance measures for early deployment of truck platooning, which includes measures covering aspects such as operations, safety, and infrastructure impacts (*20*). Recent studies have started pointing out and addressing research gaps in truck platooning and infrastructure compatibility, from aspects of contextual system design considering operational design domain or specific roadway geometric design features such as passing zone length to count for overtaking of truck platoons (*21*, *22*). More research is needed to develop comprehensive and effective regulations and guidelines for truck platooning.

2.2.2 Overtaking Longer Combination Vehicles

Longer combination vehicles (LCVs) are trucks with long multiple-trailer combinations. To some extent, LCVs are similar to truck platoons as they are both configurations to achieve a higher hauling capacity and lower energy consumption by increasing the combined cargo trailer length. However, LCVs have a much longer history of operation on modern roadways. LCVs are used in countries such as Australia, Canada, and the U.S. In Canada and the U.S., the overall length of a longer combination vehicle can range from about 29 m (95 ft) of a Rocky Mountain double to about 37 m (120 ft) of a turnpike double (*23*). In Australia, an LCV operating on public roads can have four trailers and an overall length of about 54 m (177 ft) (*24*). Studies on overtaking LCVs show that the overtaking time and distance increase as vehicle length increases. Barton and Morrall's study estimated that overtaking a Rocky Mountain Double would need 18.5 s and a distance of 623 m (2,044 ft), and a Turnpike Double would require 20 s and a distance of 674 m (2,211 ft) (*25*). Hanley and Forkenbrock's simulation analysis also indicates that the average time used when overtaking a 120-ft LCV is over 20% higher than the time used when overtaking a standard 65-ft truck (*26*). A longer vehicle also makes it more difficult to find a proper gap in the opposing traffic to complete the overtake on a two-lane road. Based on field observations of Barton and Morrall, the mean gap size accepted for passenger car drivers to overtake a 30-m Rocky Mountain Double is 39 s, compared with 17 s when overtaking a passenger car (*25*). Drivers also show more hesitation when deciding whether to accept a gap to overtake a 30-m Rocky Mountain Double, with an indecision time of 8 s compared with 3 s when overtaking a passenger car (*25*). Hanley and Forkenbrock's simulation results also confirmed that the odds of failing to overtake a 120-ft (37-m) LCV are about two to six times that of a 65-ft (20-m) truck (*26*). Due to safety concerns, the use of LCVs in the U.S. is limited to a few states and only on roadways with low traffic density and adequate bridge and interchange conditions (*27*, *28*).

2.2.3 Modeling of Overtaking

Early modeling of vehicle overtaking processes is seen in the efforts to determine proper passing sight distance (PSD) and design passing and no-passing zones for two-lane highways (*29*–*37*). The current guidelines published by the American Association of State Highway and Transportation Officials (AASHTO) use PSD models developed by Glennon and Hassan et al. (*33*, *35*, *38*). Those two models use the concept of "critical position" (i.e., the position of the passing vehicle where the sight distances required to complete or abort the pass are equal) to determine the minimum PSD. The Glennon model was the first to explicitly include lengths of passing and impeding vehicles, and the Hassan et al. model, based on previous models, refined the assumptions about the kinematic relationship between passing, impeding, and opposing vehicles involved in the overtaking process (*33*, *35*). A newer model developed by Wang and Cartmell started to consider improved vehicle capabilities and an increase in maximum permitted truck lengths (*37*). The model combines quintic polynomials and straight lines to simulate the trajectories of passing vehicles, and uses a three-stage description of the overtaking process: 1) the passing vehicle making a lane change to the left of the impeding vehicle and reaching the position where the passing vehicle front bumper and the impeding vehicle rear bumper are aligned; 2) the passing vehicle, in the left lane, passes the impeding vehicle until their front bumpers are aligned; and 3) the passing vehicle completely returns to the right lane. Tang et al. proposed an updated overtaking model describing the speed profile of the passing vehicle as a fixed-end beam deflection curve (*39*). The curve represents a speed-changing process in which the passing vehicle starts with reducing its speed to a speed greater than that of the impeding vehicle, changes to the left lane to pass the impeding vehicle, passes the impeding vehicle from the left lane, and returns to the right lane and its original speed. The overtaking time and distance in Tang et al. are modeled based on the passing vehicle speed-changing curve, but the lane change time was included in the model as an assumed constant.

2.3 Methodology

We analytically assess the safety risks in the process of a vehicle overtaking a truck platoon. The assessment results would be helpful in developing requirements for truck platooning configuration to accommodate the safety of surrounding vehicles. The analytical assessment is done in two steps. First, we establish an overtaking model, similar to that in Wang and Cartmell, considering vehicle lane change dynamics and truck platoon dimensions (*37*). Second, we assess the safety risks in the overtaking process by measuring and visualizing the distance, time, and collision risks involved in the overtaking process. The assessment is demonstrated in a numerical analysis with scenarios reflecting various roadway geometry, driver behaviors, and truck platoon lengths.

2.3.1 Overtaking Model

To analytically assess the safety risks involved in overtaking a truck platoon, the overtaking process must first be modeled. An overtaking model considering lane change dynamics and truck platooning is developed due to limitations of most conventional models. Most conventional overtaking models are developed to inform roadway geometric design, which does not require the incorporation of vehicle dynamic details needed for safety assessments. Also, conventional overtaking models assume one impeding vehicle and may not be feasible for multi-vehicle cases as in truck platooning. Different impeding vehicle lengths may have been considered in existing models. Nevertheless, a truck platoon would be much longer than a typical single tractor-trailer or a longer combination vehicle, and it would likely create a very different overtaking scenario that needs to be investigated.

The process of a vehicle overtaking a truck platoon starts with an initial state of the passing vehicle (denoted by “A”) following the impeding truck or truck platoon (denoted by “B”), followed by the following stages:

- Lane Change Stage: Vehicle A make a lane change into the left lane.
- Overtake Stage: Vehicle A passes Platoon B in the left lane.
- Back-to-lane Stage: Vehicle A merges back into the right lane.

The overtaking model should allow us to plot the trajectories of vehicles involved in the process and understand the relationships between truck platooning configuration and overtaking distance and time, as well as estimate the safety risks. Parameters involved in the overtaking model are listed in **Table 1**.

Table 1: Parameters in the Modeling of Overtaking Process

Parameter	Definition
a_x	Longitudinal acceleration of A (passing vehicle)
h_A	Gap between A and B (truck platoon) when A starts left lane change
h_{A1}	Gap between A and B when A finishes left lane change
h_B	Gap between B and A when A starts right lane change
h_{B1}	Gap between B and A when A finishes right lane change
h_O	Safety distance between A and O (opposing vehicle)
L_A	Length of A
L_B	Length of B
PSD	Passing sight distance
S_A	Total distance for A to overtake B
S_{A1}	Distance for A to accelerate from v_{A1} to $v_{A\,max}$
S'_{A1}	Distance that A travels in the left lane to pass B and reach a gap of h_B
S_O	Distance covered by O
T	Total time for A to overtake B
t_L	Time used by A to complete left lane change
t_R	Time used by A to complete right lane change
t_{OLL}	Time taken for A to overtake B in the left lane
t_1	1st part of t_{OLL} where A takes to accelerate to $v_{A\,max}$
t_2	2nd part of t_{OLL} where A passes B at $v_{A\,max}$
$TDTC$	Time difference to collision
v_A	Speed of A
v_{A0}	Initial speed of A
v_{A1}	Speed of A when it finishes left lane change
v_{A2}	Speed of A when it starts right lane change
v_{lmt}	Posted speed limit
v_{xA}	Longitudinal speed of A
v_B	Speed of B
$v_{A\,max}$	Maximum speed of A
x	Longitudinal position of A
x_e	Longitudinal displacement of A in lane changes
x_{eL}	Longitudinal displacement of A for left lane change
x_{eR}	Longitudinal displacement of A for right lane change
y	Lateral position of A
y_e	Lateral displacement of A in lane changes
y_{io}	Initial lateral offset from right edge of lane ($y = 0$)

Assumptions for the model are as follows.

Initially, vehicle A follows a truck or truck platoon B at the speed of $v_{A0} = v_B$;

A keeps a constant longitudinal acceleration, a_x, unless having reached its desired maximum speed for overtaking, $v_{A\,max}$;

B keeps a constant speed, v_B, in the process of being overtaken by A;

In the case of overtaking using the opposing lane (e.g., on two-way, two-lane highways), the opposing vehicle keeps a constant speed of $v_O = v_{lmt}$;

For analytical assessment purposes, the lane change trajectory of A is assumed to follow certain curves, as introduced in the following section about lane change trajectory models; and

All vehicles are assumed to follow smooth trajectories (i.e., lane change curves when changing lanes, and straight trajectories when moving along straight roadway segments) without any swerving.

Figure 1 illustrates the overtaking process and some parameters involved in the process. The three stages, and the compositions of total overtaking time and distance, are shown in the illustration.

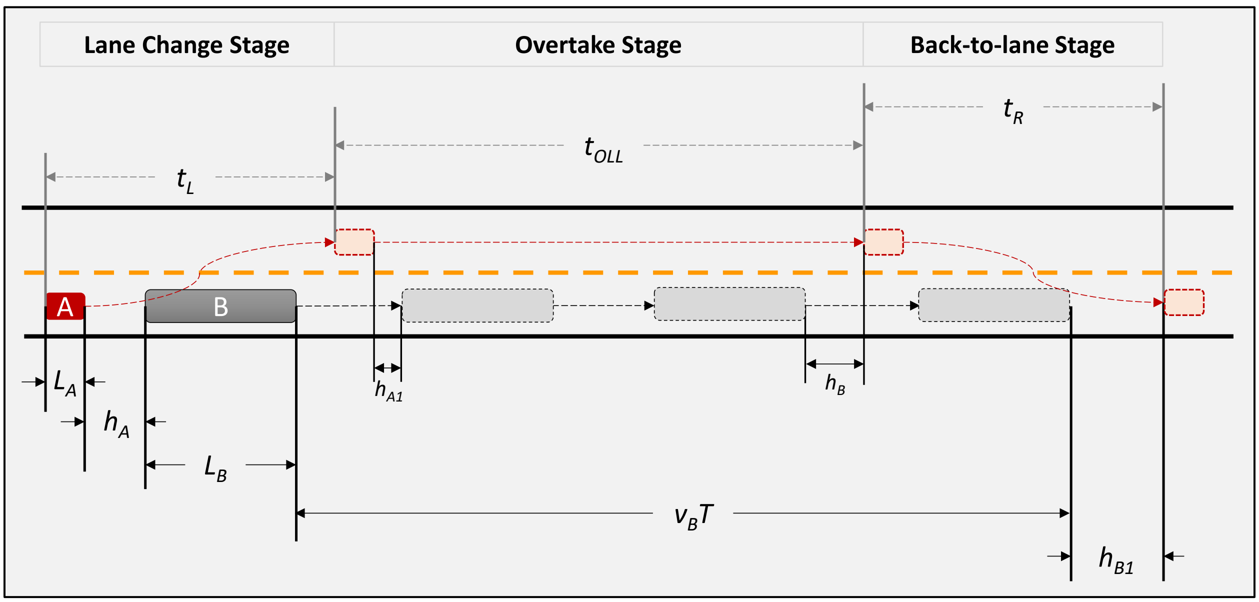

Figure 1: The overtaking process and related time and distance parameters

Lane change and back-to-lane

The lane change trajectory is formed by the longitudinal and lateral positions of a vehicle over its course of moving from a lane to the adjacent lane. A lane change curve is typically an "S" shaped curve, which has been modeled in prior studies using circular arc, polynomial, ramp sinusoidal, spiral, and Bezier spline functions, but most commonly a five or higher-degree polynomial (*40–45*). In a comparison of multiple lane change trajectory models, polynomial has been shown (*40*) to be one of the best in representing an ideal or standard lane change trajectory. The same trajectory function is also used in a PSD model in (*37*) to represent the passing vehicle's lane change trajectory. Therefore, in this section, the same five-degree polynomial function is used to model the passing vehicle's lane change trajectory. The functions for left and right lane changes are as follows.

Left lane change:

$$y(x) = y_e \left[10 \left(\frac{x}{x_e} \right)^3 - 15 \left(\frac{x}{x_e} \right)^4 + 6 \left(\frac{x}{x_e} \right)^5 \right] \quad [2\text{-}1]$$

Right lane change during back-to-lane stage:

$$y(x) = y_e - y_e \left[10 \left(\frac{x}{x_e} \right)^3 - 15 \left(\frac{x}{x_e} \right)^4 + 6 \left(\frac{x}{x_e} \right)^5 \right] \quad [2\text{-}2]$$

Per the model assumptions, the passing vehicle, A, takes a constant longitudinal acceleration, a_x. The longitudinal speed of vehicle A during the lane change is:

$$v_{xA}(t) = \frac{dx}{dt} = v_{A0} + a_x t \quad [2\text{-}3]$$

The longitudinal displacement of vehicle A during the lane change is:

$$x(t) = v_{A0} t + \frac{1}{2} a_x t^2 \quad [2\text{-}4]$$

By replacing the x in the five-degree polynomial model $y(x)$ with the function $x(t)$, the lateral displacement function can be written as:

$$y(t) = y_{io} + 10 y_e \left(\frac{v_{A0} t + \frac{1}{2} a_x t^2}{x_{eL}} \right)^3 - 15 y_e \left(\frac{v_{A0} t + \frac{1}{2} a_x t^2}{x_{eL}} \right)^4 + 6 y_e \left(\frac{v_{A0} t + \frac{1}{2} a_x t^2}{x_{eL}} \right)^5 \quad [2\text{-}5]$$

By solving the $x(t)$ Equation [4], we have the time to complete left lane change as:

$$t_L = \frac{-v_{A0} + \sqrt{v_{A0}^2 - 2 a_x x_{eL}}}{a_x} \quad [2\text{-}6]$$

The right lane change process is modeled similarly with Equations [7], [8], and [9] for longitudinal displacement, lateral displacement, and time taken to complete the process, respectively.

$$x(t) = \min(v_{A2} t + \frac{1}{2} a_x t^2, v_{A\,max} t) \quad [2\text{-}7]$$

$$y(t) = y_e - 10 y_e \left(\frac{x(t)}{x_{eR}} \right)^3 + 15 y_e \left(\frac{x(t)}{x_{eR}} \right)^4 - 6 y_e \left(\frac{x(t)}{x_{eR}} \right)^5 \quad [2\text{-}8]$$

$$t_R = \max\left(\frac{-v_{A2} + \sqrt{v_{A2}^2 - 2a_x x_{eR}}}{a_x}, \frac{x_{eR}}{v_{A2}}\right) \quad [2\text{-}9]$$

Overtake

The time needed by A to complete passing B in the left lane during the overtake stage consists of two parts and is calculated as:

$$t_{OLL} = t_1 + t_2 \quad [2\text{-}10]$$

Where t_1 is the time A takes to accelerate from v_{A1}, its speed after the left lane change, to its desired maximum passing speed, $v_{A\,max}$; and t_2 is the time for A to continue passing B at the speed of $v_{A\,max}$ until it reaches the position that the tail of it and the front bumper of B have a gap of h_B. There are two cases in the calculation of t_1 and t_2:

Case I. If the distance for A to accelerate from v_{A1} to $v_{A\,max}$, s_{A1}, is less than the distance that A travels in the left lane to pass B and reach a gap of h_B between B and A, s'_{A1}.

$$s_{A1} = v_{A1}t_1 + \frac{1}{2}a_x t_1^2 \quad [2\text{-}11]$$

$$s'_{A1} = L_A + L_B + h_{A1} + h_B + v_B t_{OLL} \quad [2\text{-}12]$$

Based on the relationship between distances traveled by A and by B during the same t_{OLL}, we have the total distance traveled by A during t_1 and t_2 equal to the sum of distance traveled by B during $(t_1 + t_2)$, the following gaps h_{A1} and h_B, and the lengths of A and B:

$$\left(v_{A1}t_1 + \frac{1}{2}a_x t_1^2\right) + v_{A2}t_2 = v_B(t_1 + t_2) + h_{A1} + h_B + L_A + L_B \quad [2\text{-}13]$$

For A to accelerate from v_{A1} to $v_{A\,max}$, it takes the time of:

$$t_1 = \frac{v_{A\,max} - v_{A1}}{a_x} \quad [2\text{-}14]$$

Then, the second part of t_{OLL} is calculated as:

$$t_2 = \frac{(v_B - v_{A1} - 0.5a_x)t_1 + (h_{A1} + h_B + L_B + L_A)}{v_{A2} - v_B} = \frac{\frac{(v_B - v_{A1} - 0.5a_x)(v_{A2} - v_{A1})}{a_x} + (h_{A1} + h_B + L_B + L_A)}{v_{A2} - v_B} \quad [2\text{-}15]$$

The speed of A at the end of the overtake stage then equals to its desired maximum passing speed:

$$v_{A2} = v_{A\,max} \qquad [2\text{-}16]$$

Case II. If A is still accelerating and yet to reach its desired maximum passing speed, which means $s_{A1} = s'_{A1}$, then we have:

$$t_1 = t_{OLL}; and\ t_2 = 0 \qquad [2\text{-}17]$$

and t_{OLL} is calculated by solving:

$$s_{A1} - s'_{A1} = 0 \qquad [2\text{-}18]$$

which is:

$$\frac{1}{2} a_x t_{OLL}^2 + (v_{A1} - v_B)t_{OLL} - (h_{A1} + h_B + L_A + L_B) = 0 \qquad [2\text{-}19]$$

The speed of A at the end of the overtake stage is:

$$v_{A2} = v_{A1} + a_x t_{OLL} \qquad [2\text{-}20]$$

Total time

The total overtaking time is the sum of times needed for the three stages of lane change, overtake, and back-to-lane (i.e., t_L, t_{OLL}, and t_R, respectively):

$$T = t_L + t_{OLL} + t_R = t_L + (t_1 + t_2) + t_R \qquad [2\text{-}21]$$

Total distance

The total overtaking distance covered by the passing vehicle, A, is the sum of the initial following gap between A and B, the final following gap between B and A, the lengths of A and B, and the distance traveled by B during the overtaking:

$$S_A = h_A + h_{B1} + L_A + L_B + v_B T \qquad [2\text{-}22]$$

Note on model validation

Validation of an overtaking model usually requires field observations or driving simulation tests. Since all model components representing the three overtaking stages have been validated by prior studies, we did not introduce a further validation (*37*, *39*). However, for adaptation to truck platooning analysis, the overtaking model would benefit from a validation, possibly using driving simulation (*46–51*). In the simulation, we would be able to set up various truck platooning scenarios and observe how drivers overtake the platoons. As suggested by prior research on overtaking LCVs, drivers behave differently when overtaking longer and larger vehicles from overtaking smaller vehicles such as passenger cars, and thus affect the vehicle trajectory and measures like overtaking distance and time (*25*). Therefore, we might see similar or more complex driver interactions with truck platoons and then incorporate the behavior in our overtaking model.

2.4 Safety Assessment

2.4.1 Overtaking distance consideration

Overtaking distance is considered part of the overtaking safety assessment because enough sight distance is required for a safe overtaking. Sight distance is considered in designing curves and two-lane, two-way passing zones. Truck platooning may pose challenges to provide enough sight distance for drivers that want to overtake platoons, as a long truck platoon may lengthen the overtaking distance. On the other hand, current geometric designs may restrict the feasible length of a truck platoon. For a case of multilane operation, the total overtaking distance, S_A, as we calculate in the previous section, would be the value to use when assessing sight distances. For one-lane operation on two-lane, two-way highways, the required PSD can be evaluated as follows.

Assuming an opposing vehicle drives at the speed limit, v_{lmt}, the distance covered by the vehicle during the period the passing vehicle completes its overtaking is:

$$S_O = v_{lmt}T \qquad [2\text{-}23]$$

The passing and opposing vehicles should maintain a safety distance, h_O, at the time point when the passing vehicle finishes its overtaking. Therefore, the PSD for the passing vehicle to complete its overtaking is:

$$PSD = S_A + S_O + h_O \qquad [2\text{-}24]$$

2.4.2 Overtaking time consideration

Overtaking time is also considered in the safety assessment as the potential lengthened overtaking time due to truck platooning may add stress to the passing vehicle driver and increase the risk of collision (*52–54*). Moreover, a long truck platoon with small following gaps may not permit enough chances for a passing vehicle to safely fall back if an overtaking maneuver is not successful, leading to increased risk of collision. The total overtaking time, T, as we calculate in the model presented in the previous section, can be used as a measurement to determine if the length of a truck platoon is appropriate considering the passing vehicle driver’s tolerance. Potentially, a long durational overtaking may affect a driver’s handling of the vehicle and affect collision risks. However, we were not able to find literature specifically on drivers’ tolerance to long-durational overtaking maneuvers yet, so we do not have an existing threshold for overtaking time to compare to the assessed T.

2.4.3 Collision risk in lane change

When executing a lane change, the passing vehicle interacts with the impeding truck platoon and potentially an opposing vehicle in one-lane operation cases. Those interactions make the passing vehicle face inherent risks of rear-end, sideswipe, or head-on collisions (*55*, *56*). A National Highway Traffic Safety Administration (NHTSA) lane change crash study showed that light vehicle passing truck related crashes take more than 8% of all passing related crashes (*57*). To measure the collision risk during lane change, we referred to a prior driving simulation study by Zhang et al., where time difference to collision (TDTC) was measured between several key points on the interacting vehicles and roadway, as shown in **Figure 2** (*56*).

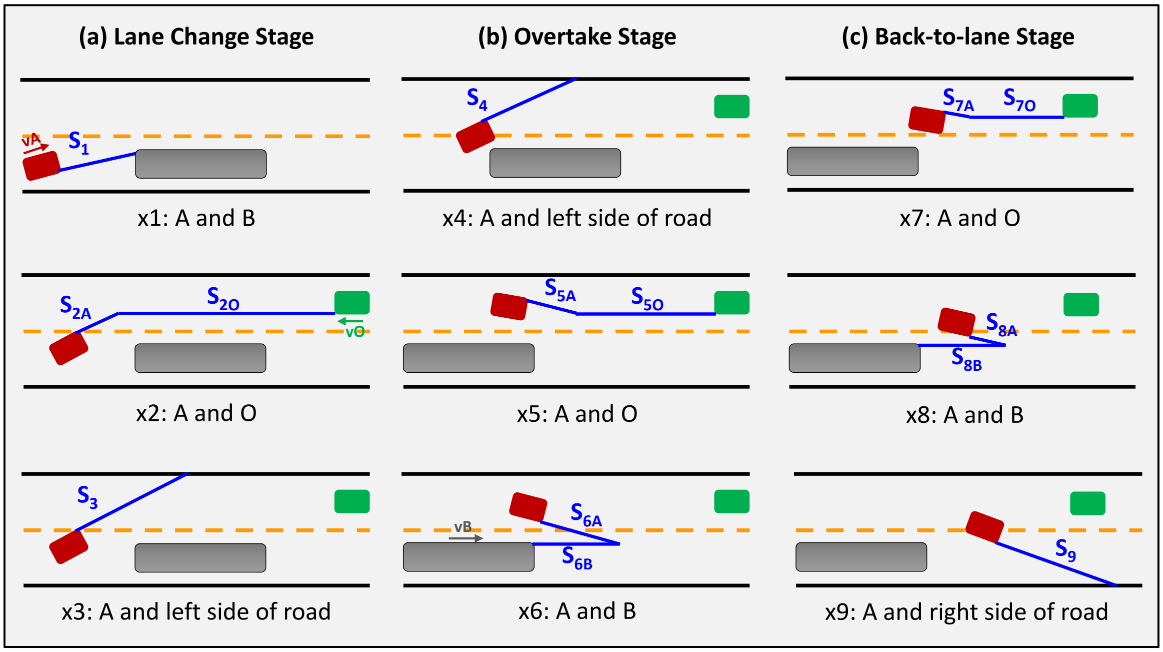

Note: Adapted from Figure 7 in (*56*).

Figure 2: Distance and speed measurements used in TDTC calculation

The TDTCs during each stage of the overtaking process are calculated based on the functions listed in **Table 2**. Then at each time step of the overtaking process, depending on the stage, the TDTCs form a vector, which can be compared against several collision safety thresholds. For example, in the lane change stage, the vector [$TDTC(x_1)$, $TDTC(x_2)$, $TDTC(x_3)$] would be compared with three safety threshold vectors [3, 3, 3], [4, 4, 4], and [6, 6, 6] (element unit: seconds). Each element of the TDTC vector is compared with its corresponding element in the three threshold vectors. The level of collision risk is determined by the smallest threshold vector that is larger than the TDTC vector, and the number of elements in the TDTC vector is smaller than their corresponding elements in the threshold vector. This comparison algorithm gives us 10 levels of collision risks ranging from level 0.1 (when the TDTC vector is greater than the 6-second threshold vector) to level 1.0 (when the TDTC vector is smaller than the 3-second threshold vector and all three elements are smaller than 3), with an increment of 0.1.

Table 2: Functions of TDTC at Each Stage of Overtaking

Lane-change Stage		Overtake Stage		Back-to-lane Stage	
$TDTC(x_1) = \frac{S_1}{v_A}$	[25]	$TDTC(x_4) = \frac{S_4}{v_A}$	[28]	$TDTC(x_7) = \frac{S_{7O}}{v_O} - \frac{S_{7A}}{v_A}$	[31]
$TDTC(x_2) = \frac{S_{2O}}{v_O} - \frac{S_{2A}}{v_A}$	[26]	$TDTC(x_5) = \frac{S_{5O}}{v_O} - \frac{S_{5A}}{v_A}$	[29]	$TDTC(x_8) = \frac{S_{8B}}{v_B} - \frac{S_{8A}}{v_A}$	[32]
$TDTC(x_3) = \frac{S_3}{v_A}$	[27]	$TDTC(x_6) = \frac{S_{6B}}{v_B} - \frac{S_{6A}}{v_A}$	[30]	$TDTC(x_9) = \frac{S_9}{v_A}$	[33]

Note: Adapted from Table 2 in Zhang et al. 2022 (*56*).

2.5 Numerical Analysis

The numerical analysis aims to show how the overtaking model and safety assessment procedure can help determine requirements for truck platooning on specific highway segments. The overtaking model is used to calculate the overtaking distance, PSD, and time for different truck platoon configurations. To assess collision risks, the model is used to calculate positions of the passing vehicle, truck platoon, and opposing vehicle (when applicable), forming corresponding trajectories. Vehicle speeds and headings are also calculated for each time point to assess the TDTC.

2.5.1 Overtaking Distance and Time

The assumed values used for the calculation of overtaking distance and time are as follows. The depicted scenario is a passenger car following a truck platoon on a two-way, two-lane highway segment, overtaking the platoon using the opposing lane. The length of the truck platoon varies as its size varies from one truck to eight trucks. The 1-second platoon following time gap was based on the suggested value from a USDOT Volpe Center research report, which considered safety, fuel efficiency, and truck driver comfort factors for truck platooning (*58*). The required overtaking distance, PSD, and overtaking time are calculated, with their relationships to the platoon length illustrated by charts.

Speed: Posted speed limit, $v_{lmt} = v_O$ = 50 mph ≈ 22 m/s
Truck speed, v_B = 45 mph ≈ 20 m/s
Passing vehicle longitudinal speed (overtaking speed), v_{Ax} = 55 mph ≈ 25 m/s

Platoon: Truck length: 70 ft ≈ 21 m
Platoon following gap: 20 m (1 s time gap at truck speed)
Lengths, L_B: 1-truck: 21 m; 2-truck: 21 × 2 + 20 = 62 m;
3-truck: 21 × 3 + 20 × 2 = 103 m; 4-truck: 144 m; 5-truck: 185 m;
6-truck: 226 m; 7-truck: 267 m; 8-truck: 308 m

Driver: "Moderate" behavior:
Following gap, $h_A = h_B$ = 66 m (3 s time gap at posted speed limit)
Lane change longitudinal displacement, $x_{el} = x_{er}$ = 100 m

Other: Longitudinal acceleration, a_x = 3 m/s^2
Vehicle widths: A: 5.9 ft ≈ 1.8 m, B: 2.6 m, O: 1.8 m

Lane width: 3.5 m
Lateral offsets: Right edge of road: 0 m
Initial offset of front center point of A, y_{io} = 3.5 × 0.5 = 1.25 m
Front center point of B: 1.25 m
Front center point of C: 3.5 × 1.5 = 5.25 m
Safety distance between A and O, h_O = 160 m

As shown in **Figure 3** (a) and (b), with the increase of platoon length, the overtaking distance, PSD, and overtaking time all increased linearly. When the truck platoon size increases from one truck to eight trucks, the overtaking distance increases from 904 m (2,966 ft) to 2,339 m (7,674 ft); the PSD increases from 1,863 m (6,112 ft) to 4,561 m (14,964 ft); and the overtaking time increases from 36 s to 94 s. The PSD increases faster than overtaking distance, at a speed of 385 m (1,263 ft) per addition of one truck to the platoon vs. 205 m (673 ft) per addition of one truck. The overtaking time increases 8.3 s per addition of one truck to the platoon.

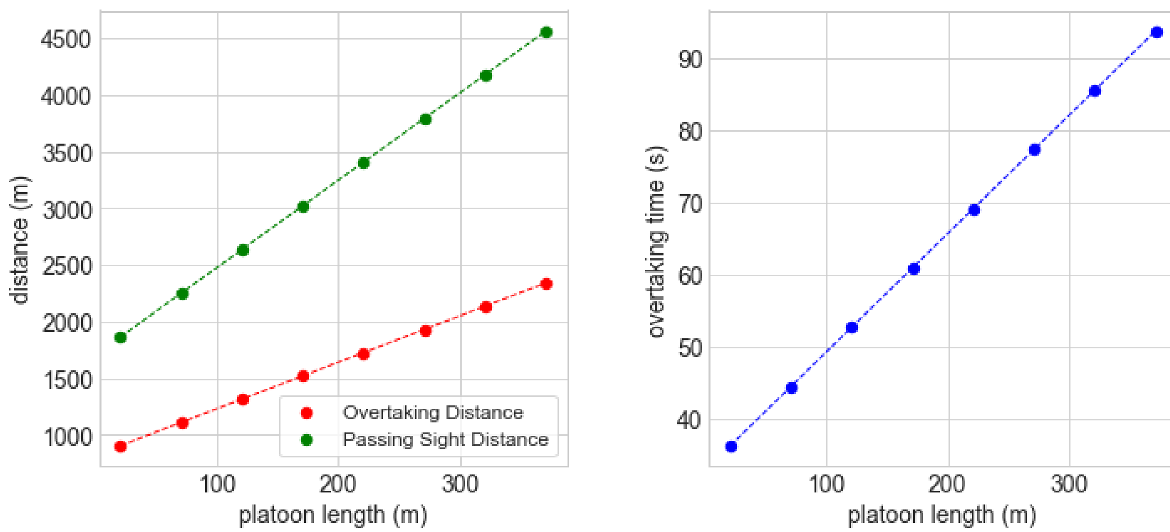

(a) Distance vs. Platoon Length (b) Time vs. Platoon Length

Figure 3: Effects of platoon length on overtaking distance, PSD, and overtaking time

2.5.2 Collision Risk

The safety risks are calculated and visualized for multiple types of overtaking behavior under the two-lane and one-lane operation scenarios. The settings are shown in **Table 3**. Based on the settings used for overtaking distance and time analysis, the only settings changed for collision risk analysis were speed, platoon, and driver behavior parameters. Parameters for the two-lane operation scenario reflect operational conditions on a single direction two-lane highway segment with a 70 mph (113 km/h) posted speed limit and without opposing traffic; and parameters for the one-lane operation scenario reflect operational conditions on a two-way, two-lane highway segment with a 50 mph (80 km/h) posted speed limit and with opposing traffic. Three types of passing vehicle driver behavior, "mild," "moderate," and "aggressive," were differentiated by the parameters of following gap and lane change longitudinal displacement. The assumption is that a more aggressive driver would use a smaller following gap and perform a more evasive lane change maneuver. The lane change longitudinal displacement values were based on a distribution found in a recent lane change trajectory study (*44*).

Table 3: Settings for Collision Risk Analysis

Speed and Platoon	Passing Vehicle Driver Behavior
Two-lane Operation Speed limit: 70 mph = 31 m/s Truck speed: 65 mph = 29 m/s Overtaking speed: 75 mph = 34 m/s Platoon length: 21*3 + 29*2 = 121 m	"Mild" - Following gap: 4 s (124 m) Lane change longitudinal displacement: 200 m
	"Moderate" - Following gap: 3 s (93 m) Lane change longitudinal displacement: 140 m
	"Aggressive" - Following gap: 2 s (62 m) Lane change longitudinal displacement: 55 m
One-lane Operation Speed limit: 50 mph = 22 m/s Truck: 45 mph = 20 m/s Overtaking speed: 55 mph = 25 m/s Platoon length: 21*3 + 20*2 = 103 m	"Mild" - Following gap: 4 s (88 m) Lane change longitudinal displacement: 170 m
	"Moderate" - Following gap: 3 s (66 m) Lane change longitudinal displacement: 100 m
	"Aggressive" - Following gap: 2 s (44 m) Lane change longitudinal displacement: 40 m

As mentioned in the Methodology section, the collision risk is measured by a 10-level TDTC, which is the result of comparing the estimated TDTC vector with three vectors representing 3-second, 4-second, and 6-second TDTC thresholds. The collision risk level ranges from 0.1 (lowest) to 1.0 (highest), with an increment of 0.1. **Figure 4** (a), (b), and (c) present color-coded collision risks in a two-way operation scenario in formats of trajectory and time-space diagrams by the three driver behavior types. **Figure 5** (a), (b), and (c) present the trajectory and time-space diagrams for the collision risks in a one-lane operation scenario.

We can observe from Figure 4 that the collision risks in the lane change and back-to-lane stages increase as the passing vehicle driver's behavior becomes more aggressive. However, the duration of exposure to higher collision risks decreases as the driver's behavior turns more aggressive. That is because the overtaking distance and time decrease due to shorter following gaps and lane change longitudinal displacements.

Figure 5 shows a slightly different pattern in the collision risk. Both the mild and aggressive driver behaviors post a higher collision risk in the lane change and back-to-lane stages, but the moderate driver behavior yields a lower collision risk. That is because, with an opposing vehicle added into the overtaking interactions, a longer overtaking distance and time add risks of collision between the passing vehicle and the opposing vehicle. When the passing vehicle enters the back-to-lane stage, the opposing vehicle may have moved to a very close position to the passing vehicle, yielding a short TDTC. The patterns in overtaking distance and time are similar to those in the two-lane operation scenario, as they decrease along with the following gaps and lane change longitudinal displacements.

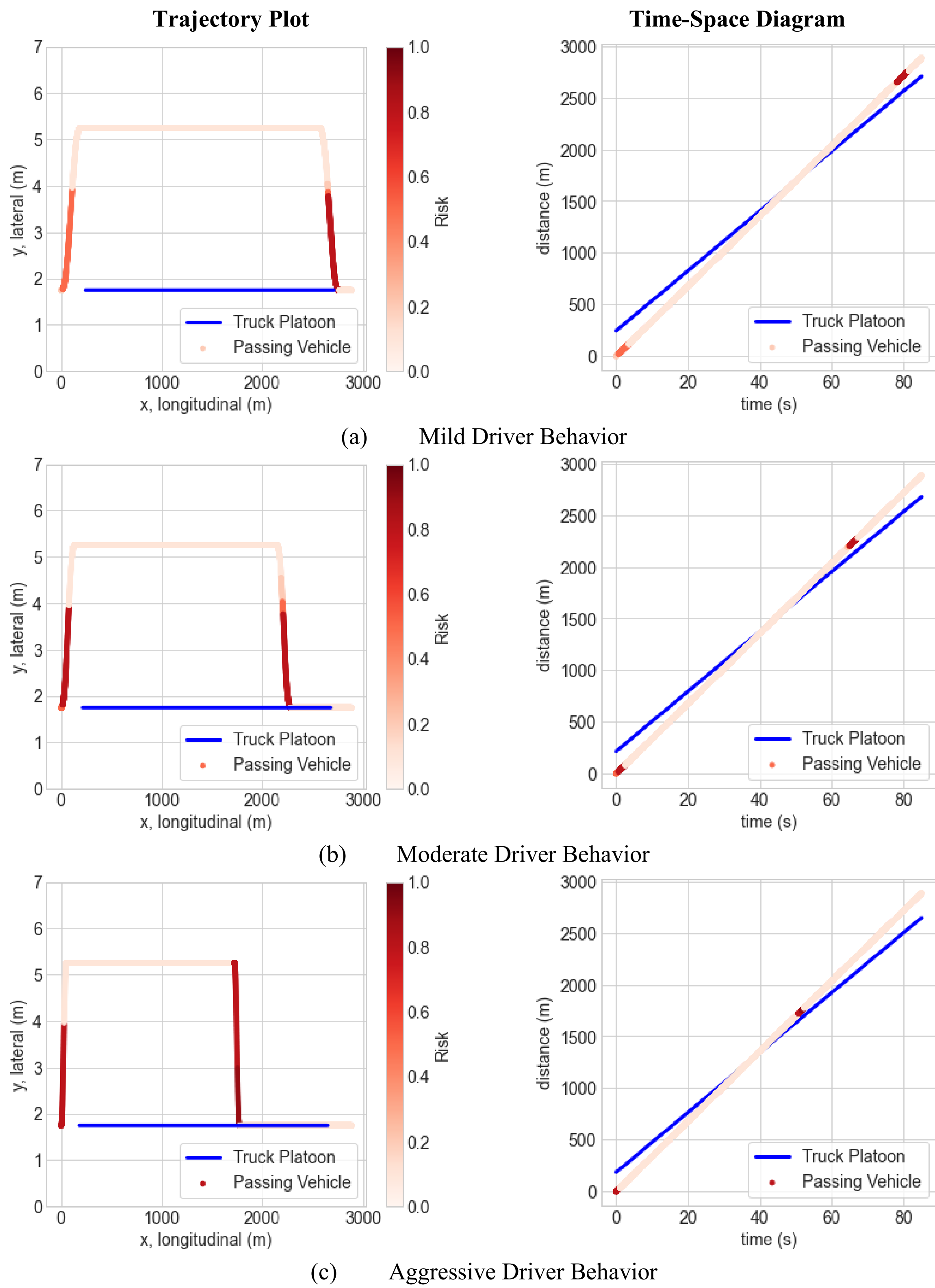

Note: Analysis duration = 85 s.

Figure 4: Collision risk in two-lane operation shown in (a) trajectory and (b) time-space diagrams.

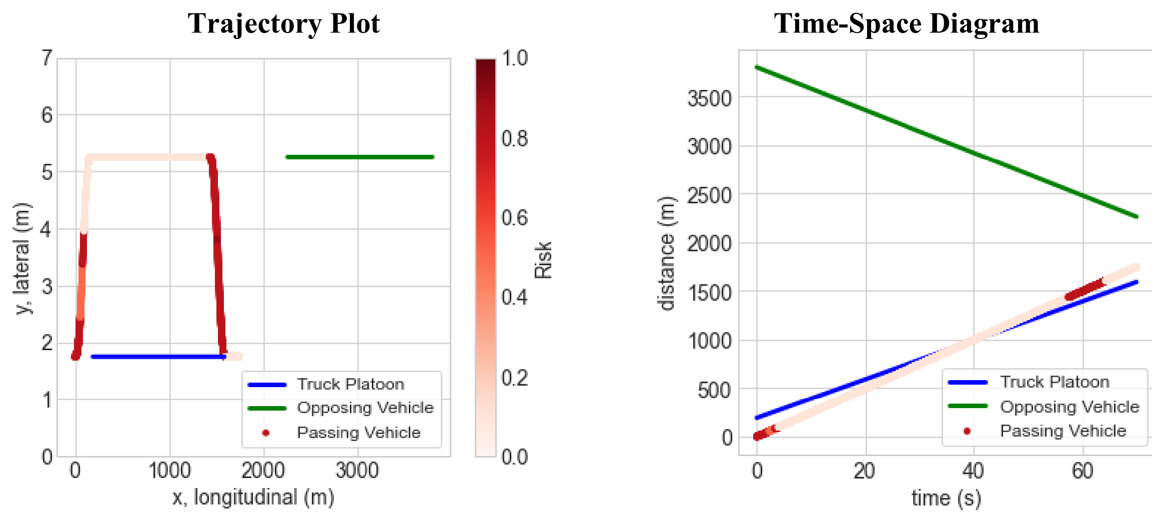

(a) Mild Driver Behavior

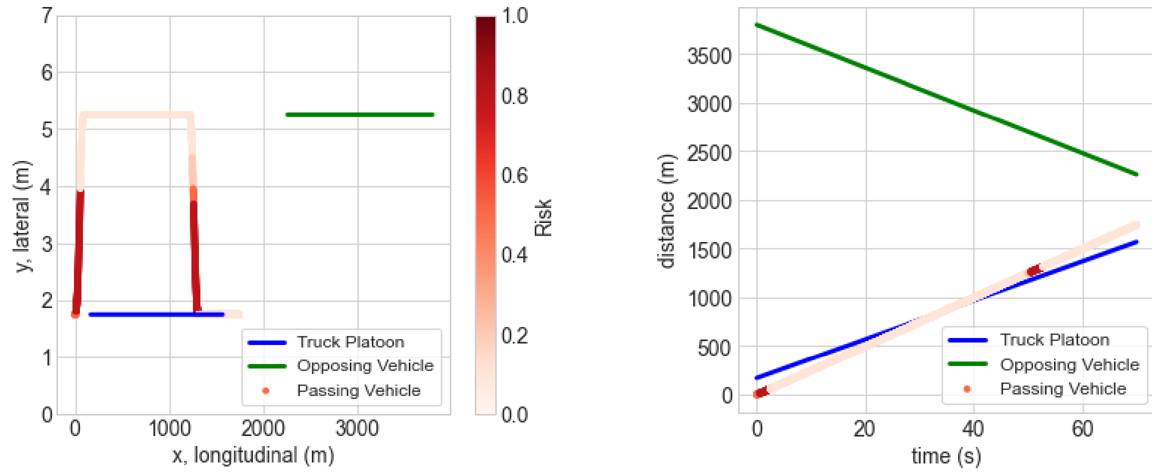

(b) Moderate Driver Behavior

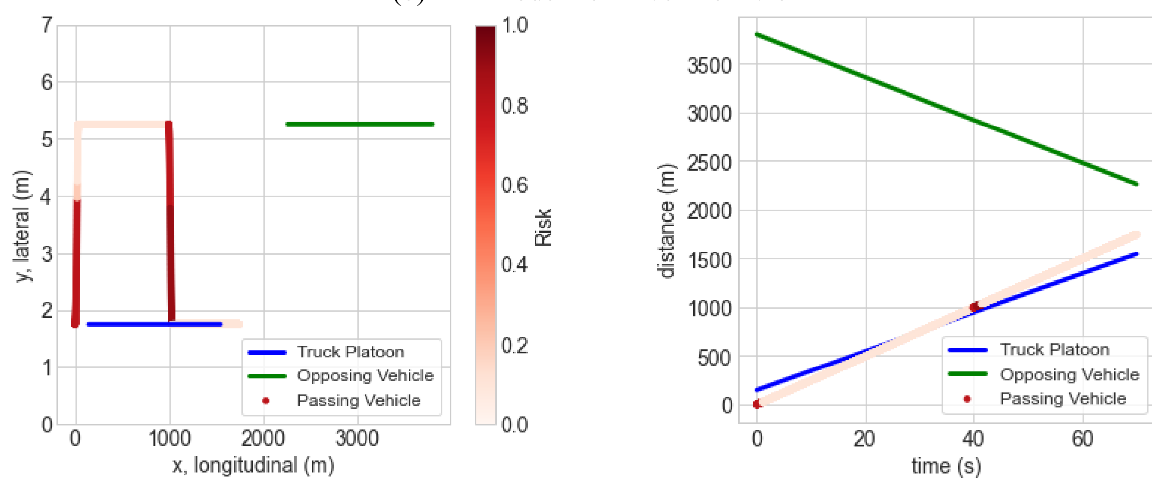

(c) Aggressive Driver Behavior

Note: Analysis duration = 70 s; opposing vehicle starts at x = 3800 m.

Figure 5: Collision risk in one-lane operation shown in (a) trajectory and (b) time-space diagrams.

2.6 Discussion

2.6.1 Aspects to Consider for Truck Platooning Requirements

Roadway geometry. The numerical analysis results show that the increased length of a truck platoon can greatly increase the overtaking distance and PSD. Current roadway geometric design guidelines have not taken that into consideration. If operating on existing roadways, truck platoon lengths should be regulated according to available sight distances for passing, especially on two-lane undivided highway segments, with a considerable number of horizontal and vertical curves, or in areas with frequent weather conditions that may limit driving visibility. On the other hand, future guidelines can be developed to incorporate truck platooning needs by defining preferable dimensions for truck platooning operation and criteria for selecting roadway segments for truck platooning operation.

Traffic conditions. Along with the increased overtaking distance, the required overtaking time also lengthens as the truck platoon length increases. Traffic conditions on a two-way, two-lane highway determine if there is a large enough gap between opposing vehicles to allow a passing vehicle to overtake a truck platoon. The small following gap between trucks in a platoon (e.g., 1 second) forces the passing vehicle to overtake the entire platoon rather than doing it one truck at a time. When a truck platoon reaches a certain length, it may add challenge for the passing vehicle driver to abort the overtaking task and thus increase the risk of collision with the truck platoon or opposing vehicle. However, the relationship between platoon length and drivers' overtaking decisions needs further investigations. Another challenge due to the increased overtaking time is the potentially added stress to the passing vehicle driver. As shown by the analysis results, under specific assumptions and settings, it would take a moderate driver over 50 seconds to overtake a three-truck platoon on a 50-mph (about 80 km/h) highway segment. A larger truck platoon would require a longer overtaking time. For example, under the same assumptions and settings, it would take a moderate driver about 70 seconds to overtake a five-truck platoon, and over 90 seconds to overtake an eight-truck platoon.

Driver behavior. Different driver behaviors would lead to different collision risks while overtaking a truck platoon. The numerical analysis briefly explores the relationship between driver behavior, truck platoon configurations, and collision risks. The results show that in two-lane operations, where the passing vehicle does not have potential conflict with traffic from the opposing direction, the more aggressive the driver behavior is, the higher the collision risks. However, in the more complex one-lane operations, with the introduction of an opposing vehicle, the relationship becomes more complicated. A milder driver behavior may not necessarily lead to lower collision risks, as the lengthened overtaking distance and time may leave a smaller distance between the passing vehicle and the opposing vehicle, posting extra risks. Apart from the inherent potential risks of driver aggressiveness, driver behavior in the overtaking process may change with the dimensions of the impeding vehicle. Prior studies have suggested that drivers show more hesitation and take more time to decide when overtaking longer vehicles (*25*). Compared with a platoon of passenger cars, the dimension of a truck platoon may impact drivers' line of sight and confidence in deciding to overtake. Further investigations into how drivers interact with truck platoons are needed to fully understand the potential risks.

2.6.2 How to Ensure Safe and Efficient Truck Platoon Operations

Regulating truck platoon configurations. Truck platoon configurations can be adapted to ensure safety operations. Basic operating parameters such as the speed, number of trucks, and following gap can be planned or determined in real-time based on general knowledge or real-time information of the three safety consideration aspects. From the perspective of infrastructure owners and operators such as state departments of transportation, rules can be developed to restrict truck platoon configurations to mitigate the potential negative safety effects of truck platooning, while keeping its operational and environmental benefits. For example, data of roadway geometry, passing zones, traffic conditions, and general driver behavior can be collected and used to develop a map of truck platooning operational design domains, showing specific restrictions on operating speed, maximum number of trucks in each platoon, and range of following gap. The map can be integrated into trucks' in-vehicle systems for truck platooning control or broadcasted through vehicle-to-infrastructure (V2I) communication networks along the routes. Real-time platooning restrictions can be implemented if real-time traffic and driver behavior data can be collected and analyzed, with updated restrictions broadcast through V2I networks. Regarding the potential impacts on traffic flow, prior research has found that truck platoons with two or three trucks do not affect traffic flow significantly, and the internal following gaps do not affect flow but should be considered for safety (*12*). On the other hand, fuel savings and emission reductions may benefit from a larger platoon size and a smaller following gap (*59*). Therefore, an optimal solution is needed to satisfy the multiple objectives.

Seeking assistance from advanced vehicle automation technologies. Advanced platoon control such as the capability to vary following gap and allow passing vehicles to merge into the platoon should be able to help address some issues in overtaking (*13*, *60*). However, that type of control has its complexities. Trucks, compared with passenger cars, are heavier, thus require more time to adjust their operating speed and following gap. A slow adjustment may not accommodate the need of a driver urgently seeking a gap between trucks to temporarily dodge an opposing vehicle. Other than truck platooning control, systems such as overtaking assistance would help drivers to complete challenging overtaking tasks (*61–68*). With overtaking assistance, drivers would receive messages informing them about available gaps, and the system can also assist steering and speed control during overtaking. These advanced vehicle automation technologies will potentially relax some regulations toward truck platooning configurations.

2.7 Section Conclusion

Through updating a vehicle overtaking model and integrating it with a safety assessment, this section investigated the safety risks associated with the maneuver of overtaking truck platoons. We explored three key aspects of safety considerations in overtaking for defining truck platooning requirements: roadway geometry, traffic conditions, and driver behavior. We found that as truck platoon length increases (due to increased number of trucks), the overtaking distance, PSD, and time increased linearly. The extent of PSD and time for overtaking a truck platoon on a two-lane highway suggests that regulations on truck platoon length may be necessary to mitigate potential difficulties in overtaking the platoons. We also found, from the collision risk assessment, that without the presence of an opposing driver, a more aggressive driver would be exposed to higher collision risks but for a shorter period, compared with a milder driver. However, with the presence of an opposing driver, a milder driver may be exposed to higher collision risks and for a longer period, compared with a more aggressive driver. It indicates that potentially increased hesitation in driver behavior (due to the large dimensions of impeding vehicles) when overtaking a truck platoon would increase collision risks. Based on these findings, we suggest that guidelines and regulations to be established for truck platoon length for operation on two-lane highways, to ensure safety in overtaking. For comprehensive guidelines and regulations on truck platooning, other operational maneuvers, truck platoon configuration parameters, and various types of roadway facilities should also be considered to ensure truck platooning safety, while maximizing the technology's operational and environmental benefits.

This section makes several contributions. First, incorporating vehicle lane changing dynamics in the overtaking model enabled the estimation of collision risks along with calculating the overtaking distance and time. We were able to quantify and visualize safety-related measures for the entire overtaking process. Second, a framework was established for defining safety requirements in truck platooning, considering roadway geometry, traffic conditions, and driver behavior, which we anticipate being helpful for practitioners and researchers in assessing the safety of overtaking a truck platoon. Furthermore, it opens new avenues for future research on truck platooning safety. Further investigations of driver behavior and truck platooning control algorithms to accommodate driver behavior would benefit the safety verification and validation of truck platooning technology. Further definition of standards and regulations for truck platooning is also a necessary next step, which requires collaborative efforts from researchers, practitioners, and technology providers.

Future research can expand upon this section to enhance the overtaking model by relaxing some of its assumptions. For instance, by gathering real-world data and acquiring localized parameter distributions, it is possible to alleviate the driver behavior assumptions. Simulation can be employed to validate the model, ensuring accurate and precise safety assessment results. Additionally, analysis methods similar to those used in this section can be employed to evaluate the safety implications of truck platooning, considering maneuvers other than overtaking. Furthermore, investigating driver interactions with different truck platoon settings would be valuable, either in a simulated environment or through staged, controlled field experiments.

3. DECIDING TRUCK PLATOONING RULES FOR TWO-LANE HIGHWAY OPERATIONS

This section has been published as the paper "Deciding Truck Platooning Operational Rules with Stochastic Approximation for Vehicle Safe Overtaking on Two-Lane Undivided Highways" in IEEE Transactions on Intelligent Transportation Systems, DOI: 10.1109/TITS.2025.3553841. Slight modifications were applied to ensure consistency in this report.

3.1 Introduction

Truck platooning is the operation of electronically linking two or more trucks in convoy using automated driving support systems and connected technology (*1*, *6*, *69*). It has great potential in reducing fuel consumption and emissions while increasing highway freight transport capacity (*8*, *70–73*). Currently, truck platooning has advanced to the stage where the technology is being improved to adapt to complex roadway infrastructure and environments. It is crucial to understand possible interactions in truck platoon operations and determine appropriate rules and requirements for deployment of the technology on existing roadways where space is shared with human drivers.

Prior research has assessed the safety impact of truck platooning and suggested general operational requirements. Platoons should operate in a way that offers safe operating conditions to surrounding vehicles when interacting with them, while under the constraints of traffic, roadway geometric, and environmental conditions (*13*, *18*, *22*, *74–77*). Simulation and field studies have shown that truck platoons, when navigating through various roadway geometry, face control challenges such as losing string stability (*72*, *75*, *78*). Environmental factors such as weather are also shown to affect truck platoon operations and safety (*76*, *79*). Adding to the complexity, truck platoons operating in mixed traffic need to avoid all types of collisions with the surrounding vehicles (*80*). Prior research has offered solutions, including applying collision avoidance systems or using complex control strategies to react to surrounding vehicles' risky maneuvers such as cut-ins (*73*, *77*, *81*).

Rather than solely relying on reactive collision avoidance, offering safe conditions for both truck platoons and surrounding vehicles by establishing operating rules and regulations would be a necessary action to ensure safe and efficient deployment of the technology, as it builds a multi-layered safety guarantee. Infrastructure owner operators such as state transportation agencies play an important role in the deployment of safe truck platooning by setting up and implementing operational rules using conventional and innovative strategies and technologies (*70*). Currently in the U.S., state laws on truck platooning are at the stage of defining operational criteria and restricting certain operational parameters. For example, 20 states have passed laws restricting truck platoons' minimum internal following gap, ranging from 250 to 500 ft (76.2 to 152.4 m) (*19*). However, a following gap as large as those would likely diminish the fuel-saving benefit of platooning, and may also induce cut-ins (*82*). To ensure safety while maintaining the desired benefits of truck platooning, appropriate operating parameters should be determined based on specific operating conditions. In addition to rules and regulations written into codes, variable platooning rules and regulations can be implemented to accommodate the dynamic changes in operating environments. Such an implementation would be similar to variable speed limit (VSL) systems, which have been shown to be effective in improving highway safety and operational efficiency (*83*, *84*).

Multilane highway settings have been the focus in prior truck platoon development and testing (*85*). However, two-lane undivided highways also have the potential to allow truck platooning (*22*, *86*). Two-lane undivided highways take up a significant portion of all types of highways in the U.S., as well as most other countries (*87*). This type of highway is especially prevalent in rural areas, serving the mobility and accessibility needs of small cities and towns. Two-lane undivided highways fall into various functional classes ranging from local roads to major arterials, carrying vastly different traffic loads. The current practice of freight truck routing already includes two-lane undivided highway segments, especially in rural areas. Therefore, allowing truck platooning on those segments would bring further benefits of this technology to a wider network and improve goods supply and accessibility to remote regions.

Deploying truck platooning on two-lane undivided highways is more challenging than deployment on multilane divided highways. The interactions between truck platoons, surrounding traffic, and roadway geometry are more complicated. Maneuvers like overtaking, for example, would be more challenging on two-lane undivided highways as an overtaking vehicle would need to use a gap in the opposite direction traffic to complete the maneuver. Analyses of truck crashes on two-lane highways have shown that overtaking-related crashes are deadlier than other types of truck crashes (*88*). Truck platoons would likely pose a higher risk for drivers attempting to overtake them, as these convoys are formed by multiple closely following, large, and heavy, tractor-trailer trucks, which bring expanded physical dimensions and additional control complexity (*6*, *74*).

Under the assumption that truck platoons, with CACC capability and sensing technology that enables surrounding information gathering and processing, are to be deployed onto existing roadways with traffic consisting of HDVs, this section focuses on addressing two research gaps:

1) The missing methodical procedure to determine operational rules for truck platooning
2) The shortage in investigation of truck platooning impacts and restrictions on two-lane undivided highways

We focus on the scenario of overtaking, as that is a primary and unique challenge faced by truck platoons when deployed on two-lane undivided highways. We propose an algorithm that determines the rules truck platoons should follow to guarantee overtaking safety, considering restrictions from traffic and roadway geometric factors. In the following sections, we summarize related work, formalize a model framework and the overtaking safety guarantee problem, and propose a solving algorithm, which is assessed using a numerical simulation.

3.2 Related Work

Related to overtaking truck platoons or longer combination vehicles (LCVs, which are trucks with long multiple-trailer combinations) on two-lane highways, prior studies have focused on modeling and simulating the effects of the convoy's or combination's large dimensions on driver passing sight distance (PSD) (*22*, *25*, *26*, *74*). A consensus of those studies is that overtaking a truck platoon or LCV requires a much larger distance than overtaking a single standard 65-ft (20-m) truck. For truck platooning on two-lane undivided highways, PSD is the most important safety parameter considered for overtaking safety. Therefore, to determine operational rules for truck platooning on two-lane highways, PSD should be the core component of the model framework that also incorporates traffic and roadway geometric factors.

In (*74*), the author proposed an overtaking trajectory model and assessed the effects of truck platoon length and overtaking driving characteristics on PSD and collision risk involved in an overtaking on two-lane undivided highways. The overtaking trajectory model from (*74*) is incorporated in this section's simulation section for PSD estimation. Note that the method in (*74*) is only one way to model overtaking trajectory and estimate PSD, and the algorithm proposed in this section is general enough that the model can be exchanged to other valid PSD estimation calculations. Some examples include models included in the guidebooks published by AASHTO (*38*), which were developed in (*33*) and (*35*) as a basis to suggest PSD values for roadway design purposes. As the models were designed for roadway design tasks, such as determining the length of passing zones, they do not model the overtaking vehicle trajectory in detail and only consider a limited number of parameters to describe kinematics. Thus, the AASHTO models do not offer a good estimation of the actual safety risks in overtaking. More advanced trajectory prediction methods that leverage real-time sensing and machine learning are also available for application to overtaking trajectories, which can be used to estimate PSD and incorporated into our platooning rule algorithm (*89–96*).

The available sight distance (ASD) is restricted by traffic and road geometric conditions without considering weather related factors. Currently, there have been few studies investigating traffic and road geometric restrictions on ASD in scenarios of overtaking a truck platoon, and (*97*) is the only found publication that investigated the impact of horizontal curves on ASD in such a scenario. The finding is that a truck platoon reduces an overtaking vehicle's ASD, but the gap between preceding and following trucks allow a slight increase in ASD. In (*97*), the authors developed an analytical procedure to calculate the ASD, which is adapted into our simulation analysis due to its simplicity for easy implementation. Nevertheless, our platooning rule algorithm can incorporate newer methods such as 3-D ASD estimation that relies on large datasets of roadway geometry, potentially obtained through advanced sensing such as LiDAR (*98–101*).

Variable traffic rules such as VSL have proven to be effective traffic management tools in an intelligent transportation system (*83*, *84*). Rules are automatically determined by algorithms, and are updated with an interval of as short as a few minutes (*84*). Depending on specific traffic management goals, VSL algorithms make decisions based on real-time data of road, weather, and traffic conditions. VSL algorithm objectives vary, for congestion management, the 85th percentile of congested traffic speeds can be used as the speed limit (*102*); for safety management, safety models relating speed, weather, and roadway conditions are used (*103*); implementations aiming at both improving mobility and reducing environmental impacts use more complex objective functions for speed limit determination (*104*). A variable truck platooning rule system would be similar to a VSL system.

3.3 Model Framework and Problem Setup

3.3.1 Model Framework

To establish rules for truck platoon operations, the relations between platoon operational parameters, traffic, and roadway geometry are modeled. This section introduces the model framework and explains how truck platooning operational rules can be determined based on the framework. **Figure 6** visualizes the framework. We are interested in knowing appropriate values for three parameters of truck platooning operations: the operating speed v, internal following gap h, and the number of trucks in a platoon n. Considering two-lane highway operations and overtaking safety, we included posted speed limit, traffic flow, horizontal and vertical curve features, and uphill grade as restricting factors. Overtaking behavior is an umbrella term for the various parameters describing the overtaking process and is included in the framework as part of the restricting factors. The three platoon operational parameters and four restricting factors are interrelated with the two sight distances, PSD and ASD, in the overtaking scenario. The definitions of variables are provided in **Table 4**.

ASD can be calculated through a function of parameters, including traffic flow, horizontal and vertical curve features, and truck platoon following gap: ASD = $f(q, R, L, A, h)$. PSD can be calculated through a function of parameters, including overtaking vehicle parameters and truck platoon parameters: PSD = $g(L_A, v_{A0}, a_x, v_{Amax}, h_A, h_B, x_{eL}, x_{eR}, d_A, v, h, n)$.

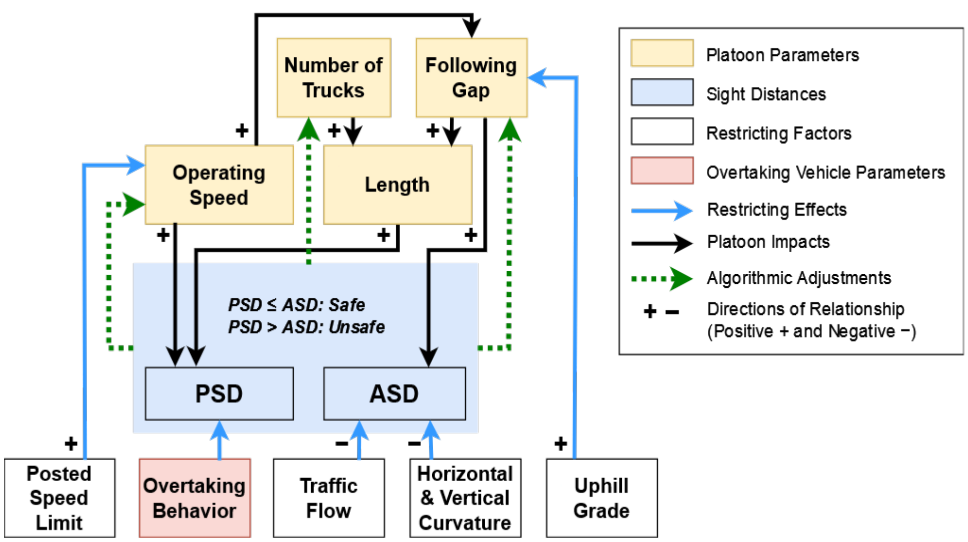

Figure 6: Relations among truck platooning parameters, sight distances, and restricting factors

Table 4: Definition of Variables

Variable	Definition
v	Truck platoon operating speed (m/s)
h	Platoon inter-truck following gap (m)
n	Number of trucks in a platoon
v_{lim}	Speed limit (m/s)
q	Traffic flow rate in the opposite direction (veh/h)
R	Horizontal curve radius (m)
L	Vertical curve length (m)
A	Vertical curve grade difference (%)
G	Uphill grade (%)
L_A	Overtaking vehicle length (m)
v_{A0}	Overtaking vehicle initial speed (m/s)
a_x	Overtaking vehicle acceleration (m/s^2)
$v_{A\,max}$	Desired overtaking speed (m/s)
h_A	Initial following gap between front bumper of the overtaking vehicle and rear bumper of the last truck in platoon (m)
h_B	End following gap between front bumper of the first truck in platoon and rear bumper of the overtaking vehicle (m)
x_{eL}	Overtaking vehicle left lane change longitudinal displacement (m)
x_{eR}	Overtaking vehicle right lane change longitudinal displacement (m)
d_A	Overtaking decision (overtake or not) with 1 = yes and 0 = no

The exact forms of functions f and g are rather complicated and are dependent on specific models chosen. Thus, we represent them here on an abstract level as it is enough for us to introduce our algorithm. In simulations, we instantiate them with specific models, whose details are presented in the Appendix section.

We use a vector, θ, to collect the overtaking vehicle parameters, and a vector, γ, to collect the traffic and roadway geometric factors: $\theta = [L_A, v_{A0}, a_x, v_{Amax}, h_A, h_B, x_{eL}, x_{eR}, d_A]$; and $\gamma = [v_{lim}, q, R, L, A, G]$.

3.3.2 Problem Setup

Given that overtaking vehicles' parameters are random, for a fixed truck platoon, PSD for any overtaking vehicle is a random variable. We introduce the overtaking safety probability, s, to be the probability that vehicles arriving behind a truck platoon are offered conditions to safely overtake the platoon or decide to keep following it. Note that s is to be achieved on the population level with respect to the distribution of overtaking vehicles' parameters. Given calculations of ASD and PSD, and definition of s, s can be calculated as:

$$s = \mathbb{E}\mathbb{1}[PSD(\theta_i, \gamma, v, h, n) \leq ASD(\gamma, h)] \quad [3\text{-}1]$$

where the indicator evaluates to one if ASD is greater than PSD, and expectation is with respect to randomness in parameter θ.

Given this setup, our goal is to search for values for variables v,h n such that s is greater than or equal to a target safety guarantee, τ. Note that this is a feasibility problem. This is possible when distribution of parameter θ is known, in which case stochastic optimization algorithms can be invoked. In reality, distribution of θ is not known, and fitting a distribution for θ takes substantial effort. More importantly, in a real time environment, the distribution of θ changes. Thus, instead of trying to achieve s and ensuring that $s \geq \tau$, which requires knowing the distribution of θ, we ensure the lower bound of s, which can be estimated quickly from a given sample, to be greater than or equal to τ.

3.3.3 Approximate Optimization Objective from Sample

Assume that a sample of k overtaking vehicles' parameters θ are available, a safety probability estimated from the sample, denoted by S, is defined as the proportion of vehicles with PSD ≤ ASD on the sample of k vehicles. We can call S the estimated safety ratio, and it is related to the truck platoon operational parameters, v,h,n:

$$S(v,h,n) = \frac{1}{k}\sum_{i=1}^{k} \mathbb{1}[PSD(\theta_i, \gamma, v, h, n) \leq ASD(\gamma, h)] \qquad [3\text{-}2]$$

where i denotes the ith vehicle in the sample. Note that $s = \mathrm{E}[S(v,h,n)]$, where the expectation here is taken over different samples. By the central limit theorem, s is within below range (*44*, *105–112*):

$$S(v,h,n) - z_{cl}\sqrt{\frac{S(v,h,n)\left(1-S(v,h,n)\right)}{k}} \leq s \leq S(v,h,n) + z_{cl}\sqrt{\frac{S(v,h,n)\left(1-S(v,h,n)\right)}{k}} \qquad [3\text{-}3]$$

Where z_{cl} is the z-score at confidence level cl.

Defining the lower bound of s as:

$$S_{ll}(v,h,n) = S(v,h,n) - z_{cl}\sqrt{\frac{S(v,h,n)\left(1-S(v,h,n)\right)}{k}} \qquad [3\text{-}4]$$

our goal is now to find v,h,n values such that $S_{ll}(v,h,n) \geq \tau$, in which case $s \geq \tau$ is also guaranteed.

Essentially, S is an estimate of the probability of success, s, calculated from the outcome of a series of success-failure experiments (i.e., the "safe-unsafe" status of each vehicle arriving behind a truck platoon). From running the comparison of PSD and ASD for each vehicle in the sample, we know the sample size, k, and the number of successes, $\sum_{i=1}^{k} \mathbb{1}[PSD \leq ASD]$. The assumption we have for the "safe-unsafe" status of vehicles is that their probabilities of being safe or unsafe are independent. To ensure that s is at least the target safety guarantee, τ, at a confidence level, cl, we need to ensure the lower confidence limit $S_{ll} \geq \tau$. To estimate the confidence interval, the distribution of each overtaking success-failure experiment can be approximated using a normal distribution, based on the central limit theorem (*105–107*). The confidence interval estimate is reliable with a large sample (i.e., $k \geq 40$) and an s not close to 0 or 1 (*105*). In the following section, we present an iterative algorithm to find feasible solutions rather than solving closed form on the sample for v,h,n. The reason is that the complex PSD and

ASD functions are difficult to differentiate and solve. We expect effective ways to be available to obtain samples of overtaking vehicle parameters using appropriate sensing techniques.

3.4 Algorithm Design

3.4.1 Algorithm

To solve the feasibility problem on the sample with the stochastic approximation objective, we designed an iterative algorithm, **Algorithm 3-1 PlatooningRules**. The reason for not using existing algorithms to solve the stochastic approximation objective is because in high dimensions, an existing algorithm relies heavily on first order or second order information (*108*, *109*). In the current problem setup, finding the gradient or hessian with respect to v,h,n is quite involved, given the inclusion of PSD models and an indicator function in objective. The algorithm we propose instead only uses zero-th order information. It evaluates PSD and ASD values and uses reductions in objective value $S_{ll}(v,h,n)$ to decide iterations. Similar to coordinate descent in spirit, we define a fixed step for each variable to take in each iteration and choose the move with the largest potential gain among all possible moves.

The algorithm takes as inputs the sample overtaking vehicle parameters, θ, restricting factors, γ, a set of initial values of the truck platooning parameters, $R_0 = [v_0,h_0,n_0]$, minimum values of the platooning parameters, $R_{min} = [v_{min},h_{min},n_{min}]$, weights on platooning parameters, $w = [w_v,w_h,w_n]$, and the step sizes for adjusting platooning parameters, $\delta = [\Delta v,\Delta h,\Delta n]$. The algorithm output is a set of truck platooning parameters, v,h,n, on the given sample of overtaking vehicles and restricting traffic and road geometric factors.

Algorithm 3-1 PlatooningRules.

Input: $(\theta,\gamma,R_0,R_{min},\tau,cl,w,\delta)$; $R0 = [v_0,h_0,n_0]$; $Rmin = [vmin,hmin,nmin]$

$w = [w_v,w_h,w_n]$; $\delta = [\Delta v,\Delta h,\Delta n]$

Output: (v,h,n)

INITIALIZE:

$v \leftarrow v_0$; $h \leftarrow h_0$; $n \leftarrow n_0$

$S_{ll}(v,h,n) \leftarrow S(v,h,n) - z_{cl}\sqrt{\frac{S(v,h,n)(1-S(v,h,n))}{k}}$

$S(v,h,n) \leftarrow \frac{1}{k}\sum_{i=1}^{k} \mathbb{1}[PSD(\theta_i,\gamma,v,h,n) \leq ASD(\gamma,h)]$

FIND FEASIBLE SOLUTION OR SUGGEST NO PASSING:

while $S_{ll}(v,h,n) < \tau$:

$v_1 \leftarrow \max((v - \Delta v),v_{min})$ $h_1 \leftarrow \max((h - \Delta h),h_{min})$ $n_1 \leftarrow \max((n - \Delta n),n_{min})$

Calculate $S_{ll}(v_1,h,n),S_{ll}(v,h_1,n),S_{ll}(v,h,n_1)$

$S_{ll,v} \leftarrow w_v \cdot S_{ll}(v_1,h,n)$

$S_{ll,h} \leftarrow w_h \cdot S_{ll}(v,h_1,n)$ $S_{ll,n} \leftarrow w_n \cdot S_{ll}(v,h,n_1)$

if max$\{S_{ll,v},S_{ll,h},S_{ll,n}\} = S_{ll,v}$: $v \leftarrow v_1$
elif max$\{S_{ll,v},S_{ll,h},S_{ll,n}\} = S_{ll,h}$: $h \leftarrow h_1$
elif max$\{S_{ll,v},S_{ll,h},S_{ll,n}\} = S_{ll,n}$: $n \leftarrow n_1$
if $v < v_{min}$ AND $h < h_{min}$ AND $n < n_{min}$:
return NO PASSING
return v,h,n

The step sizes, $\delta = [\Delta v,\Delta h,\Delta n]$, in Algorithm 3-1 can be determined based on the precision of traffic management and vehicle control. To restrict speed and following gap, Δv and Δh can take values smaller than 1 with several decimal places. To restrict the number of trucks, only integers are possible for Δn. The weights on platooning parameters, $w = [w_v,w_h,w_n]$, in estimating S_{ll}, can be set to reflect the needs of a traffic management agency wishing to prioritize certain operational features. The weights can range between 0 and 1, with a smaller value indicating less restriction. For example, if an agency wants to prioritize operating speed and implement a relatively flexible restriction on that parameter, a smaller value can be assigned to w_v than the other two weights. In Algorithm 3-1, each weight is multiplied by the corresponding new S_{ll} values obtained from updating one of v,h,n, which has been proven effective in differentiating priorities on v,h,n, as shown in the simulation. Other ways to apply the weights, on $\Delta v,\Delta h,\Delta n$ or on $v-\Delta v,h-\Delta h,n-\Delta n$, are not applied because they fail to differentiate priorities on v,h,n in the simulation, leading to a result where only changes in n affect S_{ll}. An alternative method of applying weights is to define weights as the probabilities of selecting one of v,h,n as the descent direction; so, for example, a $(w_v = 0.5,w_h = 0.3,w_n = 0.2)$ setup means that the probabilities of selecting v,h,n as the descent direction are 0.5, 0.3, and 0.2, respectively. However, the probabilistic weighting method is not used in Algorithm 3-1 because it makes the algorithm random.

3.4.2 Complexity

In the worst case, Algorithm 3-1 returns No Passing, with the initial values of v,h,n having to reduce to their corresponding minimum values by step sizes $\Delta v,\Delta h,\Delta n$, respectively. The time taken is: $T_v = (v_0 - v_{min})/\Delta v$, $T_h = (h_0 - h_{min})/\Delta h$, and $T_n = (n_0 - n_{min})/\Delta n$, respectively. Therefore, the "while" loop would take max$\{T_v,T_h,T_n\}$. The ASD-PSD calculation costs different amounts of time depending on the specific mathematical models implemented. In the models used in our simulation, the calculation of PSD for a trailing vehicle involves 43 operations, and the calculation of ASD for a road segment involves 140 operations. For a given road segment and a sample of k trailing vehicles, the number of operations taken to calculate an S_{ll} is $(43k + 140)$. Therefore, the worst-case runtime of Algorithm 3-1 is $T(k) = \max\{T_v,T_h,T_n\}(43k + 140) = O(k)$. Linear time is good enough for a variable regulatory system using real-time traffic data. Similar to a VSL system, the most frequent update of regulatory information is once every few minutes, and in practice, truck platooning operating rules should not be expected to change as frequently.

3.4.3 Sensitivity

Assume that in the current traffic, vehicles' parameters (for overtaking modeling) follow a distribution D. True proportion of vehicles with PSD ≤ ASD, $E_D S(v,h,n)$ can be thought of as:

$$E_D S(v,h,n) = E_D 1[\text{PSD}(\theta,\gamma,v,h,n) \leq \text{ASD}(\gamma,h)] = P_D(\text{PSD}(\theta,\gamma,v,h,n) \leq \text{ASD}(\gamma,h)) \quad [3\text{-}5]$$

Thus, the sensitivity of $E_D S(v,h,n)$ with respect to, for example, changes in v, denoted Δv can be thought of as:

$$E_D S(v + \Delta v,h,n) = P_D(\text{PSD}(\theta,\gamma,v + \Delta v,h,n) \leq \text{ASD}(\gamma,h)) \quad [3\text{-}6]$$

For fixed γ,h, ASD(γ,h) is a constant. Thus, a change in the above two probabilities when PSD is evaluated at $v + \Delta v$ and v, respectively, is decided by changes in PSD and changes in the distribution function. If we approximate changes in PSD with respect to Δv by a multiplicative factor $r(v)$, which can be decided by taking derivative of function for PSD and evaluating at v:

$$\frac{\text{PSD}(\theta,\gamma,v,h,n)}{\Delta v,h,n)} \approx r(v) \quad [3\text{-}7]$$

The changes in probability mass [3-6] can be written as:

$$P_D(\text{PSD}(\theta,\gamma,v + \Delta v,h,n) \leq \text{ASD}(\gamma,h)) \approx P_D(\text{PSD}(\theta,\gamma,v,h,n) \leq r(v) \cdot \text{ASD}(\gamma,h)) \quad [3\text{-}8]$$

Thus, the increase in $ES(v,h,n)$ can be written as:

$$ES(v + \Delta v,h,n) - ES(v,h,n) = P_D(\text{PSD}(\theta,\gamma,v,h,n) \leq r(v) \cdot \text{ASD}(\gamma,h)) - P_D(\text{PSD}(\theta,\gamma,v,h,n) \leq \text{ASD}(\gamma,h)) \quad [3\text{-}9]$$

Note that this increase is dependent on distribution D of θ from here on. To be more exact, how much density of this distribution is between ASD and $r(v)$·ASD. **Figure 7** shows an illustration of two densities of PSD values under the same distribution but evaluated at v and $v + \Delta v$, respectively. We note the same style of analysis applies to changes in n and h.

In some cases, if the distribution of current traffic and a vehicle's parameters follow a specific parametric form, its density function can be assumed to be Lipschitz with constant L_D, with respect to PSD values. For example, Lipschitz constant for Gaussian densities can be calculated. Then the changes in $ES(v,h,n)$ can be succinctly expressed as:

$$ES(v + \Delta v,h,n) - ES(v,h,n) \approx LD(r(v) \cdot \text{ASD} - \text{ASD}) \quad [3\text{-}10]$$

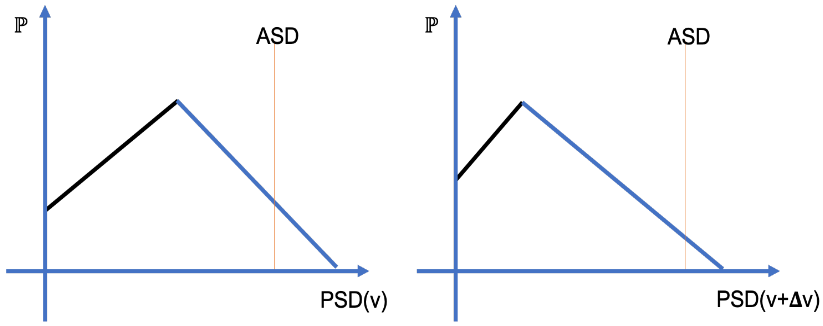

Figure 7: An illustration of two densities of PSD, evaluated at v and v +Δv, respectively: In density of PSD(v + Δv), less probability densities are on the right side of fixed ASD value

3.5 Simulation

To assess Algorithm 3-1, we carry out simulation analysis with a large sample of overtaking vehicles, with parameters θ generated based on the distributions shown in **Table 5** and **Table 6**. We run 10 simulations, each with a pseudo-random sample consisting of 10,000 vehicles. Integer random seeds of 1, 2, ..., 10 are used. We consider various vehicle lengths, initial speeds, accelerations, desired overtaking speeds, longitudinal displacements in lane change, and starting and ending following gaps. The overtaking decision is determined by a conditional probability based on the speed difference between the overtaking vehicle and the platoon. The conditional probability distribution is from (*110*).

We first assess how sensitive the safety ratio is to the change in input variables v,h,n in Algorithm 3-1. By varying one of the three input variables v,h,n while holding the other two constant, we can observe how many steps it takes for each of them to reach the target. The second aspect of the assessment is the effects of target safety guarantee, τ, in which we are interested in knowing the maximum τ that can be reached, and how platoon operational rules change to achieve the targets for the given data sample. The third aspect of the assessment is to see how the restricting factors in γ affect the platoon operational rule output.

The initial values of the platoon operational parameters v_0,h_0,n_0 are set to 27 m/s (60.4 mph), 30 m (98.4 ft), and 10 trucks. The reduction step sizes $\Delta v,\Delta h,\Delta n$ are set to 0.45 m/s (1 mph), 0.3 m (0.98 ft), and 1 truck, respectively. The minimum values v_{min},h_{min},n_{min} are 18 m/s (40.3 mph), 13.2 m (43.3 ft), and 2 trucks, respectively. The one-sided confidence level, *cl*, is set to 0.975. The detailed models and other assumed values for calculating ASD and PSD are listed in **Table 21** in the Appendices.

Table 5: Overtaking Vehicle Parameters

Parameter	Distribution	Source
Vehicle length (m): L_A	Normal: mean = 5.5; s.d. = 0.56	[64]
Initial speed (m/s): $v_A0 = c \cdot v_B$	c: Lognormal: mean = 1.08; s.d. = 0.04	[65]
Acceleration (m/s^2): a_x	Lognormal: mean = 1.31; s.d. = 0.68	[65]
Desired speed (m/s): $vAmax = vA0 + f \cdot ax$	f: Lognormal: mean = 2.8; s.d. = 0.1	[65]
Following gaps (m): hA, hB	h_A: Normal: mean = 7.5; s.d. = 3.7 h_B: Normal: mean = 21.2; s.d. = 8.2	[65]
Lane change longitudinal displacements (m): xeL, xeR	Normal: mean = 100; s.d. = 35	[66]
Overtaking decision d_A:	Conditional probability	[63]

Table 6: Overtaking Decision Probability Distribution

Decision: d_A	Speed Difference: $v_A - v_B$ (m/s)					
	(-∞, -1.67]	(-1.67, -0.83]	(-0.83, 0]	(0, 0.83]	(0.83, 1.67]	(1.67, ∞)
1 = yes	0.17	0.47	0.64	0.93	0.95	1.00
0 = no	0.83	0.53	0.36	0.07	0.05	0.00

Source: (*110*).

3.5.1 Sensitivity of S_{ll} to (v,h,n)

We know that the overtaking safety ratio must be negatively correlated with each of (v,h,n), based on intuition and the mathematical model framework (**Figure 3-1**). We can validate that statement by running the simulation with one of the parameters (v,h,n) varying and the other two parameters fixed. Simulations are run with the assumed parameters and distributions in **Tables 3-2, 3-3, and 8-1**, with varying τ. In each iteration of the algorithm, we keep track of how much the lower limit of safety ratio S_{ll} increased and plotted the results, as shown in **Figure 3-3**. Mean values of S_{ll} at each step of (v,h,n) change are plotted, with τ varying from 0.5 to 0.9 and increasing by 0.05. Note that the standard error of S_{ll} at each step, from the 10 simulation results, ranges from 0.09 to 0.19, so the confidence intervals are very small considering the magnitude of S_{ll} and are omitted from the plots. The varying line widths do not indicate confidence intervals but are used to avoid total overlapping between lines.

We observe that S_{ll} is not as sensitive to the change in v or h in the simulation when the other parameters are fixed (i.e., with weight = 0). Neither descending only on v nor on h can help S_{ll} reach the target τ. On the other hand, n affects S_{ll} significantly when the weights are set to $w_v = w_h = 0, w_n = 1$, as shown in **Figure 8** (a). Under a different preset τ, as n decreases, S_{ll} increases.

We adjust the weights to $w_v = w_h = 1, w_n = 0.6$, to investigate how the descent on v,h,n works together to reach the target τ. **Figure 8** (b), (c), and (d) show the curves of S_{ll} vs. n,v and h. We observe that as n is given a smaller weight, it is kept at the initial value 10, initially, with descent in h contributing to the increase in S_{ll}, then v, then at the final stage, n. The pattern is recognized by observing the density of plotted round dots in **Figure 8** (b), (c), and (d). Each dot represents an S_{ll} value obtained at each iteration.

We adjust the weights to $w_v = w_h = 1, w_n = 0.6$, to investigate how the descent on v, h, n works together to reach the target τ. **Figure 8** (b), (c), and (d) show the curves of S_{ll} vs. n, v and h. We observe that as n is given a smaller weight, it is kept at the initial value 10, initially, with descent in h contributing to the increase in S_{ll}, then v, then at the final stage, n. The pattern is recognized by observing the density of plotted round dots in **Figure 8** (b), (c), and (d). Each dot represents an S_{ll} value obtained at each iteration.

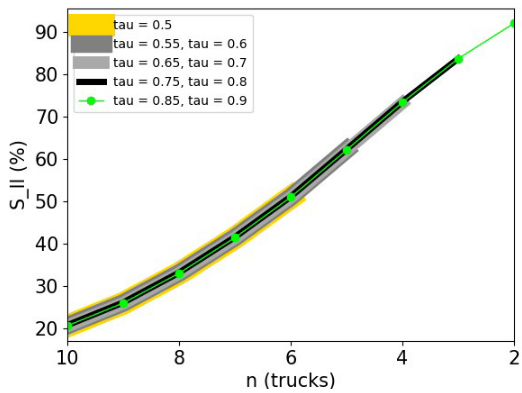

(a)

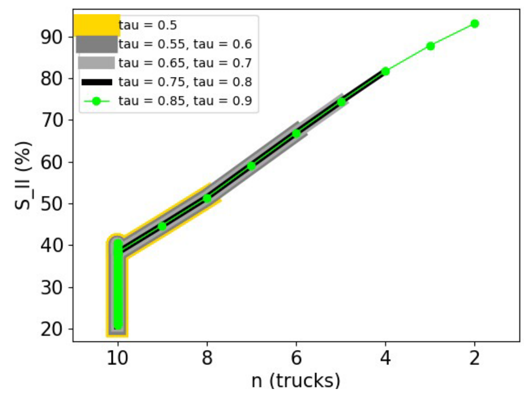

(b)

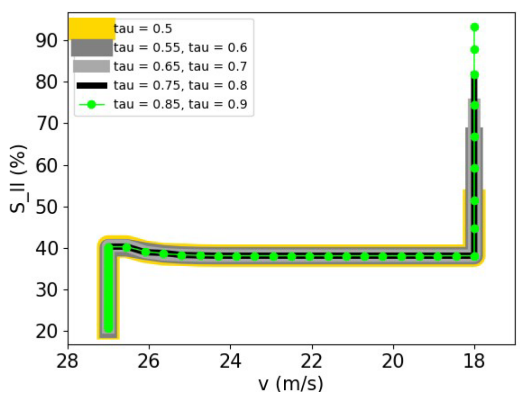

(c)

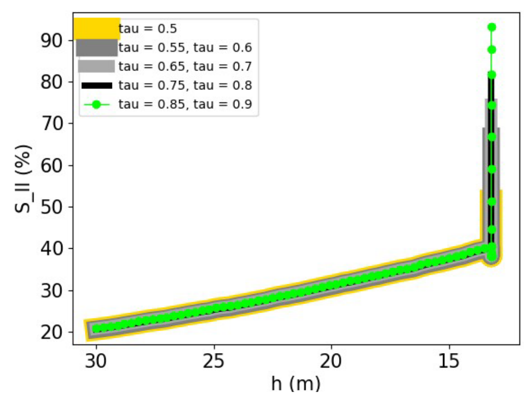

(d)

Figure 8. Change in the lower limit of safety ratio, S_{ll}, with: (a) number of trucks, n (weights $w_v = w_h = 0, w_n = 1$). (b) number of trucks, n (weights $w_v = w_h = 1, w_n = 0.6$). (c) speed, v (weights $w_v = w_h = 1, w_n = 0.6$). (d) following gap, h (weights $w_v = w_h = 1, w_n = 0.6$).

3.5.2 Effects of Target Safety Guarantee, τ

We wanted to evaluate, given the 10,000-vehicle sample in the simulation, how large a safety ratio we can guarantee. Thus, we vary the τ input from 50% to 100% and run the simulation with two sets of weights: $(w_v = w_h = w_n = 1)$ and $(w_v = w_h = 1, w_n = 0.6)$. The roadway conditions are set to: $q = 30$, $R = 999{,}999$, $L = 0$, $A = 0$, and $G = 0$, which describe a straight and flat segment with sparse opposing traffic. The results are shown in **Figure 9** (a) and (b), respectively. We found that the maximum safety ratio S_{ll} that we can reach is around 93% for both cases. With equal weights, as τ increases, n decreases to obtain a desired S_{ll}, but v and h do not contribute much until τ is over 90% and n is at its minimum of 2. With a smaller weight on n, we are discouraging the reduction in number of trucks; therefore, we observe in **Figure 9** (b) that n is kept at higher numbers while v and h decrease from the beginning to obtain the desired S_{ll}. However, for a τ as high as 90%, n has to be limited to 2 to provide enough safety guarantee.

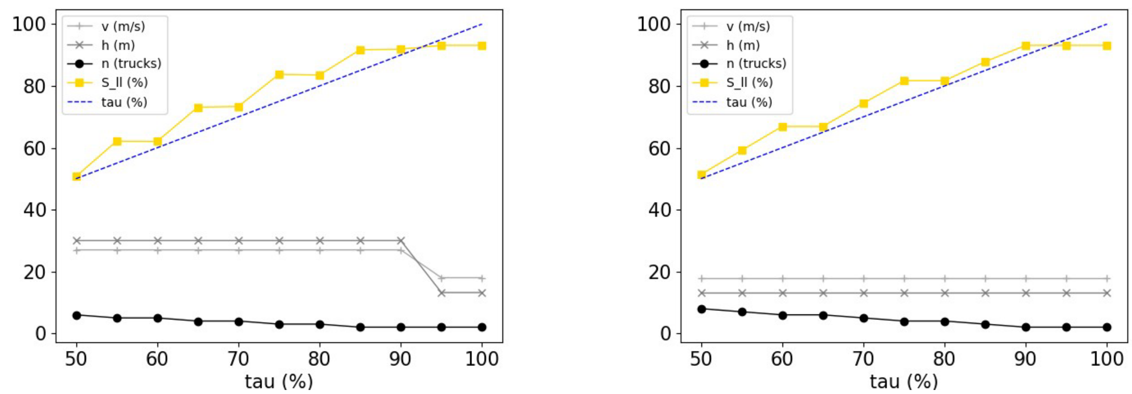

(a) (b)

Figure 9: Change in platooning rules and the estimated lower limit of safety ratio, S_{ll} (%), with the preset safety guarantee, τ. Weights: (a) $w_v = w_h = w_n = 1$. (b) $w_v = w_h = 1, w_n = 0.6$.

3.5.3 Effects of Restricting Factors in γ

We are also interested in how the restricting factors in γ affect the output truck platooning rules. Thus, we vary the inputs' traffic flow, q, horizontal curve radius, R, crest vertical curve grade difference, A, and uphill grade, G, in the simulations, and observe the results. The target safety guarantee, τ, is set to 75%. As the sample size of 10,000 vehicles is large, the same results are obtained from the 10 simulation runs.

Traffic Flow: The simulations of platooning rule determination with varying traffic flow, q on the opposite direction is done by keeping the other input parameters in γ constant. The road geometric features are set to: $R = 999{,}999$, $L = 0$, $A = 0$, and $G = 0$. Simulation results are shown in **Figure 10** (a) and (b), for equal weights and ($w_v = w_h = 1, w_n = 0.6$), respectively. As shown in **Figure 10** (a), starting with a flow of 10 veh/h, Algorithm 3-1 determines that to guarantee the safety of 75% of overtaking vehicles, n should be limited to 4, while v and h can be kept at the initial values of 27 m/s (60.4 mph) and 30 m (98.4 ft). We can observe that the actual safety ratio, S_{ll}, that can be achieved by this feasible solution is 79.4%. With q increasing, n decreases further and reaches the minimum value of 2 at q = 50 veh/h. The safety guarantee fluctuates but stays above the target of τ = 75%. Once q exceeds 50 veh/h, the target τ cannot be achieved.

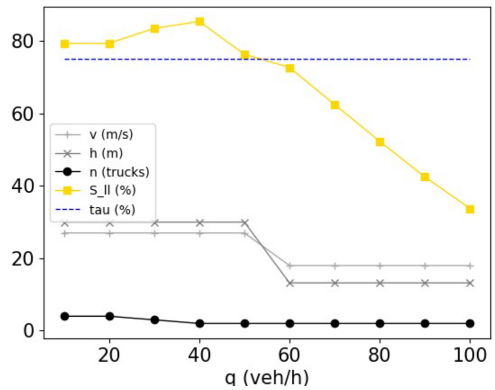

(a)

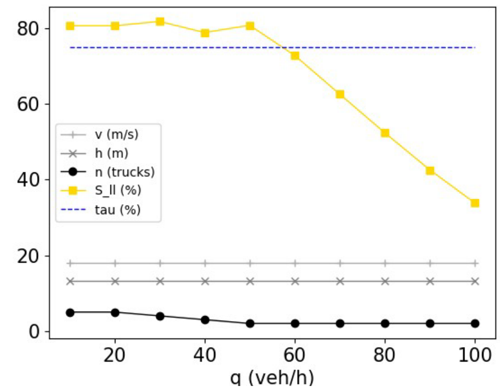

(b)

Figure 10: Change in platooning rules and the estimated lower limit of safety ratio, S_{ll}, with the opposite direction traffic flow rate, q. Weights: (a) $w_v = w_h = w_n = 1$. (b) $w_v = w_h = 1, w_n = 0.6$.

Horizontal Curve: To assess the effects of horizontal curves on platooning rules, traffic flow is kept at 30 veh/h in the simulations, and *L, A, G* are kept at 0. We can observe from the results, as plotted in **Figure 11** (a) and (b), that the target safety guarantee cannot be achieved until curve radius reaches 200 km (124 mi). As shown in **Figure 11** (a), at 200 km horizontal curve radius, Algorithm 3-1 determines that a maximum *v* of 27 m/s (60.4 mph), *h* of 15.9 m (52.2 ft), and *n* of 2 would guarantee at least 75.06% of overtaking vehicles to be safe. As curve radius increases, the output *h* increases and reaches the initial value of 30 m at curve radius of 250 km (155.3 mi). The output *n* stays at 2 throughout the change in curve radius from 100 km (62.1 mi) to 300 km (186.4 mi). The safety guarantee increases as curve radius increases, reaching 78.95% at 300 km. When weights ($w_v = w_h = 1$, $w_n = 0.6$) are applied, as shown in **Figure 11** (b), the outputs *v,h,n* are restricted to 18 m/s, 13.2 m, and 2 trucks.

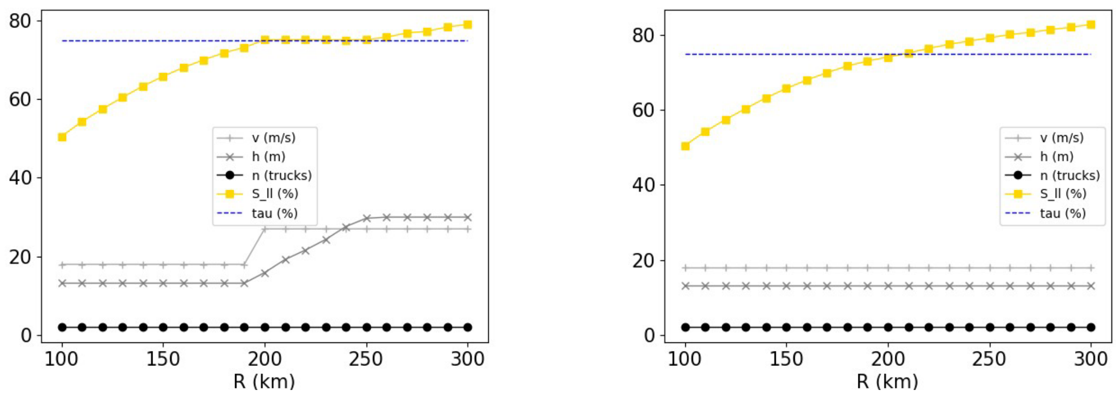

(a) (b)

Figure 11: Change in platooning rules and the estimated lower limit of safety ratio, S_{ll}, with the horizontal curve radius, R. Weights: (a) $w_v = w_h = w_n = 1$. (b) $w_v = w_h = 1, w_n = 0.6$.

Crest Vertical Curve: Crest vertical curve is controlled by two parameters, L and A. In the simulations, L is kept constant at 1,609 m (1 mi), with A varying from 0 to 0.6%. All other parameters were kept constant, with $q = 30$, $R = 999{,}999$, and $G = 0$. The simulation results, as shown in **Figure 12** (a) and (b), suggest that a crest vertical curve with $A > 0.3\%$ will result in a restriction on overtaking of any truck platoon. **Figure 12** (a) shows that, when using Algorithm 3-1, with A between 0% and 0.15%, n should be limited to 3 to reach a safety guarantee of 75%, but $v = 27$ m/s and $h = 30$ m do not need to change. From $A = 0.15\%$ to 0.4%, n starts to be further restricted, followed by the reduction in allowed operating speed and desired following gap. **Figure 12** (b) shows that when weights ($w_v = w_h = 1, w_n = 0.6$) are applied, v and h are restricted to 18 m/s and 13.2 m. When A is between 0% and 0.15%, n can be as large as 4, but further restricted to smaller numbers as A increases. Once A is larger than 0.3%, S_{ll} falls below 75%.

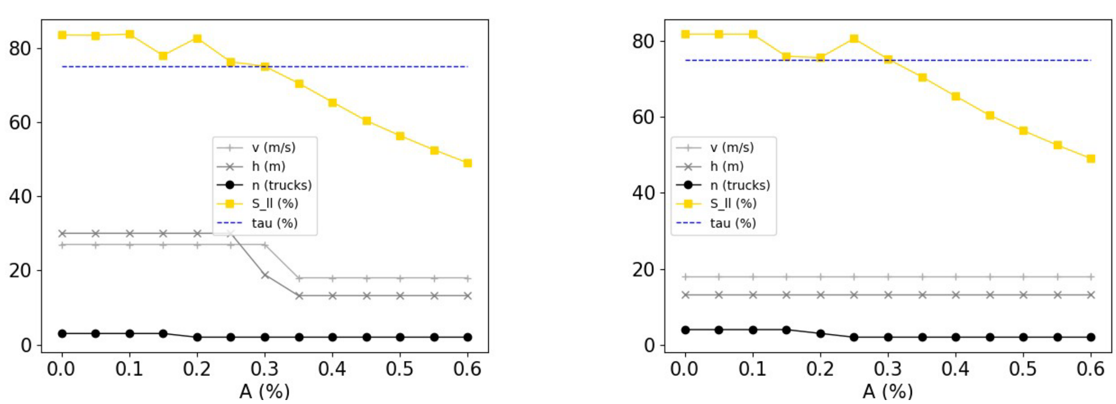

(a) (b)

Figure 12: Change in platooning rules and the estimated lower limit of safety ratio, S_{ll}, with the vertical curve grade difference, A. Weights: (a) $w_v = w_h = w_n = 1$. (b) $w_v = w_h = 1, w_n = 0.6$.

Uphill Grade: Uphill grade varies from 0% to 20% in the simulations. Other parameters are kept constant with q = 30, R = 999,999, and L and A both set to 0. Results shown in **Figure 13** (a) indicate that Algorithm 3-1, with equal weights, determines that v and h can stay at the initial values of 27 m/s and 30 m, but n should be restricted to 3. The safety guarantee stays above 80% within the simulated range of uphill grade. When weights ($w_v = w_h = 1, w_n = 0.6$) are applied, as shown in **Figure 13** (b), n can be as high as 4 when the uphill grade is below 15%. Operating speed, v, is restricted to 18 m/s and does not change as the grade increases. The following gap, h, can be restricted to 13.2 m when grade is less than 8%, but it cannot hold to that value as it increases due to the increasing uphill grade and the limited truck acceleration capability. The safety guarantee is maintained above 75% by compensating for the increasing following gap with a decreased n.

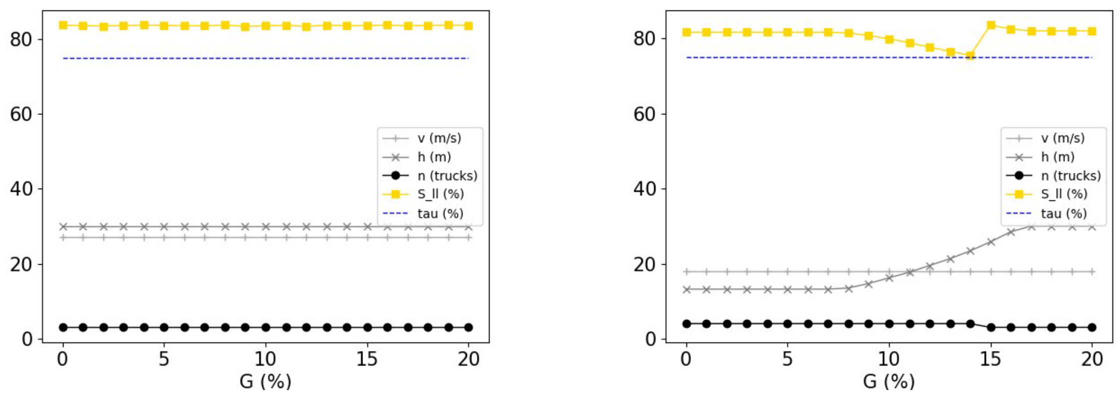

(a) (b)

Figure 13: Change in platooning rules and the estimated lower limit of safety ratio, S_{ll}, with the uphill grade, G. Weights: (a) $w_v = w_h = w_n = 1$. (b) $w_v = w_h = 1, w_n = 0.6$.

Combined Effects: The combined effects of restricting factors on the platooning rule output is determined by the strictest restriction, as we are essentially looking for an upper bound of the truck platooning parameters. For example, when we have a traffic flow that is high enough to restrict the platooning parameters more than the horizontal curve radius, traffic flow would become the determining factor for the output.

3.6 Section Conclusion

We proposed an algorithm to determine operational rules for truck platooning on two-lane undivided highways, considering overtaking safety. Based on existing models of vehicle dynamics and driver sight distance in overtaking scenarios, we constructed a framework that describes the relationship between truck platoon operational parameters and traffic and roadway geometric factors. The core component of the framework is comparing PSD and ASD. If ASD cannot satisfy the needed PSD, safe overtaking then cannot be achieved. Based on existing models, truck platooning parameters, operating speed, and length affect PSD, along with overtaking vehicle's physical and behavioral parameters. ASD is affected by traffic flow and horizontal and vertical curves. In addition, truck platooning parameters are directly related to posted speed limit and uphill grade.

We formulated the problem of guaranteeing overtaking safety of truck platoons on two-lane highways as a feasibility problem. By solving the problem, we look for a set of operational parameters for truck platooning, v,h,n, which would guarantee a desired percentage of trailing non-platoon vehicles can safely overtake or continue following the platoons. To find feasible solutions, the algorithm employs a method similar to coordinate descent, which runs iteratively along the dimensions of the three operational parameters. The output can be a feasible solution, or a recommendation to forbid overtaking, depending on the input of traffic and roadway geometric factors, and the trailing vehicles' physical and behavioral parameters.

The algorithm has a running time of O(k), where k is the input vehicle sample size, showing that it can provide a performance similar to a typical VSL system with an update frequency of once in several minutes. In terms of safety guarantee, the simulation assessment shows that given a straight, flat two-lane highway with sparse traffic, the algorithm can generate platooning rules that guarantee up to 93% of trailing vehicles' overtaking safety. Among the input truck platooning parameters, v,h,n, we found that n affects the safety guarantee most significantly. By comparing the results obtained from applying equal and unequal weights on v,h,n, we found that lower-weight parameters receive less restrictions and are kept at higher values until they are required to contribute to the increase of safety guarantee.

From the applications perspective, the iterative algorithm can be used to generate variable platooning rules to be displayed or broadcast to truck platoons on segments of two-lane highways. Surrounding vehicles' physical and behavioral parameters can be collected in real time by roadside sensors or mobile sensors on trucks and transmitted to a traffic management center, where platooning rules are determined and quickly updated by the iterative algorithm. For future research, the algorithm can be improved by incorporating more restrictive factors that are likely to affect truck platooning operations and surrounding traffic safety such as weather. Efforts can also be put into calibrating sets of weights for the weighted rule-determining algorithm, to meet specific management needs. The current algorithm, under the assumption that HDVs overtake platoons in one take, tends to suggest small platoon sizes, n. A future research effort can focus on investigating if coordinated driving behavior and improved ASD-PSD models can lead to a larger n. The scope of this section is limited to overtaking safety on two-lane highways. To expand the scope and make the algorithm more comprehensive, we can identify and incorporate other potentially risky interactions between human drivers and truck platoons by collecting data using driving simulation.

4. EVALUATING TRUCK PLATOONING RULES FOR TWO-LANE HIGHWAY OPERATIONS

4.1 Introduction

This section presents a study evaluating truck platooning rules on a segment of U.S. Highway 287 in Wyoming using microscopic traffic simulation. The segment is between the U.S. 287 junction with Interstate 80 in Laramie, Wyoming, to the state border of Wyoming and Colorado, a corridor of strategic importance to freight transportation within the state. This segment was chosen because of its unique blend of rural highway attributes, a multilane divided highway alongside a two-lane undivided highway. The two-lane undivided segment of the roadway offers an optimal setting for assessing the impacts of potential implementations of regulations for overtaking the truck platoon by HDVs in a mixed traffic scenario.

The assumptions made in this analysis are as follows:

- As this part of the project concentrates only on traffic interactions and the effects of platooning, dry and sunny weather conditions were assumed. The impact of weather changes was not considered in the simulations.
- To reflect a realistic close following gap in platooning operation through CACC and V2V communication, an aggressive driving behavior with a 0.6-second following gap was used for the platooned trucks in PTV VISSIM simulations.
- In order to simulate typical mixed-traffic behavior without adding needless complexity, standard car-following and lane-changing models built in VISSIM were applied to HDVs.
- To simplify the analysis and to compare the pure effects of platooning regulations, the segment used for this part of the project was considered as a long continuous roadway. Merging lane scenarios were not considered.

The objective was to evaluate the network operation performance and safety impacts of truck platooning regulations application on Wyoming's rural two-lane undivided highways, with the consideration for overtaking maneuvers by HDVs in mixed-traffic environments. To achieve this goal, the following objectives were defined:

- Develop a microsimulation model of U.S. Highway 287 using real-world geometric and traffic data
- Implement and evaluate truck platooning regulations derived from Song's (*113*) stochastic approximation-based algorithm
- Analyze the network-level performance by microsimulation PTV VISSIM software with varying traffic demands and truck compositions scenarios
- Evaluate safety implications using surrogate safety assessment modeling
- Conduct statistical modeling to quantify factor significance and variable interactions on operation performance and safety assessment
- Contribute to optimizing truck platooning performance and safety on rural highways by providing a foundation for evidence-based policy development and future field testing in Wyoming

4.2 Methodology

4.2.1 Network

The study area selected for the simulation is a segment of U.S. Highway 287, starting from the Wyoming-Colorado state border to the I-80 and U.S. 287 interchange near the 3rd Street intersection in Laramie, Wyoming. This pathway was chosen because of its unique blend of rural highway attributes and being multilane divided highway alongside a two-lane undivided highway. The length of this U.S. 287 segment is around 25 miles, starting from milepost 401 to ending at milepost 425, as shown in **Figure 14**. Each of the two different corridor types (multilane divided and two-lane undivided) constitutes roughly 50% of the total segment length, making it an ideal location for analyzing corridor type impact on traffic flow and safety for overtaking truck platoons by HDVs.

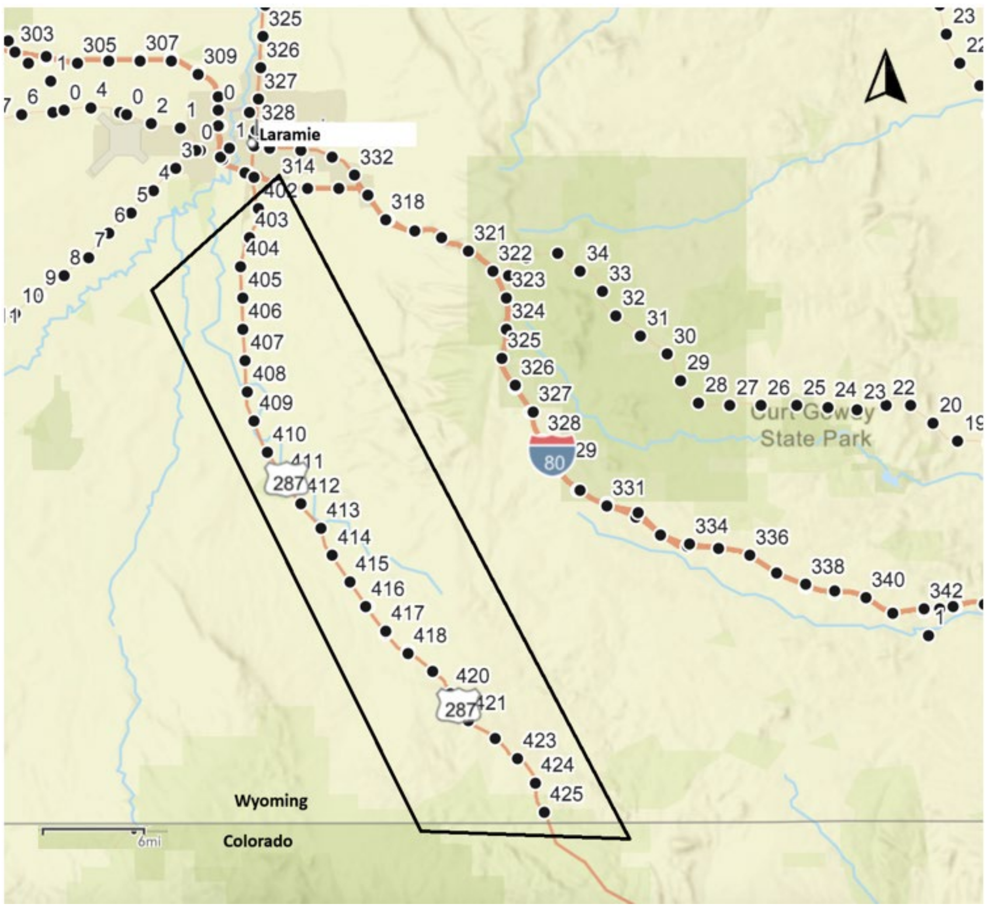

Figure 14: Study location: Map of U.S. 287 roadway segment (study area shown in black outline)

4.2.2 Data Collection

Data were collected from multiple sources, including the Wyoming Department of Transportation (WYDOT), Google Earth, and Google Street Map. The roadway geometry data such as horizontal curve radius, vertical curvature, elevation, grades, and geographic coordinates (latitude and longitude) were collected from WYDOT's roadway inventory databases. Additional roadway information such as the number of lanes, posted speed limits, and classification of roadway sections (i.e., multilane divided highways and two-lane undivided segments) was extracted through visual assessment using Google Earth and Google Street View imagery. Traffic-related data, including average annual daily traffic (AADT) volumes, vehicle speed distributions, and AADT disaggregated by vehicle type, were obtained from WYDOT. For the traffic volumes, the April 2024 Monthly Hourly Volume Report, publicly available data from WYDOT, was utilized. Collectively, the integration of geometric, traffic, and roadway classification data from these diverse sources ensured a robust and comprehensive dataset to support the study's analytical objectives.

By using the roadway geometry data together with geographic coordinates information obtained from WYDOT, the following maps (**Figure 15**, **Figure 16**, and **Figure 17**) were created for identifying the location and value ranges of horizontal curves, grades, and crest vertical curves by using the ArcGIS.

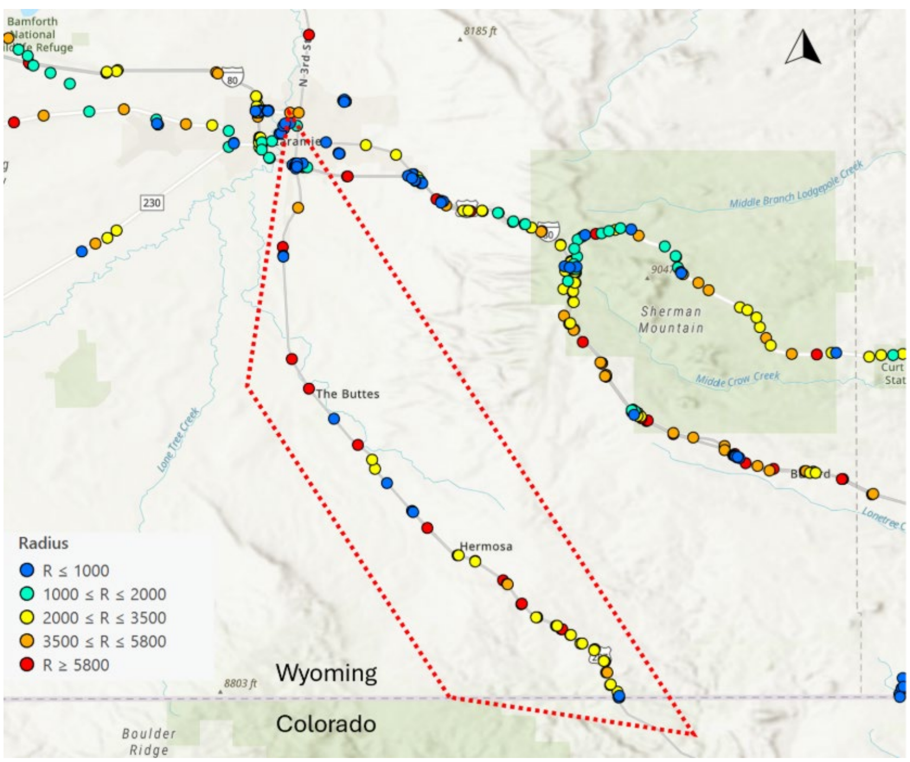

Figure 15: Map of horizontal curves locations along the study corridor (study area shown in red dotted outline)

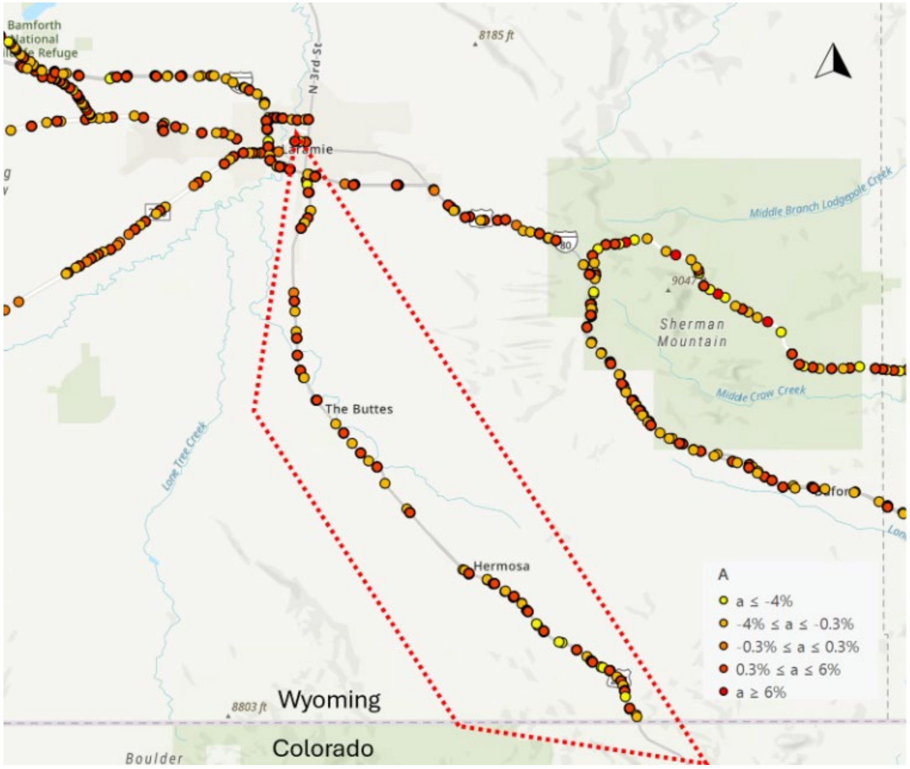

Figure 16: Map of vertical curves (crest/sag) locations along the study corridor (study area shown in red dotted outline)

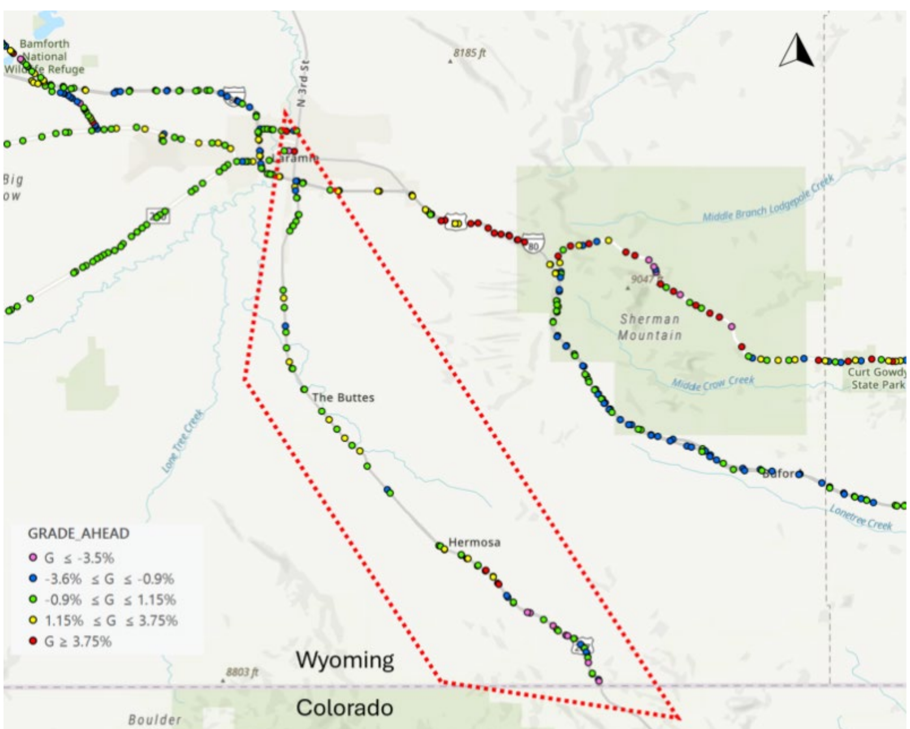

Figure 17: Map of grade ahead locations along the study corridor (study area shown in red dotted outline).

4.2.3 Algorithm and Model Setup

By using the roadway geometry data, truck platooning operation rules were established to the required sections of the roadway. The assigned operational rules for truck platoon were implemented based on the stochastic approximation-based algorithm developed by Song (*113*). Song's algorithm provides a systematic method to determine the platooning parameters that maintain overtaking safety on a two-lane undivided highway. The core component of the stochastic model framework, introduced by Song (*113*), was comparing passing sight distance (PSD) and available sight distance (ASD) to ensure overtaking safety. Song's algorithm was designed to determine the operational rules for truck platooning, considering factors such as horizontal and vertical curvature, uphill grade, traffic flow, vehicle dynamics, and the safety threshold for overtaking. The algorithm's simulations generated platooning regulation guidelines for two-lane undivided highways, focusing on overtaking safety, in terms of three key parameters: 1) the operating speed of the truck platoon, 2) the inter-truck following gap in the truck platoon, and 3) the number of trucks in the platoon.

Only the number of trucks in the platoon was set as a variable parameter for platoon regulations in the simulation. Values of the other two parameters (speed and following) were pre-determined for this part of the project. The operating speed of the truck platoon is limited to a range that is practically operable, considering the posted speed limits along the roadway segments. Similarly, the inter-truck following gap in the truck platoon was also set into a fixed gap of 0.6 seconds, matching the assumption of the VISSIM simulation model for aggressive automated vehicles in driving behavior settings.

By using the WYDOT data for restricting factors such as horizontal and vertical curvature, uphill grade, traffic flow, and posted speed limit, Song's algorithm (*113*) was used to reference an approximate representation of the recommended truck platooning rules for the minimum number of trucks in the platoon. To maintain methodological consistency and to reflect CACC capability, Song's algorithm was executed exactly as described in (*113*)–except that a modification of using the operating speed of the truck platoon with respects to the posted speed limit along the study segment of U.S. 287 and fixed inter-truck following gap parameter of 0.6s instead of around 1s–is used in the published results. The algorithm generated platooning rules were then applied to respective sections of the roadway.

The length of each section along the roadway segment to assign different platooning regulations was determined to be one mile through detailed calculations that considered the inter-vehicle following gaps within the platoon, the length of the vehicles, the operating speed, and the distance required for the platoon to adjust its operational parameters when assigned rules were changed.

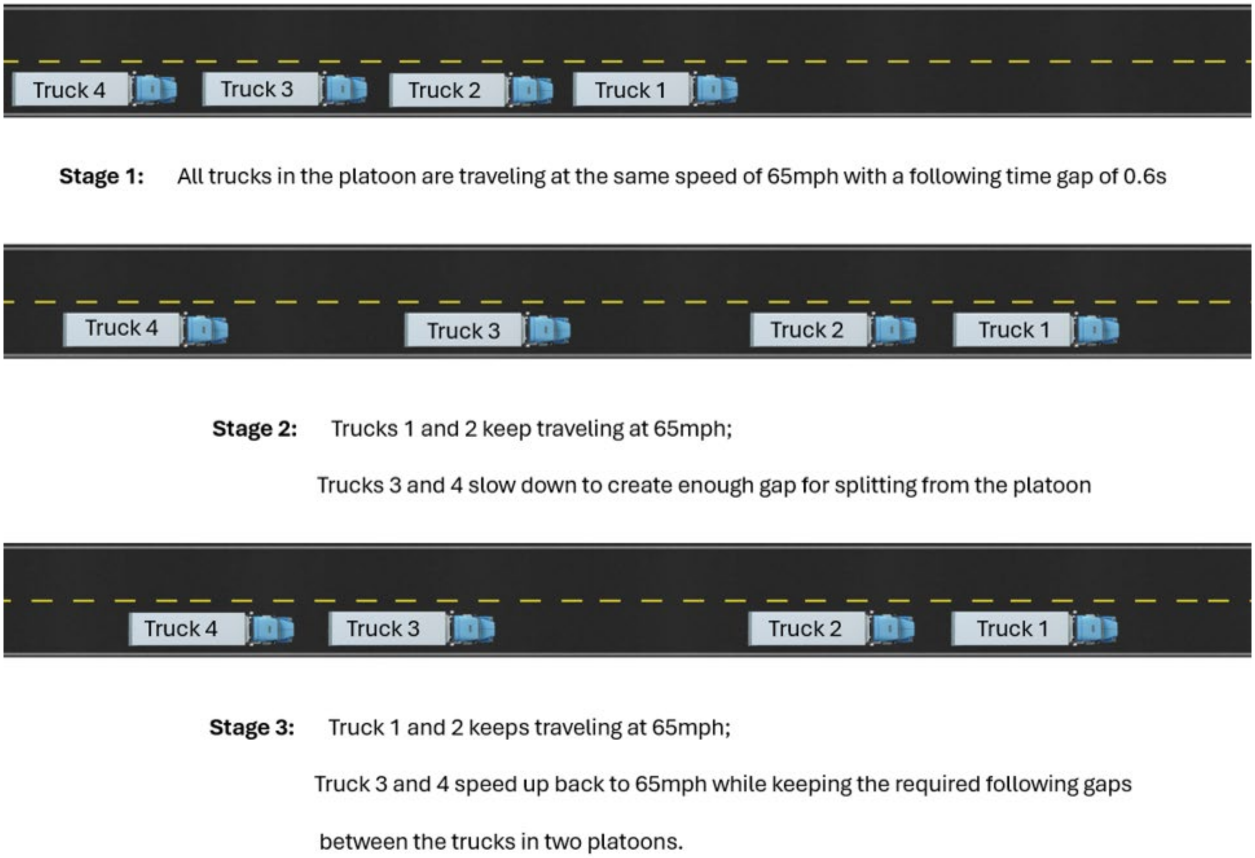

Figure 18: Three stages of truck platooning splitting procedure (when the platoon operating speed is 65 mph)

As shown in **Table 6**, different regulations on the maximum allowable numbers of trucks to form a platoon were assigned to each section of the roadway based on the algorithm guidelines. However, to maintain consistency in comparing multiple simulation scenarios with various traffic input levels, the strictest regulation was picked from all the restricting factors. Therefore, the lowest number of trucks (n=2) was assigned for nearly all two-way undivided highway sections, except for a few sections where the overtaking safety ratio dropped below 75%, and the no-overtaking rule was applied. When the platoons enter the sections, assigned with different platooning rules than they were traveling with before, they will adjust by splitting into smaller platoons or by merging two or more platoons into one. According to the PTV VISSIM 2024 Manual (*114*), platoon splitting in a VISSIM simulation model occurs by the speed adjustments of the leaving vehicle and its following vehicles. An example procedure of the platoon splitting steps is shown in **Figure 18**.

The number of trucks on the multilane segments of the highways were not restricted with the algorithm generated platoon regulations as HDVs can overtake the platoons via adjacent lanes (*115*). Restrictions were applied only in the two-lane undivided sections of the highway as overtaking on those sections amplify hazardous risks for the passing vehicles where they must share the same lane with the opposing traffic (*74*, *97*, *116*, *117*), (*118*). To compare the effects of having restrictions on the maximum number of trucks allowed to form a platoon on two-lane undivided highway segments, two model groups (A and B) were set up differently on the two-lane undivided highway segments as follows:

- Group A (with regulations): the maximum number of trucks allowed to form a platoon on two-lane undivided highway segments were restricted according to algorithm-generated values
- Group B (without regulations): the maximum number of trucks allowed to form a platoon on two-lane undivided highway segments were not restricted according to algorithm-generated values

Therefore, in this project, the platoon regulation assigned means having a restriction on the maximum number of trucks allowed to form a platoon on two-lane undivided highway segments according to algorithm-generated values. The maximum number of allowed trucks to form a platoon for the U.S. 287 two-lane undivided highway segments are shown in **Table 7**.

Table 7: Platoon Regulations Assigned to each Section of U.S. 287 (Group A vs. Group B)

Sections	Milepost Startpoint	Milepost Endpoint	Horizontal Curve R	Uphill Grade G	Crest Vertical Curve A	Roadway Type	Platooning Regulations of Group A (Maximum allowed number of trucks in a platoon)	Platooning Regulations of Group B (Maximum allowed number of trucks in a platoon)
1	402	403				Multilane	8	8
2	403	404				Multilane	8	8
3	404	405	☑	☑	☑	Two-Lane Undivided	8	8
4	405	406	☑	☑	✗	Two-Lane Undivided	No Overtaking Zone	No Overtaking Zone
5	406	407	☑	☑	✗	Two-Lane Undivided	2	8
6	407	408	☑	☑	✗	Two-Lane Undivided	2	8
7	408	409	✗	☑	☑	Two-Lane Undivided	2	8
8	409	410	✗	☑	☑	Two-Lane Undivided	2	8
9	410	411	☑	☑	✗	Two-Lane Undivided	2	8
10	411	412	☑	✗	✗	Two-Lane Undivided	2	8
11	412	413	✗	✗	✗	Two-Lane Undivided	No Overtaking Zone	No Overtaking Zone
12	413	414	✗	☑	☑	Two-Lane Undivided	No Overtaking Zone	No Overtaking Zone
13	414	415	☑	✗	✗	Two-Lane Undivided	No Overtaking Zone	No Overtaking Zone
14	415	416	☑	☑	☑	Two-Lane Undivided	8	8
15	416	417				Multilane	8	8
16	417	418				Multilane	8	8
17	418	419				Multilane	8	8
18	419	420				Multilane	8	8
19	420	421				Multilane	8	8
20	421	422				Multilane	8	8
21	422	423				Multilane	8	8
22	423	424				Multilane	8	8
23	424	425				Multilane	8	8

☑	No Restriction
✗	Restriction

By assigning the different platoon regulations to each section of the roadway, simulation models with 20 different scenarios were built to evaluate the operational effects of truck platooning regulations under varying traffic and composition conditions, as shown in **Figure 19**. Those 20 simulation scenarios were then grouped into two main groups (Group A and Group B) to be compared under a structured set of traffic input levels and truck percentage compositions to assess performance sensitivity. Traffic volumes varied across five levels [50, 100, 150, 300, and 400 vehicles per hour (vph)] to represent a range from light to moderately dense to peak-hour rural highway conditions. For each traffic volume, two different truck composition ratios were applied: 20% (low truck share) and 50% (high truck share). This resulted in a total of 10 simulation scenarios per model.

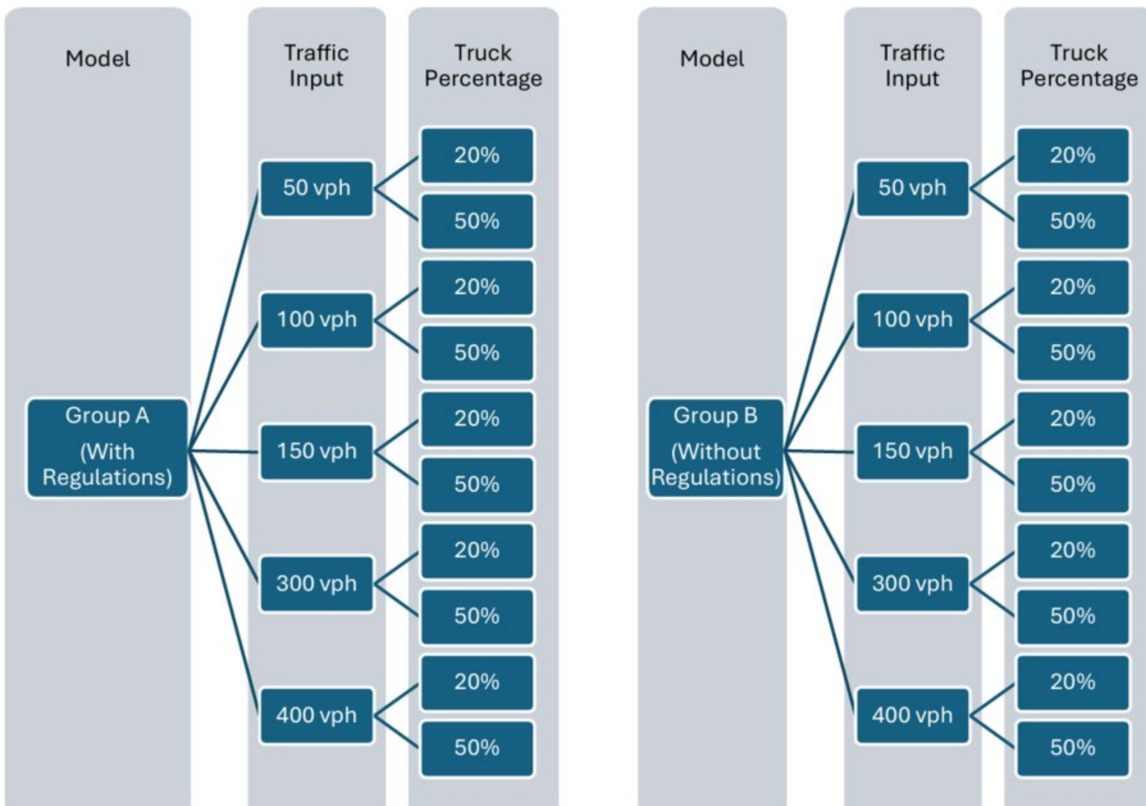

Figure 19: Simulation scenarios

4.2.4 Microsimulation Model Development in VISSIM

The simulation models were developed in VISSIM by using the data and model setup described in previous sections. The simulation setup consists of the following steps: 1) network development, 2) driving and link behavior parameterization, 3) speed calibration, 4) vehicle route decision and traffic inputs according to 20 model scenarios, 5) simulation parameters, and 6) evaluation parameter configurations. The simulation network was developed by replicating the actual roadway geometry using Google Maps and Google Street View as references. Links and connectors were manually constructed to match the real-life lane configurations, road curvature, and intersections along the selected study corridor. This process ensured the spatial accuracy of the modeled environment and preserved the realism of vehicle dynamics throughout the simulation. Traffic demand was generated using VISSIM's Vehicle Input and Vehicle Composition objects. Vehicle inputs were defined at the network entry points of each traffic direction. To ensure vehicles followed the appropriate paths through the network, static route assignments and desired route decisions were utilized. Speed distribution was set up with real-world speed distribution data obtained from WYDOT traffic data. The simulation incorporated two distinct driving behavior profiles using VISSIM's Driving Behavior settings (Wiedemann 99 model) (*114*).

For HDVs, the default Wiedemann 99 car-following model parameters were used with slight calibration to reflect better typical freeway car-following behavior, lane-change aggressiveness, and response times. Adjustments were made to parameters such as desired safety distance (CC1) and headway time to match observed driver behavior in mixed traffic. The parameters of the car following model for HDVs are shown in **Figure 20**.

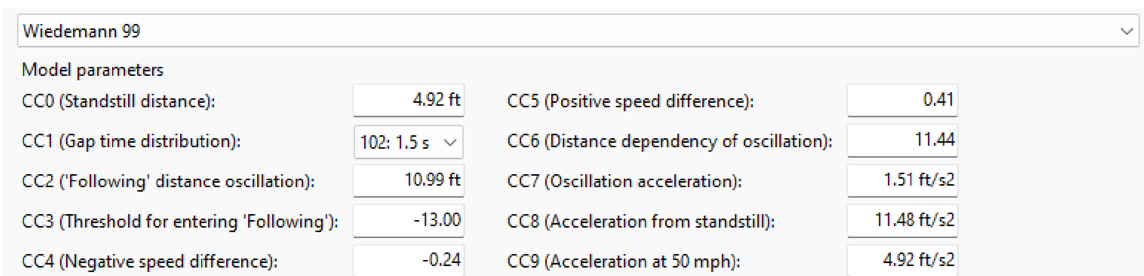

Figure 20: Parameters of the car following model for HDVs in VISSIM

For platooned trucks, a separate driving behavior type called AV aggressive (CoExist) driving behavior was used to represent connected and autonomous vehicle (CAV) operations in platoons. These profiles included:

- Shorter standstill distance (CC0)
- Reduced desired safety distance (CC1) according to platoon time gap
- Lower thresholds for speed difference (CC4/CC5)
- Increased look-ahead distance to simulate vehicle-to-vehicle communication effects

These adjustments were made to enable CACC dynamics, enabling tighter headways and smoother acceleration/deceleration behavior within platoons (*119*). The parameters of the car following model for the trucks in the platoon are shown in **Figure 21**.

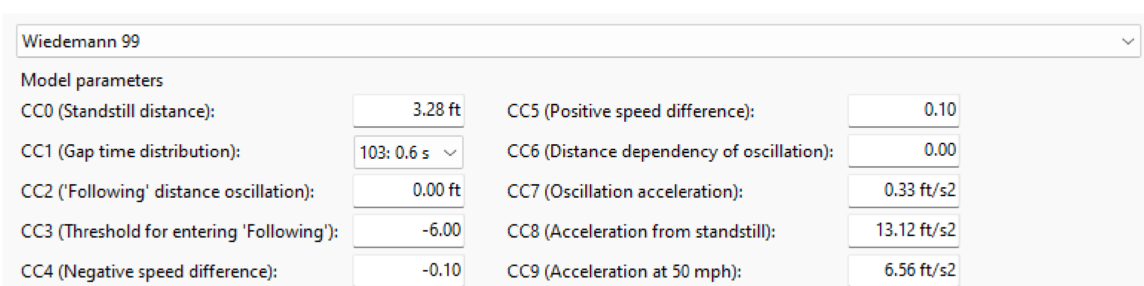

Figure 21: Parameters of the car following model for platoon trucks in VISSIM

Configuring platooning behavior involves setting several parameters that define how vehicles operate within a platoon. One of the key settings is the maximum number of vehicles that can form a single platoon. According to the regulations assigned at different corridor types, the platooning behavior was built into two types, one for eight-truck platoons and another one for two-truck platoons. Platooning sizes can impact factors like roadway capacity, string stability, and aerodynamic benefits. Another important parameter is the maximum desired speed, which specifies the highest speed at which both the lead and following vehicles in the platoon are allowed to travel. In this part of the project, the maximum desired speed was controlled by the posted speed limit. This helps ensure consistent movement among the vehicles in the platoon and prevents speed mismatches that could disrupt formation or create instability.

Additionally, the maximum distance for catching up to a platoon defines how far behind the last vehicle in a platoon another vehicle can be and still be eligible to join. If a vehicle falls within this distance, VISSIM allows it to accelerate and merge into the platoon. This is important for enabling dynamic platoon formation in traffic streams. The time gap parameter controls the desired time headway between vehicles within the platoon. This time gap is usually much shorter than in normal traffic since platooned vehicles, particularly autonomous or CACC-enabled trucks, are designed to maintain close distances safely using synchronized acceleration and braking. Finally, the minimum clearance sets the physical bumper-to-bumper distance that a following vehicle must keep from the vehicle in front of it. This ensures that even at low speeds or stops, the platoon maintains a realistic and safe following distance. **Figure 22** shows the parameters that were used to develop platooning behaviors in VISSIM. Different roadway segments were designated to simulate variable platooning regulations by assigning different driving behavior profiles and vehicle compositions to each segment. This was achieved by using Vehicle Routing Decisions and Route Decisions in VISSIM, which allowed for platooned and non-platooned vehicles to follow specific paths based on the simulation scenario.

The simulation parameters were set up with 10 simulation runs, as shown in **Figure 23**. The simulation period was 5,400 s (1,800 s warm-up period + 3,600 s simulation period). A warm-up time of 1,800 s was applied to allow the network to reach a stable traffic flow state before data collection began, as recommended by the VISSIM User Manual for large-scale freeway models (*114*). Each scenario was simulated 10 times (n=10) to account for the stochastic variability in vehicle behavior and ensure statistically reliable outputs. These replications were generated using different random seeds, configured under Simulation Parameters > Random Seed in VISSIM.

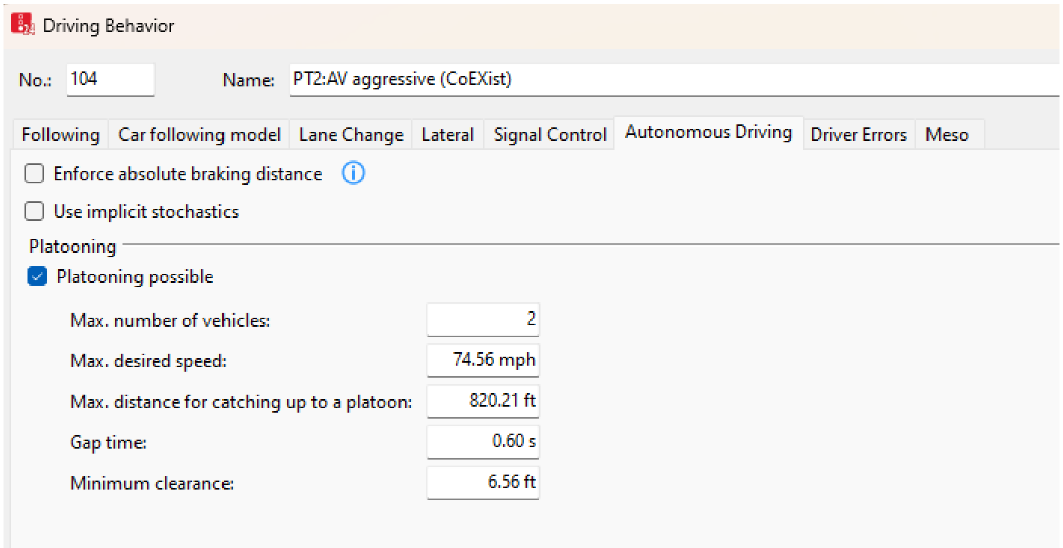

Figure 22 Platooning parameters in VISSIM.

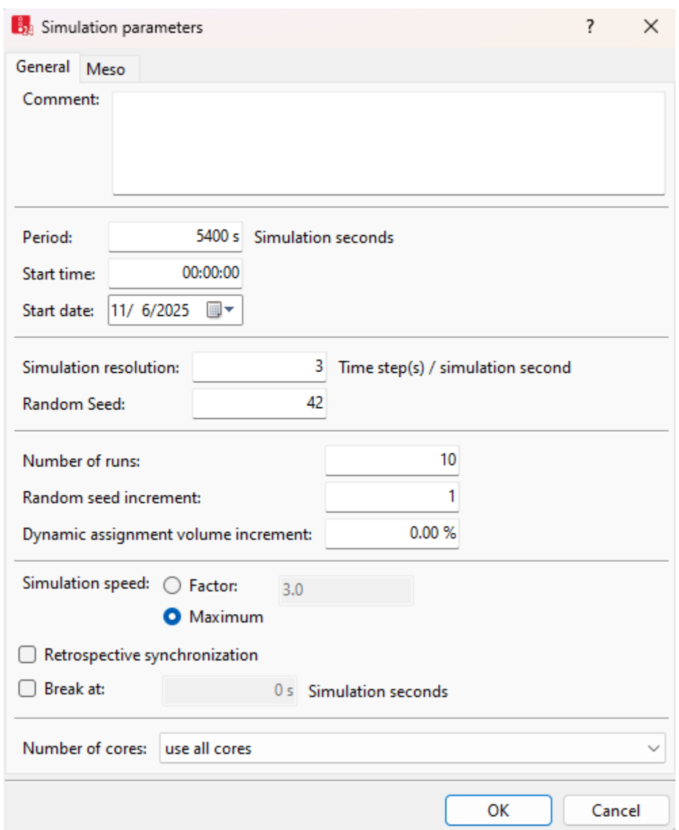

Figure 23: Simulation parameters in VISSIM.

4.2.5 Model Calibration and Validation by Using a Base Model

Before evaluating the operational and safety impacts of truck platooning, the baseline (non-platooning) VISSIM model was calibrated to accurately represent existing traffic behavior on the U.S. 287 study corridor. Calibration consists of adjusting model parameters so that simulated traffic performance measures closely match real-world field observations. This step is essential to ensure that all platooning scenarios are assessed within a reliable and representative simulation environment.

The model was calibrated using two primary parameters: traffic volume and speed. These parameters are widely recommended for freeway and rural highway calibration because they reflect fundamental traffic flow characteristics. Observed data were obtained from WYDOT traffic monitoring stations along the corridor.

GEH Statistic:

In microscopic traffic simulation, the GEH statistic is commonly used to assess how well simulated and observed traffic volumes match. The GEH formula is:

$$GEH = \sqrt{\frac{2\,(Q_{\text{sim}} - Q_{\text{obs}})^2}{Q_{\text{sim}} + Q_{\text{obs}}}} \qquad [4\text{-}1]$$

where:

Q_{sim} = simulation traffic volume (vph) from VISSIM

Q_{obs} =observed traffic volume (vph) from WYDOT traffic data

GEH = Geoffrey E. Havers statistic for traffic volume validation

Speed calibration was evaluated using multiple statistical measures to demonstrate agreement between simulated and observed traffic conditions.

Percent Error / Normalized RMSE (NRMSE):

$$\text{Percent Error} = \left| \frac{V_{\text{sim}} - V_{\text{obs}}}{V_{\text{obs}}} \right| \times 100 \qquad [4\text{-}2]$$

where:

V_{sim} = Simulated average speed (mph) obtained from VISSIM

V_{obs} = Observed average speed (mph) collected from WYDOT traffic data

In VISSIM, a traffic input of 300 vph was used for the base model as it was close to the monthly average traffic volume at the 2 p.m. to 3 p.m. time period in the WYDOT field observations document. Regarding truck percentage, 84.19% was used for the passenger vehicles and 15.81% was used for the trucks to match the average WYDOT traffic data. An average speed of 72 mph under free-flow conditions was calculated from WYDOT's 2024 speed distribution data. These values served as calibration targets. The baseline VISSIM model was run for 3,600 seconds after an 1,800-second warm-up period, using 10 random seed replications to account for stochastic variation. Results from the simulations were averaged across the 10 replications to provide stable performance estimates. The baseline simulation produced a mean traffic volume of 295 vph and an average speed of 63.6 mph, as shown in **Table 8**.

Table 8: Model Calibration Test Results

Measure	Observed	Simulated	Statistic	Threshold	Result
Traffic Volume (vph)	300	295	GEH = 0.29	GEH < 5	Pass
Average Speed (mph)	72	63.6	Error = 11.67%	< 15% acceptable	Pass

A GEH value below 5.0 is typically considered an excellent match, and a value below 2.0 indicates near-perfect agreement. The calculated GEH of 0.29 indicates that the simulated throughput closely corresponds to the actual field volume, thereby meeting volume calibration requirements with a high level of confidence. Similarly, the percent error for speed calibration is 11.67%. This value falls within the widely accepted 10%–15% error range recommended for rural highway microsimulation models, indicating that the model adequately reproduces field speed conditions. In summary, the calibration results demonstrated that the baseline VISSIM model closely replicates observed traffic conditions on U.S. 287.

4.2.6 SSAM, Surrogate Safety Measures

The study utilized the Surrogate Safety Assessment Model (SSAM) developed by the FHWA to perform a surrogate safety analysis based on vehicle trajectory data generated from microsimulation modeling in PTV VISSIM 2024. This approach enables a proactive safety assessment by identifying and quantifying vehicle interactions that have a high potential for collision but do not necessarily result in actual crashes. Each model scenario underwent 10 independent simulation runs to account for the stochastic nature of driver behavior and traffic flow variability. These multiple replications increase the reliability and statistical robustness of the resulting safety evaluation. For each simulation run, VISSIM generated a vehicle trajectory file. These files recorded the time, position, speed, and acceleration of every vehicle at each simulation time step and were subsequently used as inputs for the safety analysis in SSAM. The flow steps of the SSAM analysis are shown in **Figure 24** (*120*).

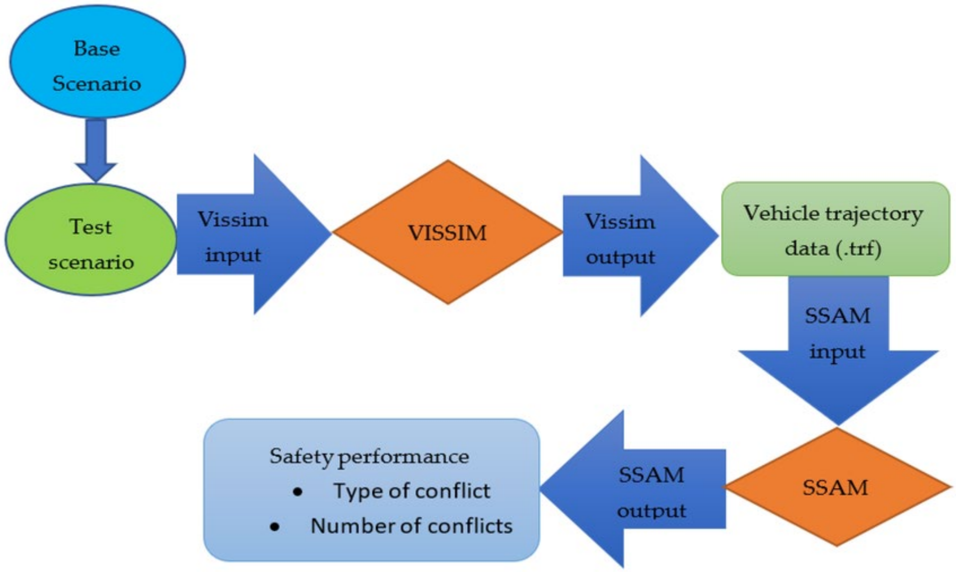

Figure 24: Procedure of SSAM analysis (120)

A conflict is defined in SSAM as "a situation in which two road users would collide unless at least one of them performs an evasive action" (*121*). SSAM was used with its default conflict detection thresholds, time-to-collision (TTC) < 1.5 seconds and post-encroachment time (PET) < 5.0 seconds, as shown in **Figure 25**.

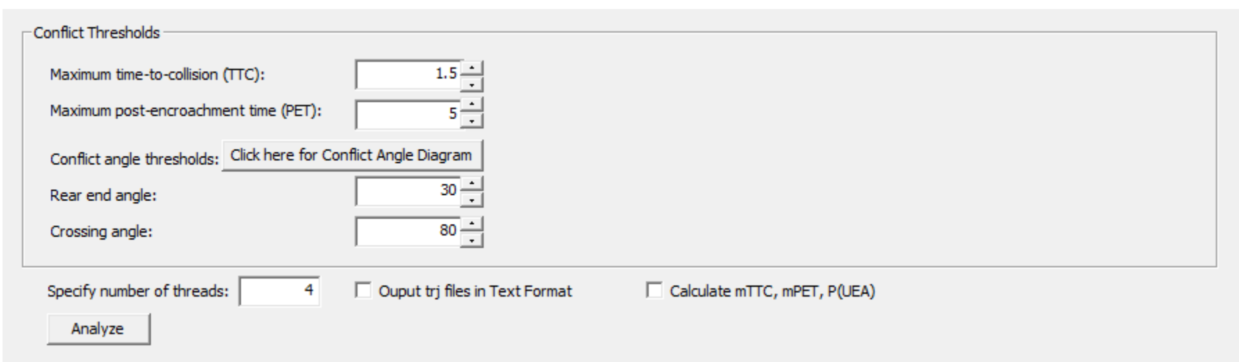

Figure 25: Parameters of conflict thresholds in SSAM

For each scenario, SSAM classified conflicts into the following types:

- Unclassified
- Crossing conflicts
- Rear-end conflicts
- Lane-change conflicts

The total number of conflicts identified across all 10 replications per scenario were aggregated to assess and compare safety performance. These conflict categories provide insight into the nature of potential safety issues within the simulated traffic system.

4.3 Analysis

The analysis includes two parts: 1) Network operation performance analysis and 2) Safety performance analysis. The objective of this analysis is to determine how different platooning regulations influence key operational measures and safety performance under varying traffic inputs, vehicle compositions, and roadway geometries. By distinguishing between multilane divided and two-lane undivided segments, the study captures the impact on traffic dynamics arising from differences in lane configuration, overtaking opportunities, and interactions between platooned and non-platooned vehicles.

4.3.1 Network Operation Performance Analysis

To accurately assess the effects of truck platooning on traffic network operation under varying roadway corridor types, the performance evaluation was conducted separately for multilane divided and two-lane undivided highway segments. This separation was essential because traffic behavior, vehicle interaction patterns, and assigned platoon regulations differ substantially depending on whether opposing traffic streams are physically separated. Two-lane undivided segments, in which both directions of travel share the same carriageway without a physical median or barrier, typically exhibit greater variability in speed, higher potential for interference from opposing vehicles, and increased delay due to overtaking limitations. In contrast, multilane divided segments generally provide a more consistent traffic flow environment, allowing for smoother platoon movement and fewer disruptions.

The undivided segment was designated as the control condition, representing the baseline or reference scenario for performance comparisons. Using the undivided section as a control enables the assessment of how roadway geometry influences the overall benefit of platooning. In addition to the comparison of different corridor types (Group A, representing conditions with the application of truck platoon regulations, and Group B, representing conditions without restrictions on platoon regulations), two groups of simulation models within the same type of corridors were analyzed as well. Therefore, this design produced four distinct comparison scenarios:

- Comparison between Groups A and B for divided segments
- Comparison between Groups A and B for undivided segments
- Comparison between undivided segments and divided segments using Group A
- Comparison between undivided segments and divided segments using Group B

The comparison was conducted in two main stages. First, within each corridor segment type, the results of Model A and Model B were compared to quantify the effect of implementing platoon regulations under that specific geometric condition. In the second stage, comparisons between different corridor segment types were performed to determine how the effect of restricted platooning regulations differentiate between divided and undivided segments. Using the undivided segment results as the baseline, performance metrics from the divided segments were expressed as relative improvements or degradations. This two-level comparison approach provided a structured way to evaluate not only the overall benefit of platooning but also its dependency on roadway configuration.

Through this analytical framework, the study ensured that performance differences attributed to platooning were interpreted in the context of geometric conditions. The approach also allowed for a clearer identification of whether platooning regulations yielded consistent benefits across different highway types or whether their effectiveness was influenced by roadway division characteristics.

To assess the effects of applying platooning rules on the traffic network, average speed and average delay were selected as the primary performance metrics. Both parameters are widely used in traffic simulation and performance analysis studies due to their strong correlation with mobility and operational efficiency, which are most affected by the application of platooning rules.

Data Processing of Evaluation Results:

To evaluate the network operation performance, raw link evaluation outputs, containing over 110,000 records for each link of each model scenario from 10 VISSIM simulation runs, were collected. To get meaningful data from over 110,000 records, the data cleaning process was performed, which involved removing incomplete or zero-volume records and excluding any entries with physically unrealistic values, such as negative speeds or excessively high delays. After that, the average speed for each link was calculated across all runs to obtain a stable estimate of link-level performance. The links were then grouped according to their corridor type, classified as either divided or undivided based on the roadway geometry. As both segment types are long, continuous sections of the corridor instead of frequently switching into different types, it was possible to meaningfully group the segments by corridor type and average the speeds and delay along the entire divided and undivided portions of the network.

The overall average speed and delay for each segment type was therefore computed as the means of all roadway links' average speeds. This method provides a representative measure of corridor-level performance for each segment type while retaining the geometric and operational continuity of the simulated roadway. It also allows a direct comparison between the divided and undivided segments under each traffic and platooning scenario by minimizing the local noise from individual link-level fluctuations.

4.3.2 Statistical Analysis of Network Operation Performance

Statistical Model Design and Structure:

The simulation results data of the 20 scenarios from VISSIM microsimulation software were structured as shown in **Table 9**. Each parameter set i=1, 2, …, 10 appears under all combinations of (j,k), and the resulting data represent a within-subject factorial design. Consequently, the analysis focused on paired-sample statistical methods that account for the dependency among repeated measurements within the same scenario.

Table 9: Data Structure of Statistical Model

Scenario Parameter Set (i)	Models Group (j)	Corridor Segment Type (k)	Simulation results
1 - 10	A, B	Multilane Divided, Two-lane Undivided	Average Speed, Average Delay

Paired Comparison Tests:

As each Group A observation corresponds directly to a Group B observation under identical traffic and truck percentage conditions, the samples are dependent (paired). Similarly, within each group, the results for the divided and undivided segments are also paired for each scenario. Independent sample methods such as one-way ANOVA would ignore this dependency and inflate error variance; therefore, paired t-tests were used. Four paired comparisons were performed:

- Group A vs Group B on divided segments
- Group A vs Group B on undivided segments
- Group A (divided vs undivided)
- Group B (divided vs undivided)

Paired t-Test Formulation:

The paired t-test evaluates whether the mean difference between two related measurements differs by using the following hypotheses:

$H_0: \mu_D \neq 0$ [4-3]
$H_1: \mu_D \neq 0$ [4-4]

where $D_{1=}X_{A,i} - X_{B,I}$ is the difference between paired observations for the ith parameter set. The test statistic is:

$$t = \frac{\bar{D}}{s_D/\sqrt{n}s_D/\sqrt{n}} \quad [4\text{-}5]$$

where $\bar{D}$= mean of differences, s_D= standard deviation of differences, and n= number of paired observations. A significant level of α=0.05 was used for all tests.

Validation of Test Assumptions:

To make sure the statistical analysis fits the model and does not violate the model's assumptions, the following tests were done for validation. The normality assumption of the paired t-test was verified using the Shapiro-Wilk test:

$$W = \frac{\left(\sum_{i=1}^{n} a_i x_{(i)(i)}\right)^2}{\left(\sum_{i=1}^{n}(x_i - \bar{x}\right)^2} \quad [4\text{-}6]$$

where a_i are constants derived from the expected order statistics of a standard normal distribution, x(i) represents the i^{th}ordered sample value (from smallest to largest), x_i denotes each individual observation in the sample, and $\bar{x}$ is the arithmetic mean of all observations. A p-value greater than 0.05 indicates that the differences do not deviate significantly from normality. Additionally, QQ plots of residuals were visually inspected to confirm the normal distribution of paired differences.

Nonparametric Robustness Check:

To ensure robustness, a Wilcoxon signed-rank test was performed as a nonparametric alternative to the paired t-test. The test statistic, W, sums the ranks of absolute differences, preserving signs. It evaluates the null hypothesis that the median difference equals zero without assuming normality.

Effect Size and Confidence Intervals:

To quantify the magnitude of differences, Cohen's d_z for paired designs was computed as follows:

$$d_z = \frac{\bar{D}}{s_D} \quad [4\text{-}7]$$

where s_D is the standard deviation of the paired differences and $\bar{D}$ is mean of differences.

In interpreting Cohen's $d_z$values, the magnitude of the effect provides insight into the practical significance of the observed difference. According to Cohen's (*122*) conventional benchmarks, a value of approximately 0.2 indicates a small effect, around 0.5 shows a medium effect, and 0.8 or greater signifies a large effect. These thresholds help translate statistical differences into meaningful interpretations, where larger $d_z$values imply that the difference between paired conditions is more substantial relative to the variability in the data (*122*).

To obtain distribution-free uncertainty estimates, bootstrapping (10,000 resamples) was applied to compute 95% confidence intervals for the mean differences. The percentile method was used:

$$CI_{95\%} = [P_{2.5}(\bar{D}^*), P_{97.5}(\bar{D}^*)]CI_{95\%} = [P_{2.5}(\bar{D}^*), P_{97.5}(\bar{D}^*)] \quad [4\text{-}8]$$

where $\bar{D}^*$ are bootstraps resampled mean differences.

Multi-Factor ANOVA Analysis:

The analysis of network-level performance was performed by using a multi-factor ANOVA framework designed to evaluate how platooning regulations interact with roadway geometry and traffic conditions. A three-way ANOVA was conducted for each performance metric to quantify the contributions of the primary factors and their interactions.

This approach was selected because the study involves multiple independent variables that may influence each other, and ANOVA provides an efficient way to detect both main effects and interaction effects within a unified model structure. It also allows for the comparison of numerous factor levels simultaneously, which is necessary when evaluating networks that vary by segment type, traffic input, and truck percentage. The structure of the ANOVA model followed the general expression:

$$Y = \mu + \alpha i\ + \beta j\ + \gamma k\ + \delta l\ + (\alpha\beta)ij\ + (\alpha\gamma)ik\ + (\beta\gamma)jk\ + \varepsilon \qquad [4\text{-}9]$$

Where, α represents the effect of the platooning regulation group, β represents the effect of segment type, γ denotes the influence of traffic input, δ corresponds to truck percentage, and ε captures the random error term.

Statistical significance for each factor and interaction was determined using F-statistics and corresponding p-values to evaluate whether each term contributed meaningfully to variations in average speed and average delay. Before interpreting the ANOVA results, assumption checks were performed to ensure model validity. ANOVA relies on three core assumptions: normality, homoscedasticity, and independence. Each assumption was evaluated using standard diagnostic tools. Normality was assessed using Shapiro–Wilk tests applied to the residuals, and QQ plots confirmed an approximately normal distribution.

Homoscedasticity, defined as the equality of variances across factor levels, was evaluated using Levene's test, which indicated sufficiently stable variance for our data. Independence was ensured by the simulation design, as each scenario was generated and executed separately without influence from previous runs. These diagnostics supported the reliability of the model. This method was chosen because it provides a statistically robust and computationally efficient approach to determining whether platooning regulations introduce significant performance differences after accounting for the dominant effects of roadway geometry and traffic input.

4.3.3 Safety Performance Analysis and Results

This section presents the traffic safety performance results of the microsimulation case study and evaluation on the effects of truck platooning regulations on a rural highway based on different characteristics of traffic inputs (50, 100, 150, 300, and 400 vph) and truck percentages in the traffic (20% and 50%).

Surrogate Safety Measures:

Traditional crash-based safety evaluation usually relies on existing observed crash data. However, crashes are rare, random, and often unavailable for new or hypothetical designs. The SSAM methodology allows for safety assessment before crashes occur by using simulated vehicle trajectories to identify "conflict events," situations where two vehicles would likely collide without evasive action (*121*). Moreover, conflict frequency has been shown to correlate with crash risk, thus serving as a reliable surrogate safety measure (SSM) in transportation safety research (*121*).

The major advantages include:

- Ability to assess safety of new designs or interventions where crash history is not available

- Derivation of quantitative measures (conflict counts, severity metrics such as TTC, PET, etc.)
- Ability to compare alternative scenarios (group A vs B) in a consistent microsimulation-based environment

Because of these advantages, we consider that using SSAM conflict-point metrics is appropriate and robust for our analysis purposes.

Conflict Types:

Traffic conflicts were analyzed not only in terms of the total number of conflicts but also by each conflict type, to provide a more detailed understanding of how different operational and traffic conditions influence roadway safety. Examining the overall number of conflicts alone can mask important behavioral patterns; therefore, disaggregating conflicts by type allows for identification of specific risk mechanisms associated with truck platooning, such as following behavior, lane-changing maneuvers, or lateral interactions.

According to the FHWA (*123*) surrogate safety methodology, vehicular conflicts can be categorized into four main types based on the relative trajectories and potential points of collision between vehicles: rear-end conflicts, lane-change (sideswipe) conflicts, crossing conflicts, and unclassified conflicts.

Unclassified Conflicts: The "unclassified" conflicts category essentially captures interactions between vehicle pairs that do not meet the stricter geometric or lane-link change criteria to be reliably classified as rear-end, lane-change, or crossing conflicts. While less descriptive, these events still indicate proximity and evasive action potential, and thus they represent latent risk. The SSAM documentation notes that every conflict event is assigned a type "rear-end, lane-change, or path-crossing (crossing)" but acknowledges that some events may remain unclassified due to incomplete link data (*121*).

Crossing Conflicts: "Crossing" conflicts occur when two vehicles' paths intersect at appreciable angles such that one vehicle crosses the path of another (for example a turning vehicle crossing through-traffic or adjacent-lane weave). SSAM classifies a path-crossing event when the conflict angle is greater than a threshold (e.g., ||ConflictAngle|| > 80°) if link/lane information is insufficient (*121*).

Rear-End Conflicts: "Rear-end" conflicts represent vehicle pairs in which one vehicle trails another in the same lane/link without a lane change or link change during the conflict (or the conflict angle is small: ||ConflictAngle|| < 30°) (*121*). In practice, rear-end conflicts are one of the most frequent surrogate conflict types because trailing vehicles reacting to slower lead vehicles or platoons are a common source of collisions, particularly in dense-flow or platooned scenarios.

Lane-Change Conflicts: "Lane-change" conflicts involve maneuvers in which at least one vehicle changes lanes (or occupies different lanes at start and end of conflict) and interacts with another vehicle because of the lane change. SSAM uses lane/link data and conflict angle logic to identify such events (*121*).

4.3.4 Statistical Analysis of Safety Performance

The primary advantage of using conflict-point and conflict types as surrogate safety measures via SSAM enables the quantification of safety risk by identifying potential collisions (or conflicts) drawn from simulated trajectories, thus allowing a proactive rather than reactive safety assessment (*121*). Traffic conflicts were analyzed not only in terms of their total frequency but also by conflict type, to provide a more detailed understanding of how different operational and traffic conditions influence roadway safety. By evaluating each conflict category type separately, our analysis captures not only the overall safety but also the nature of interactions most affected by platooning regulations and different input factors. This level of detail enables a better interpretation of safety trends. It also supports the identification of targeted countermeasures for specific conflict types.

The analytical framework employed a two-stage approach combining nonparametric and factorial ANOVA models. To make sure the statistical analysis fits for the model and does not violate the model's assumptions, the following tests were performed for validation and initial assumption checks were performed for Shapiro–Wilk normality and Levene's homogeneity of variances. Given the small sample size and non-normal data, the Mann-Whitney U test was selected for overall pairwise comparisons between the two groups. This nonparametric method does not assume normality and is suitable for independent samples with potentially unequal distributions.

For a more comprehensive understanding of factor interactions, two-way factorial ANOVA models were conducted for each conflict type. The factors included group, traffic input level, and truck percentage. The inclusion of interaction terms is crucial in transportation simulation analysis, as the combined influence of flow rate and truck percentage can nonlinearly affect car-following and lane-changing behaviors.

4.4 Results and Discussion (Network Operational Performance)

We use two metrics to evaluate the network operation performance: average speed and average delay. The analysis for both metrics' results proceeds in two layers for statistical tests as follows:

- Paired comparisons across corridor types and groups to test specific hypotheses with minimal assumptions
- ANOVA analysis to quantify combined and interaction effects of roadway geometry (divided vs. undivided), platoon configuration (Group A vs. Group B), and traffic composition (traffic input and truck percentage), while accounting for between-scenario heterogeneity.

The platoon regulations assigned to Groups A and B differ only in undivided segments (Group A limits platoons to two trucks, while B allows up to eight). On multilane divided segments, overtaking the platoon is not restricted by opposing traffic. Therefore, both Groups A and B were allowed to have up to eight trucks, serving as a functional control for comparing configurations under high-maneuverability conditions.

4.4.1 Average Speed

Comparison by Corridor Segment Types (Divided vs. Undivided):

The results from the statistical analysis of the average speed comparison were shown in **Table 10**. The table summarizes the outcomes of the paired statistical comparisons between Group A and Group B across the divided and undivided highway segments. Four sets of paired t-tests were conducted to evaluate differences in average speed performance:

1. Group A vs Group B on divided segments (as both groups A and B were assigned the same number of trucks allowed to form a platoon on multilane divided highway segments, the results from this comparison were used as a control condition to make sure the results in the rest of the three comparisons are not caused by model bias)
2. Group A vs Group B on undivided segments
3. Group A divided vs undivided segments
4. Group B divided vs undivided segments

Table 10: Statistical Analysis Results for Average Speed Comparison by Segment Types

Comparison	Pairs	t_stat	T_p	Wilcoxon Stat	Wilcoxon p	Shapiro W on diffs	Shapiro_p On diffs	Cohen d_z	Boot CI_low	Boot CI_high
A vs B (Divided)	10	-0.7980	0.4454	22	0.62501	0.9677	0.8688	-0.2524	-0.7831	0.2819
A vs B (Undivided)	10	2.8152	0.0202	6.0000	0.0273	0.9039	0.2420	0.8902	0.2412	1.0961
A (Divided vs Undivided)	10	6.6297	0.0001	0.0000	0.0020	0.9120	0.2951	2.0965	3.8719	6.8749
B (Divided vs Undivided)	10	6.5300	0.0001	0.0000	0.0020	0.9481	0.6466	2.0650	4.2742	7.6516

Group A vs Group B on multilane divided segments (Validation of the control condition)

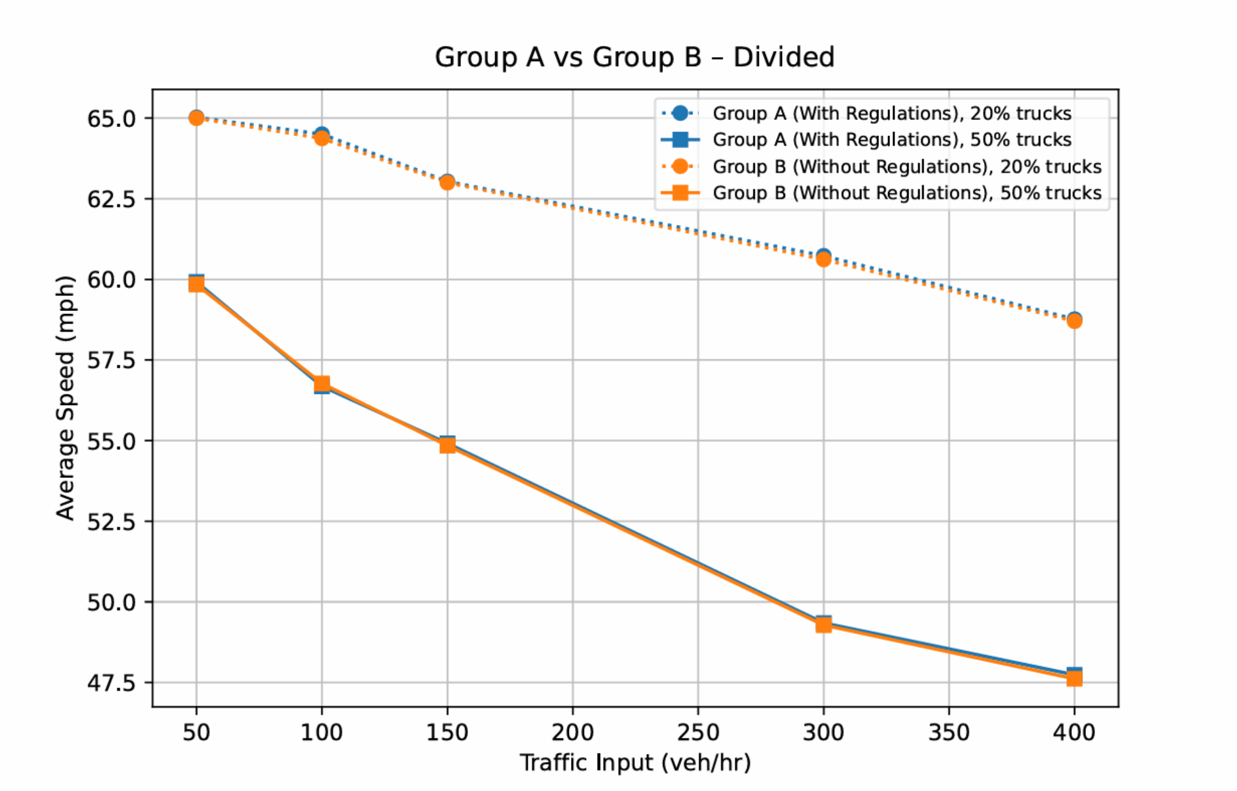

Figure 26: Average speeds comparison for multilane divided highway segments between Group A (with platooning regulations) and Group B (without platooning regulations) across various traffic input levels and truck percentages.

Figure 26 shows the average speed results of divided highway segments for Group A (with platooning regulations) and Group B (without platooning regulations) under two truck percentages (20% and 50%) across increasing traffic inputs. Overall, both groups A and B exhibit a distinct pattern of decreasing speed as traffic volumes increase, which is consistent with the effects of congestion. Average speeds are consistently lower for the 50% truck scenarios than for the 20% truck cases, indicating that even on divided highways, higher truck proportions more severely restrict the traffic flow. However, in comparison of the groups A and B, all average speed results are nearly identical. As both groups A and B were assigned the same number of trucks allowed to form a platoon on multilane divided highway segments, these results align with the model setup and show that the control is performing as it should be.

However, the statistical comparison between Group A and Group B on multilane divided segments did not show a significant difference ($t = -0.8$, $p = 0.445$), with Group A showing a slightly higher average speed (58.07 mph vs 58.00 mph), a difference of only 0.07 mph. As the speed difference is insignificantly minimal, it is negligible in practical terms, suggesting that both platooning regulations groups (A and B) performed nearly identically under divided highway conditions. Therefore, these results confirm the validity of the control condition and clearance of the model bias on the following three comparisons according to segment types.

Group A vs Group B on undivided segments

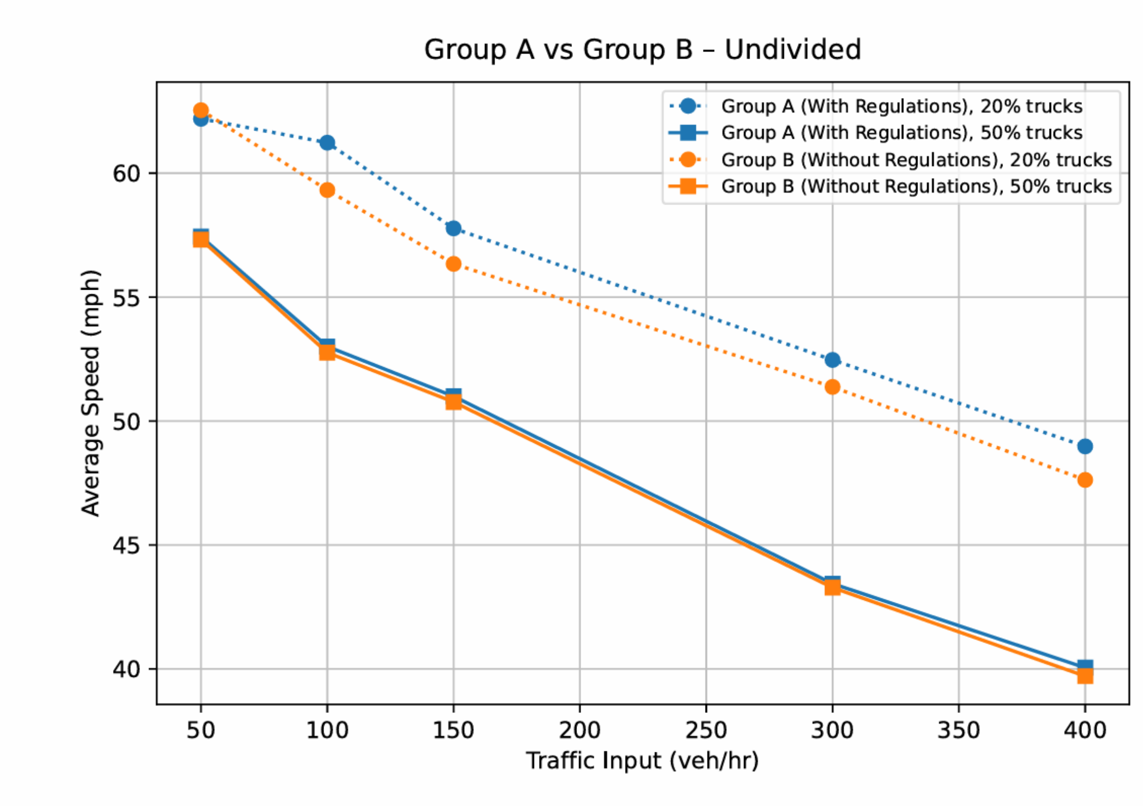

Figure 27: Average speeds comparison for two-lane undivided highway segments between Group A (with platooning regulations) and Group B (without platooning regulations) across various traffic input levels and truck percentages

As shown in **Figure 27**, regulations help maintain smoother flow at lower traffic volumes. However, the difference between the two groups (A and B) becomes minimal at truck percentages (50%), indicating that the presence of heavy trucks reduces the effects of platooning regulations on undivided highway segments.

Statistical analysis showed that group A (with platooning regulations) had a slight but statistically significant speed advantage over Group B ($t = 2.82$, $p = 0.020$), averaging 0.65 mph faster. This difference suggests that the assigned platooning regulations in Group A may provide slightly improved mobility benefits on two-lane undivided segments.

Group A comparison of divided vs undivided segments and Group B comparison of divided vs undivided segments

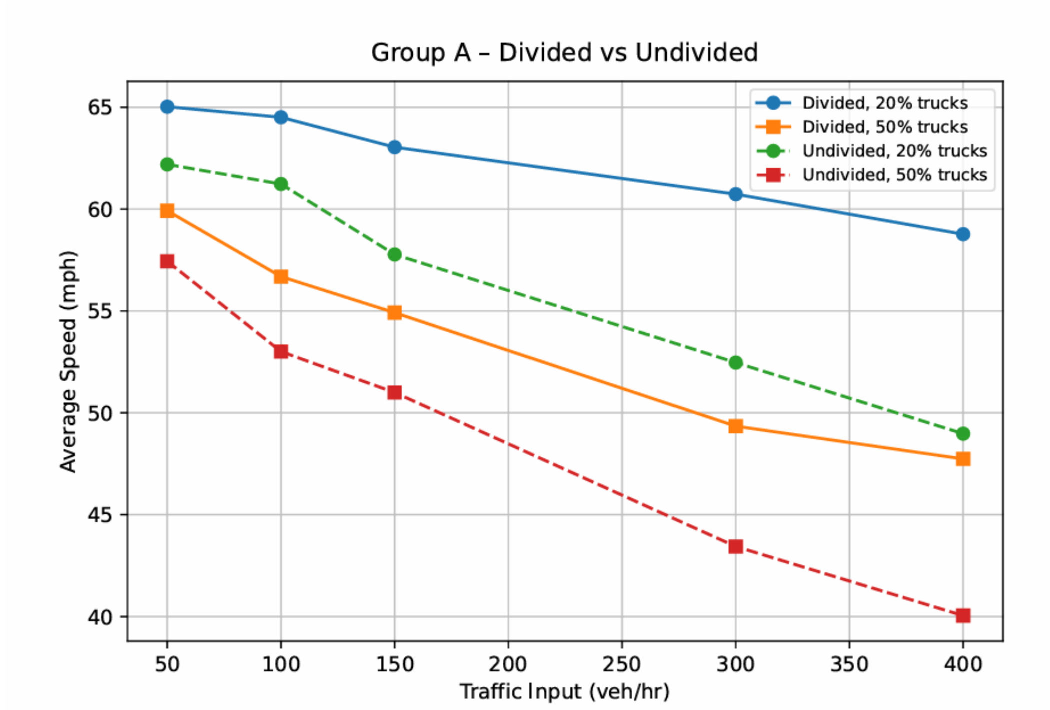

Figure 28: Average speeds comparison for Group A (with platooning regulations) on divided and undivided highways across varying traffic inputs and truck percentages

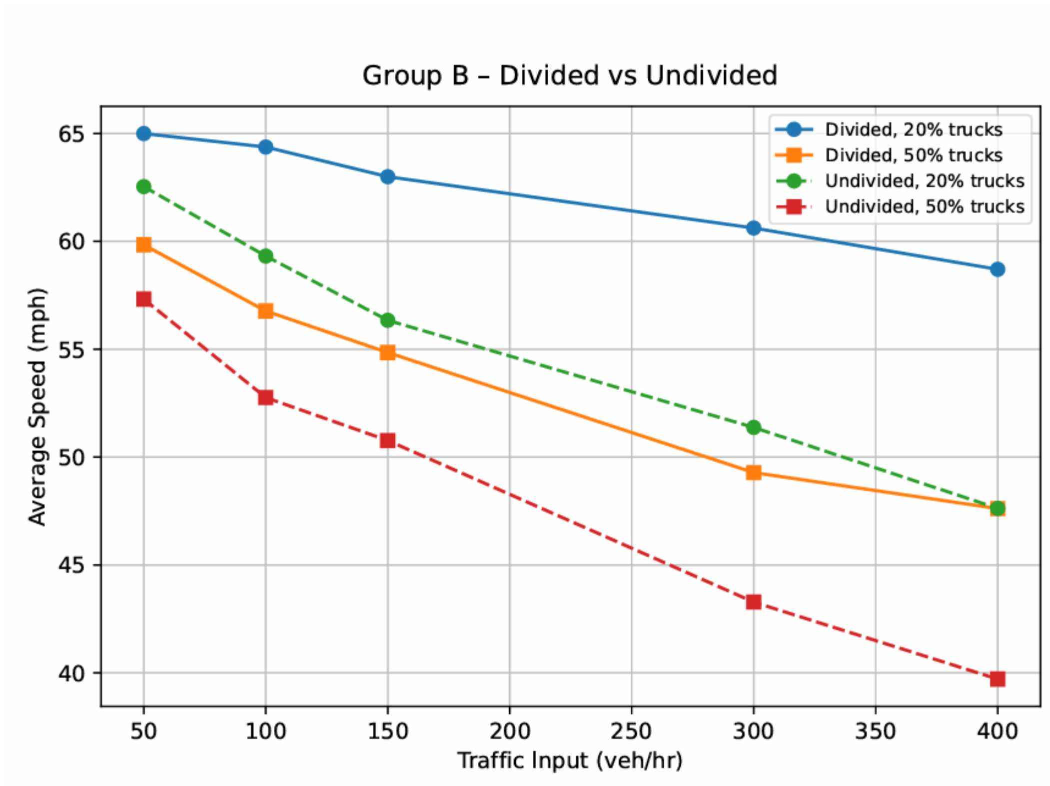

Figure 29: Average speeds comparison for Group B (without platooning regulations) on divided and undivided highways across varying traffic inputs and truck percentages

The results from **Figure 28** and **Figure 29** demonstrate higher average speeds in divided segments than in undivided segments across all conditions. Similarly in statistical analysis, the comparisons of each Group A and B between divided and undivided segments revealed very strong effects for both groups. When comparing divided segments to the undivided segments, Group A had an average speed difference of approximately +5.31 mph ($t = 6.63$, $p < 0.001$) on divided segments, while Group B showed an average speed difference of +5.90 mph ($t = 6.53$, $p < 0.001$) on divided segments. Additionally, Cohen's d_z result was greater than 2.0, which also confirms a large effect size that roadway geometry type is the dominant factor influencing overall traffic performance, outweighing any differences attributable to the platooning regulations differences. Overall, the results demonstrate that while significant differences exist between the two platooning regulations scenarios (Groups A and B), the impact of the roadway type is far greater.

Comparison by Factors and Interaction Effects:

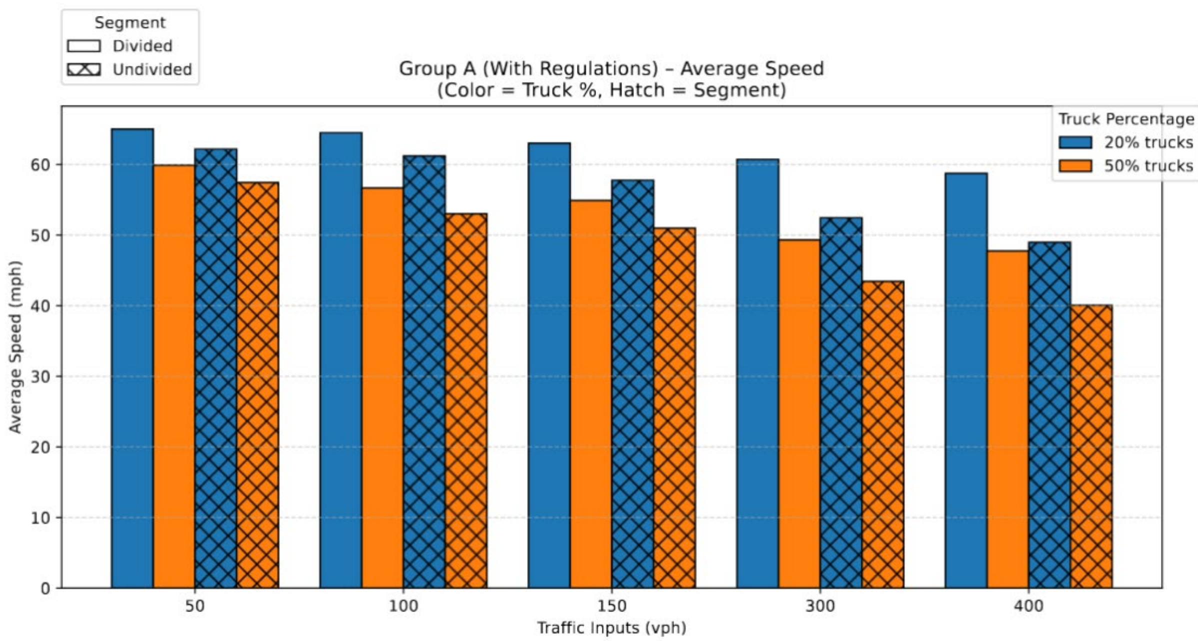

Figure 30: Average speeds comparison for Group A (with platooning regulations) across divided and undivided highway segments for varying truck percentages and traffic input levels

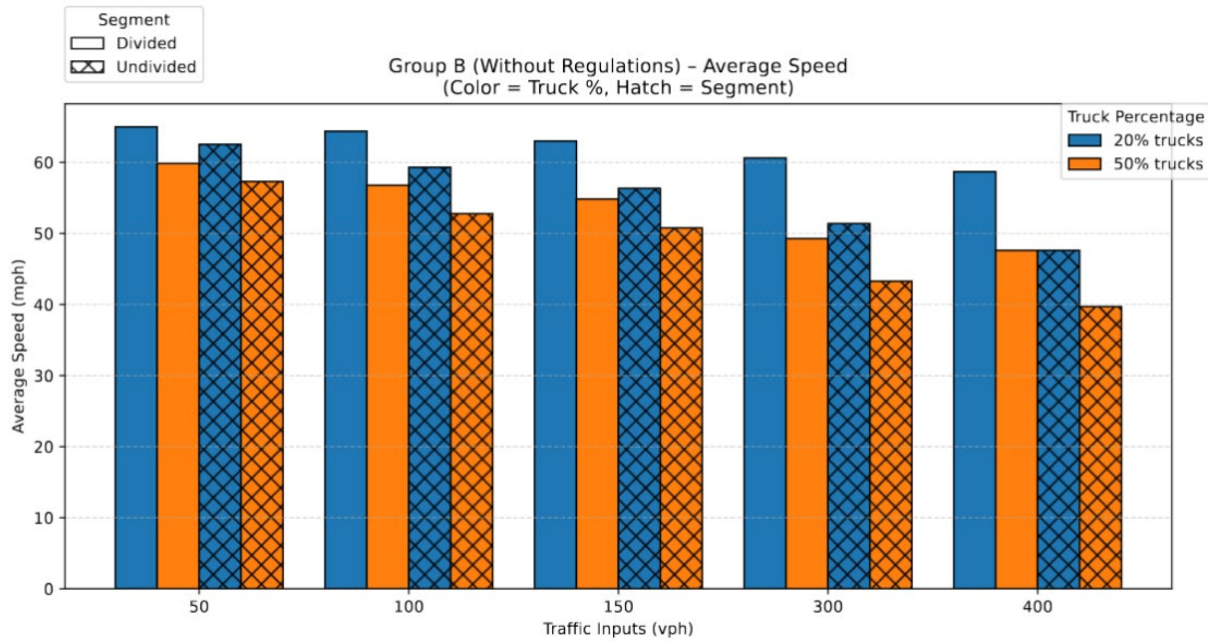

Figure 31: Average speeds comparison for Group B (without platooning regulations) across divided and undivided highway segments for varying truck percentages and traffic input levels

As shown in **Figure 30** and **Figure 31**, both Group A (with platooning regulations) and Group B (without platooning regulations) have higher average speeds on divided segments compared with undivided segments. Additionally, both groups have downward trends on average speeds as traffic input increases. The downward trend is steeper in undivided segments compared with divided segments. These findings fit with the practical terms as undivided segments have overtaking limitations and the impacts of the opposite traffic. The effect of the truck percentage is also evident, with a higher truck percentage (50%) causing the reduction of speeds in both groups.

Table 11: ANOVA Results for Average Speed Comparison by Factors and Interaction Effects

Effect	**Sum Sq**	**Effect Size (η^2_p)**	**F**	**p-value**	**Interpretation**
Groups A vs B (Regulations)	1.28	0.012	0.401	0.531	Not significant
Segment Type	314.15	0.744	98.519	<0.001	Highly significant effect
Group × Segment Type	0.87	0.008	0.273	0.604	Not significant
Traffic Input	843.33	0.886	264.472	<0.001	Significant negative effect
Truck Percentage	622.88	0.852	195.336	<0.001	Significant negative effect

The ANOVA test results shown in **Table 11** indicate that segment types (divided vs. undivided), traffic input, and truck percentage are the three factors that have significant effects on the average speed. In contrast, the effect of regulation groups, A (with platooning regulations) vs B (without platooning regulations), does not show a significant difference. This is because the scale of speed difference caused by platoon regulations is overshadowed by the large effect sizes of the segment types, traffic input, and truck percentages on speed differences. Regulations differences (the number of trucks allowed to form a platoon) affect microscale behavior, but their impact on macroscopic speed is small compared with the other three factors: segment types (divided vs undivided), traffic input, and truck percentage.

4.4.2 Average Delay

Comparison by Corridor Segment Type

The statistical comparison between Groups A and B, as well as between divided and undivided roadway configurations, reveals several notable trends in traffic performance. Similar to the average speed analysis, four sets of paired tests were conducted to evaluate differences in average speed performance:

1. Group A vs Group B on divided segments (as both groups A and B were assigned the same number of trucks allowed to form a platoon on multilane divided highway segments, the results from this comparison were used as a control condition to make sure the results in the rest of the three comparisons are not caused by model bias)
2. Group A vs Group B on undivided segments
3. Group A divided vs undivided segments
4. Group B divided vs undivided segments

Table 12: Statistical Analysis Results of Average Delay Comparison by Segment Types

Comparison	Pairs	t_stat	T_p	Wilcoxon Stat	Wilcoxon p	Shapiro W on diffs	Shapiro_p On diffs	Cohen d_z	Boot CI_low	Boot CI_high
A vs B (Divided)	10	-3.52	0.00651	0	0.001953	0.77033	0.00631	-1.1132	-8.2984	-2.7232
A vs B (Undivided)	10	-2.7916	0.021	3	0.009766	0.87071	0.10188	-0.8827	-28.066	-6.2738
A (Divided vs Undivided)	10	-4.8907	0.00087	0	0.001953	0.92275	0.38053	-1.5465	-207.95	-93.0646
B (Divided vs Undivided)	10	-4.9380	0.00080	0	0.001953	0.93109	0.4587	-1.5615	-223.363	-100.861

Both parametric (paired t-test) and non-parametric (Wilcoxon signed-rank) tests were applied to verify statistical significance, and Cohen's d_z was used to evaluate the magnitude of the effect size. Normality of paired differences was assessed using the Shapiro-Wilk test. The statistical analysis results are shown in **Table 12**.

Group A vs Group B on multilane divided segments (Validation of the control condition)

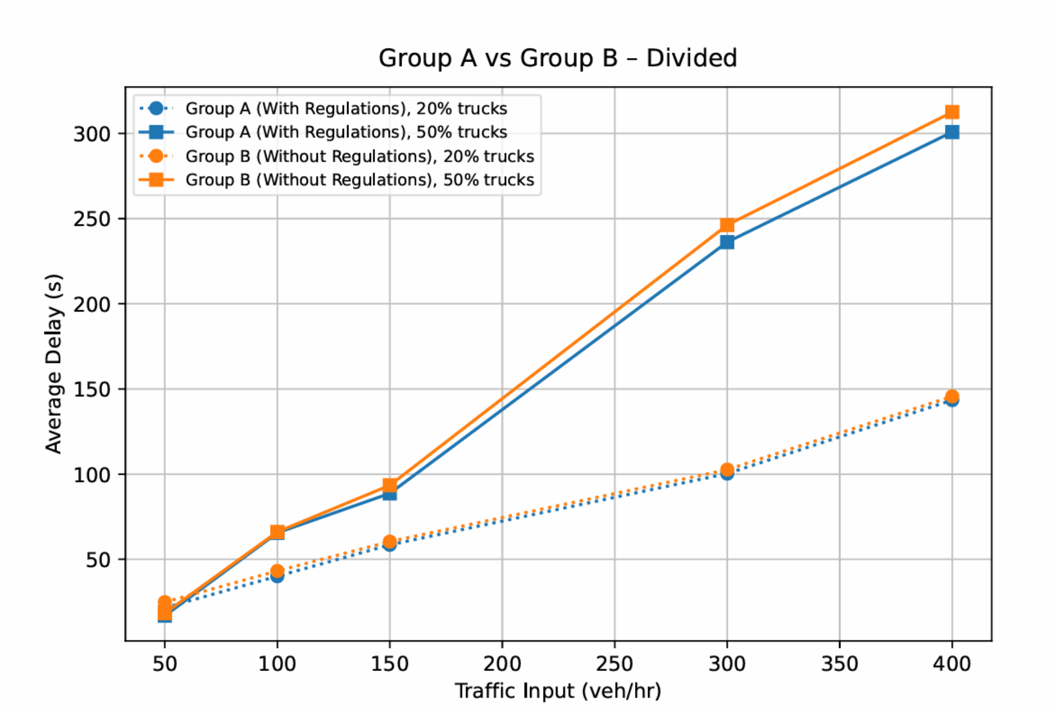

Figure 32: Average delays comparison for multilane divided highway segments between Group A (with platooning regulations) and Group B (without platooning regulations) across various traffic input levels and truck percentages

The comparison in **Figure 32** shows an upward trend in delays as traffic input increases under all circumstances, as expected given the higher vehicle interactions at higher volumes. When comparing the average delay results between groups A and B at 50% truck percentage, a slight increase in the average delay difference is observed as the traffic input increases. As the same platooning regulations were assigned to both groups A and B on the divided highway segments, vehicles arriving from the undivided segments with varying headways, speeds, spacing patterns, and lane usage distributions start with different initial conditions in A vs. B. Therefore, this results in a difference in performance when the truck percentage is high enough to create a tailgate impact from the undivided segments.

The statistical comparison between groups A (with platooning regulations) and B (without platooning regulations) on multilane divided highways also showed a significant difference ($t=-3.52$, $p=0.0065$), with Group A exhibiting lower delay than Group B. However, the magnitude of the mean difference is small, approximately 5.2 seconds on average. As shown in Figure 21, the difference becomes more visible primarily at the 50% truck percentage level as the traffic input increases. This pattern suggests that the observed difference was not generated by the divided segment itself but originated externally by the carry-over effect of the vehicle flow from the undivided segments, which had substantially higher delays. In practice, small stochastic fluctuations in vehicle entry times, lane changes, and spacing patterns could easily account for the observed sub-second differences in the divided segments. Therefore, despite the presence of statistical significance, the multilane divided segment still functions as an appropriate and technically justified control condition.

Group A vs Group B on undivided segments

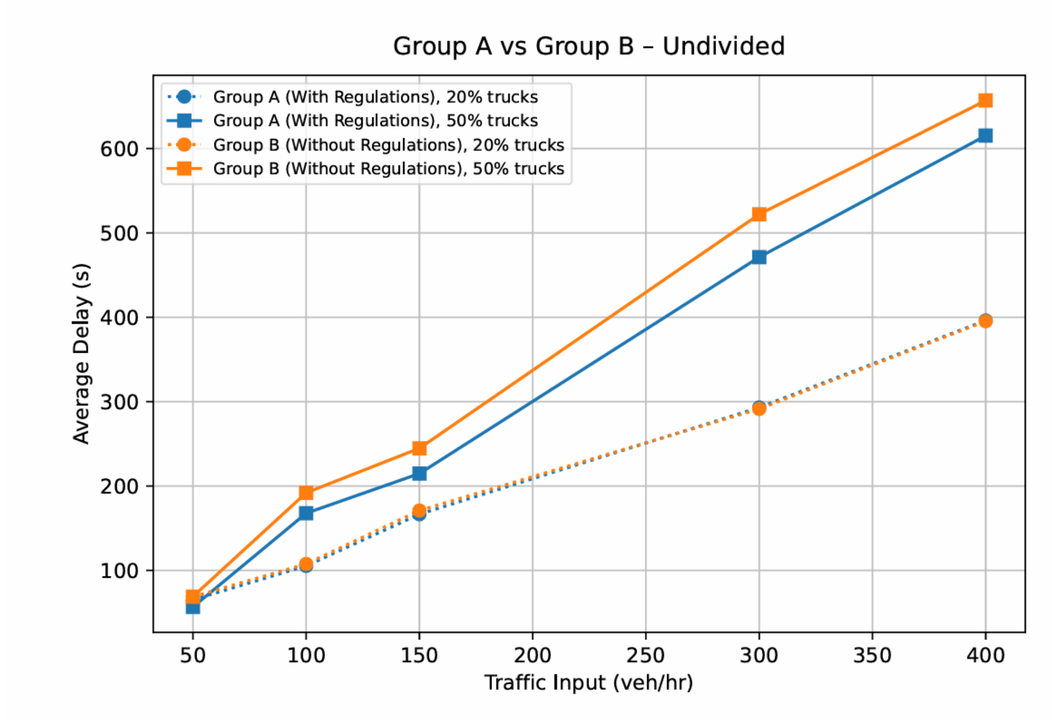

Figure 33: Average delays comparison for two-lane undivided highway segments between Group A (with platooning regulations) and Group B (without platooning regulations) across various traffic input levels and truck percentages

Due to the limited passing opportunities and significant impact of slow-moving trucks on two-lane undivided highways, average delays increase dramatically with volume across all traffic input levels. Group A consistently outperforms Group B at the higher truck percentage of 50%, while the difference in average delays between Group A and B is minimal at the lower truck percentage of 20%.

As shown in **Figure 33**, on undivided highway segments, Group A recorded higher performance with an average delay (255.19 s) compared with Group B (271.87 s), with a mean difference of −16.68 s ($t = -2.79$, $p = 0.021$). The Wilcoxon test confirmed this significance ($p = 0.0098$). The 95% bootstrap CI [−28.07, −6.27] further validates that the longer platoon (Model B) consistently produced higher delay time in undivided highway segments. This finding can be explained by the effects of platoon length and the overtaking constraints inherent to undivided highways. This result is consistent with realistic traffic flow expectations: longer platoons considerably reduce the opportunities for following traffic to overtake on undivided, single-lane-per-direction roads.

When an eight-truck platoon occupies the lane, HDVs must wait for extended passing gaps, causing local queuing and increased average delay. In contrast, when the number of trucks allowed to form a platoon is restricted in Group A, shorter two-truck platoons in Group A create more frequent overtaking opportunities, allowing general traffic to recover faster after slowdowns or interruptions. Therefore, the higher delay observed in Model B is directly linked to longer platoons acting as mobile bottlenecks on undivided segments. Model A's shorter platoons produced lower total delays, confirming that on constrained two-lane highways, platoon size should remain limited to maintain operational fluidity.

Group A comparison of divided vs undivided segments and Group B comparison of divided vs undivided segments

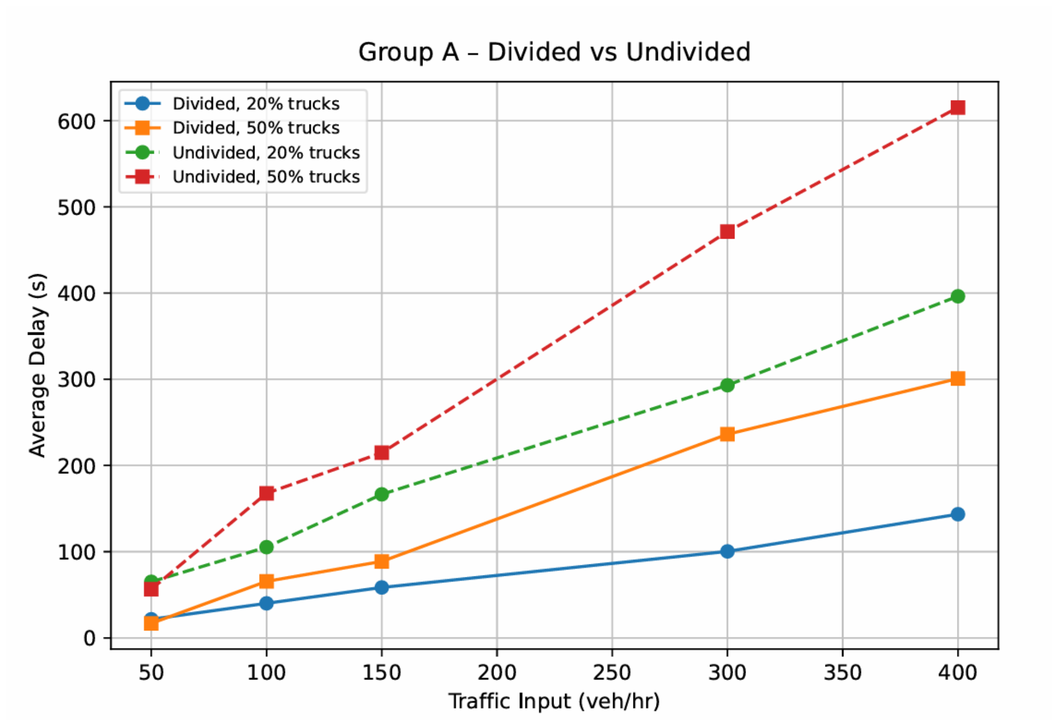

Figure 34: Average delays comparison for Group A (with platooning regulations) on divided and undivided segments across varying traffic inputs and truck percentages

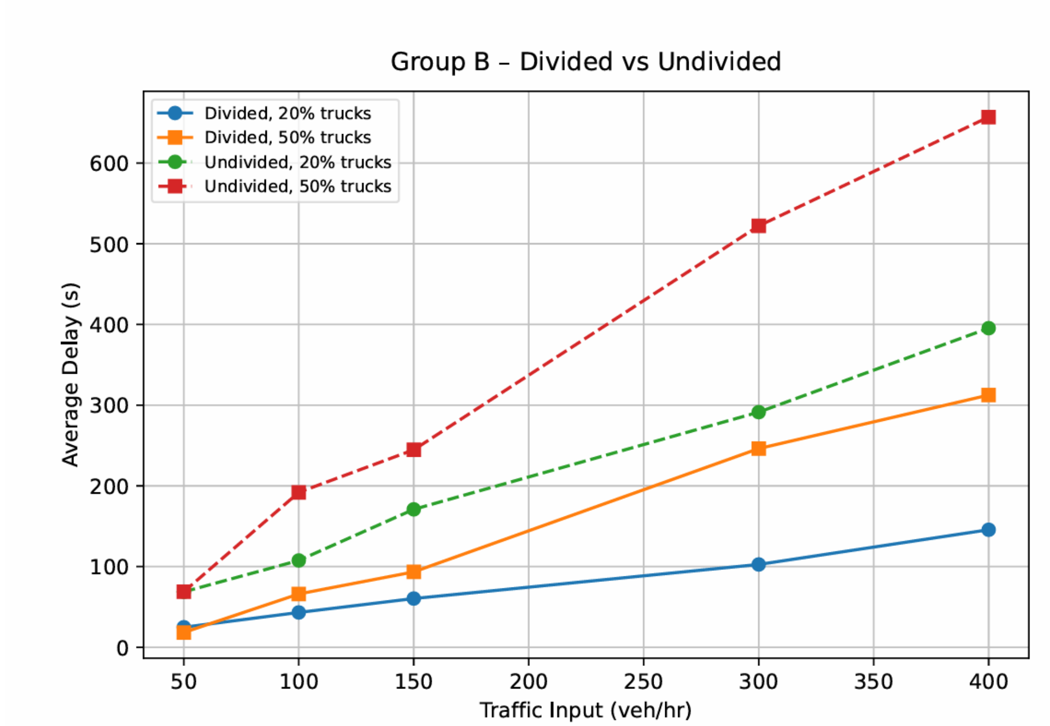

Figure 35: Average delays comparison for Group B (without platooning regulations) on divided and undivided segments across varying traffic inputs and truck percentages

The delay patterns in both **Figure 34** and **Figure 35** demonstrate a clear and consistent difference between divided and undivided highways. Delays are significantly reduced on the divided multilane segment in both Groups A (with regulations) and B (without regulations), and they progressively rise with increased traffic volumes. In both comparisons, a truck percentage of 50% creates higher delays than 20% at each traffic input level. This illustrates the compounding effects of mixed traffic and few opportunities for overtaking: as trucks slow down, lines quickly form behind them, constricting the flow of traffic.

Similarly in statistical results, both comparisons of segment types (divided vs undivided) for group A and B exhibited significantly higher average delay on undivided segments compared with divided ones. For Group A, the average delay increased from 106.71 s (divided segments) to 255.19 s (undivided segments), resulting in a mean difference of 148.48 s ($t = -4.89$, $p = 0.0009$; $d_z = -1.55$). For Group B, the average delay increased from 111.92 s (divided segments) to 271.87 s (undivided segments), resulting in a mean difference of 159.95s ($t = -4.94$, $p = 0.0008$; $d_z = -1.56$).

Therefore, both effects are statistically significant with very large effect sizes, indicating that a multilane divided segment type produces a significantly greater improvement in performance than a two-lane undivided segment type. The average reduction of approximately 150–160 seconds demonstrates that roadway geometry (corridor segment type) greatly impacts the delay outcomes.

Average Delay Comparison by Factors and Interaction Effects:

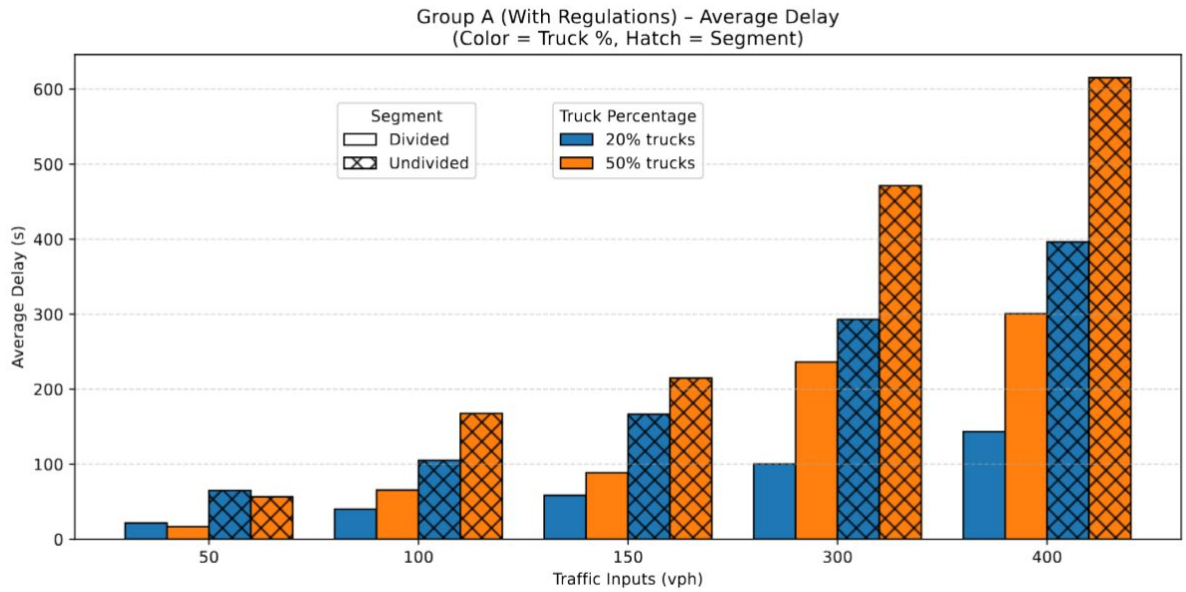

Figure 36: Average delays comparison for Group A (with platooning regulations) across divided and undivided highway segments for varying truck percentages and traffic input levels

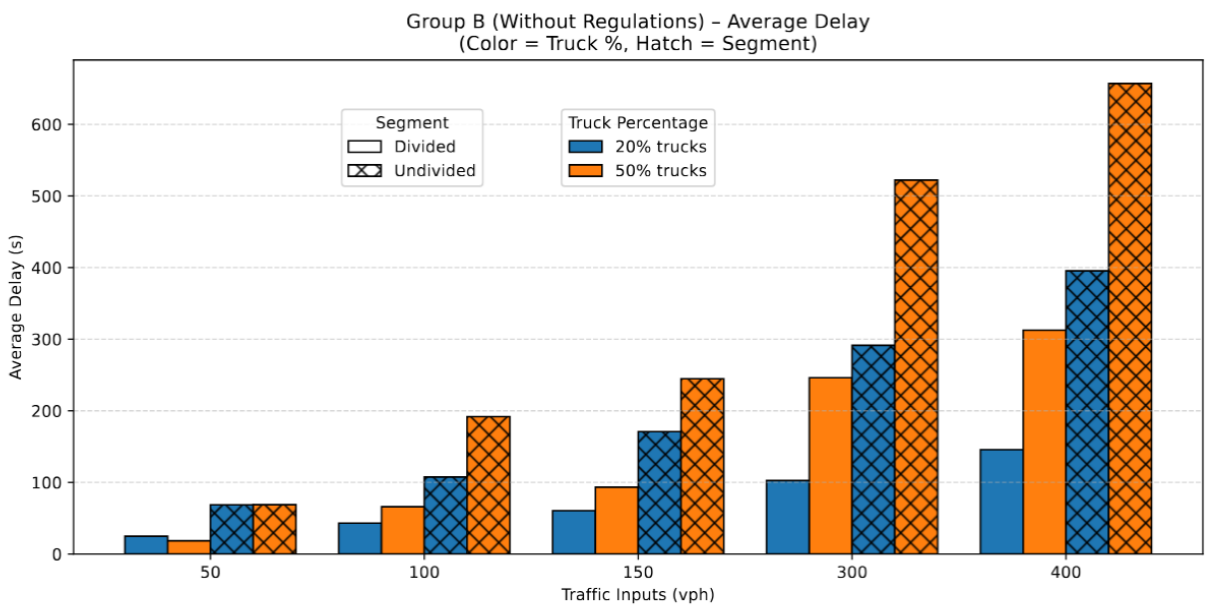

Figure 37: Average delays comparison for Group B (without platooning regulations) across divided and undivided highway segments for varying truck percentages and traffic input levels

According to **Figure 36** and **Figure 37**, undivided segments have substantially higher average delays than the divided segments. The average delay difference between divided and undivided segments grows dramatically with increasing traffic input. When traffic input exceeds 150 vehicles per hour, average delays increase sharply in undivided segments, while those in divided segments increase gradually. The truck percentage also shows a disproportionate increase, from 20% to 50% generally.

Table 13: ANOVA Test Results for Average Delay Comparison by Factors and Interaction Effects

Effect	**Sum Sq**	**Effect Size (η^2_p)**	**F**	**p-value**	**Interpretation**
Group	1,196.95	0.008	0.265	0.610	Not significant
Segment Type	237,818.55	0.608	52.684	<0.001	Highly significant effect
Group × Segment Type	329.13	0.002	0.073	0.789	Not significant
Traffic Input	591,783.25	0.794	131.097	<0.001	Significant
Truck Percentage	85,808.73	0.358	19.009	<0.001	Significant

Similar to the average speed comparison, segment types (divided vs. undivided), traffic input, and truck percentage are the three factors that had significant effects on the average delays, according to the ANOVA test results shown in **Table 13**. The effect of regulation groups, A (with platooning regulations) vs B (without platooning regulations), did not show a significant difference ($p = 0.610$, $\eta^2_p = 0.008$). This is because the scale of the differences in average delay caused by Groups A and B is minimal compared with the large effect sizes of the segment types, traffic input, and truck percentages. Therefore, platooning regulations did not generate significant changes at network-scale congestion levels. Traffic input had the strongest effect on delay ($\eta^2_p = 0.794$), indicating that higher traffic input disproportionately increases delay, even before the system reaches full capacity. This outcome aligns with established traffic engineering principles and reflects the expected behavior of mixed traffic operation. In conclusion, segment types (divided vs. undivided), traffic input, and truck percentage dominated the average delay outcomes.

4.5 Results and Discussions (Safety Performance)

This section focuses on conflict-based surrogate safety outcomes generated using the SSAM. Safety evaluation is performed across a full factorial combination of traffic input and truck percentage, allowing systematic examination of how operating conditions influence conflict patterns. The results from SSAM analysis for Group A (with regulations) and Group B (without regulations) are summarized in **Table 14**.

Table 14: SSAM Results

Groups	Traffic Input	Truck Percentage	Total Conflicts	Unclassified Conflicts	Crossing Conflicts	Rear End Conflicts	Lane Change Conflicts
A (With Regulations)	50 veh/hr	20%	13	0	0	12	1
		50%	12	0	3	9	0
	100 veh/hr	20%	49	0	3	42	4
		50%	68	0	6	56	6
	150 veh/hr	20%	397	0	26	348	23
		50%	342	0	25	310	7
	300 veh/hr	20%	342	0	25	310	7
		50%	8,687	0	334	8,216	137
	400 veh/hr	20%	13,091	0	1,886	10,539	666
		50%	18,392	0	2,868	15,062	462
B (Without Regulations)	50 veh/hr	20%	5	0	0	3	2
		50%	17	0	3	13	1
	100 veh/hr	20%	89	0	4	80	5
		50%	89	0	7	78	4
	150 veh/hr	20%	517	0	47	449	21
		50%	551	0	27	515	9
	300 veh/hr	20%	5,824	0	390	5,224	210
		50%	11,233	0	302	10,811	120
	400 veh/hr	20%	14,031	0	2,029	11,285	717
		50%	19,675	0	2,998	16,298	379

4.5.1 Total Conflicts

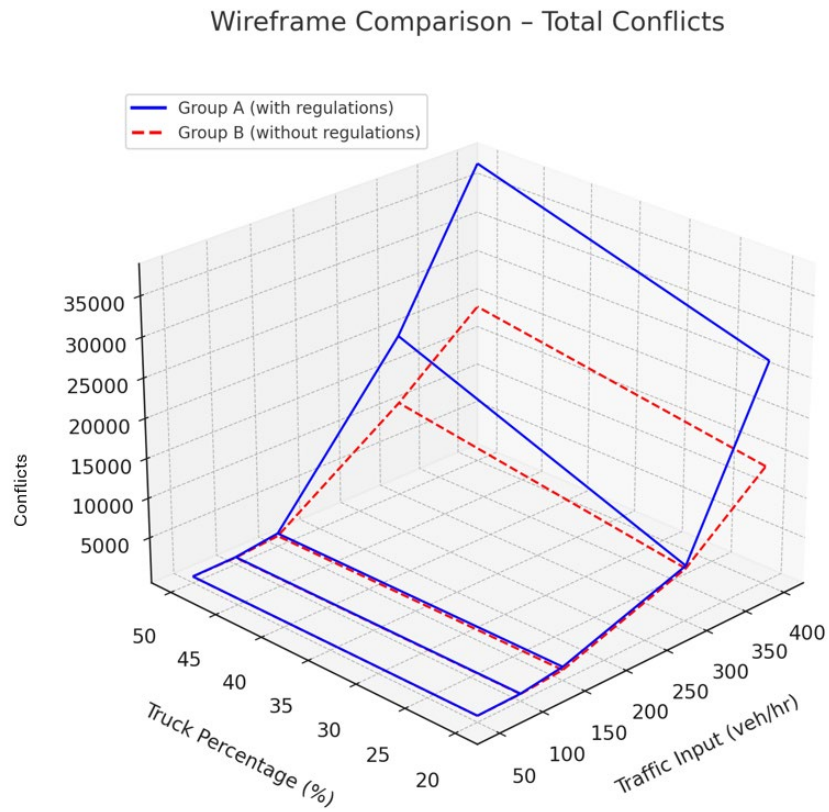

Figure 38: 3D wireframe comparison of total conflicts between Group A and B

Wireframe plots in **Figure 38** demonstrate that Group A (with platoon regulations) have higher total conflict counts than Group B, especially at traffic inputs of 300 vehicles per hour or more. This reduction is caused by the stabilizing influence of longer platoons in the network. An eight-truck platoon performs as a cohesive and predictable unit, which reduces speed variance and minimizes overtaking maneuvers. Conversely, limiting platoons to two trucks, as in Group A, produces a greater number of small platoons distributed throughout the network. The frequent formation and dissolution of these small platoons generate more interactions with surrounding traffic, increasing turbulence and the likelihood of conflicts. Consequently, the higher number of small platoons directly contributes to the elevated conflict counts observed in Group A.

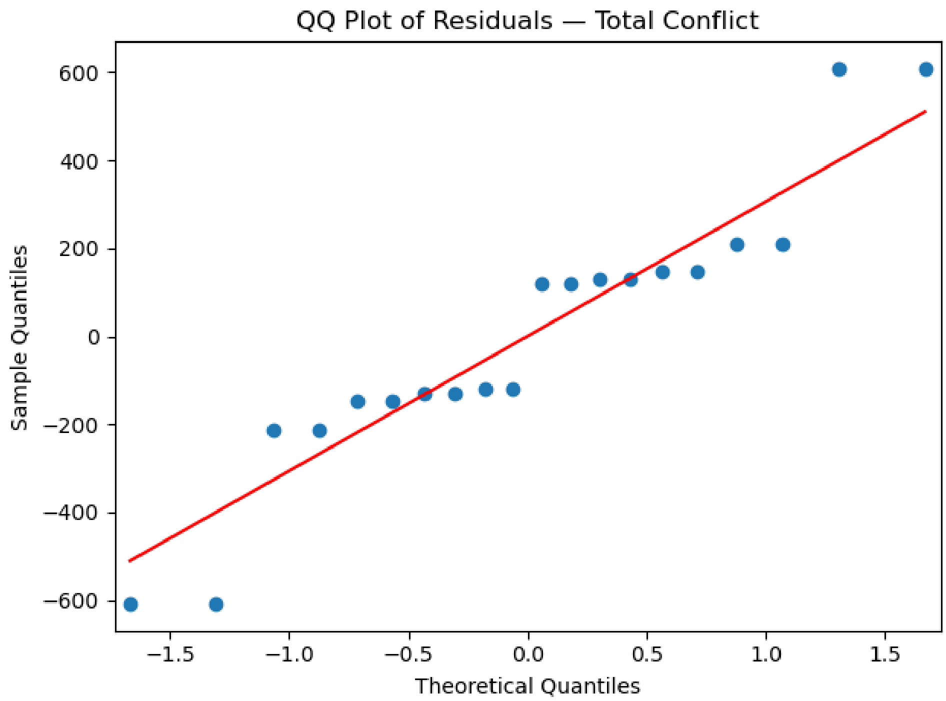

Figure 39: QQ plot of residuals for total conflicts

The Shapiro-Wilk test ($p = 0.0925$) supports the assumption of normality, and the QQ plot (**Figure 39**) shows residuals closely following the theoretical diagonal, indicating acceptable distributional symmetry and homoscedasticity.

Table 15: ANOVA Test Results Summary for Total Conflicts

Source	Sum Sq	df	F-Value	P-Value (PR(>F))
Group	5,658,352.2	1.0	12.093442	0.025408
Traffic Input	796,957,711.2	4.0	425.829001	0.000016
Truck Percentage	30,524,263.2	1.0	65.238676	0.001276
Group & Traffic Input	11,717,268.8	4.0	6.260750	0.051681
Group & Truck Percentage	315,005.0	1.0	0.673252	0.458002
Traffic Input & Truck Percentage	46,717,352.8	4.0	24.961931	0.004337

The ANOVA results shown in **Table 15** indicate significant main effects for Group ($p = 0.025$), Traffic Input ($p < 0.001$), and Truck Percentage ($p = 0.001$). The Group × Traffic Input interaction approached significance ($p = 0.052$), suggesting that platooning regulations' impact on total conflicts may vary across traffic demand levels.

4.5.2 Crossing Conflicts

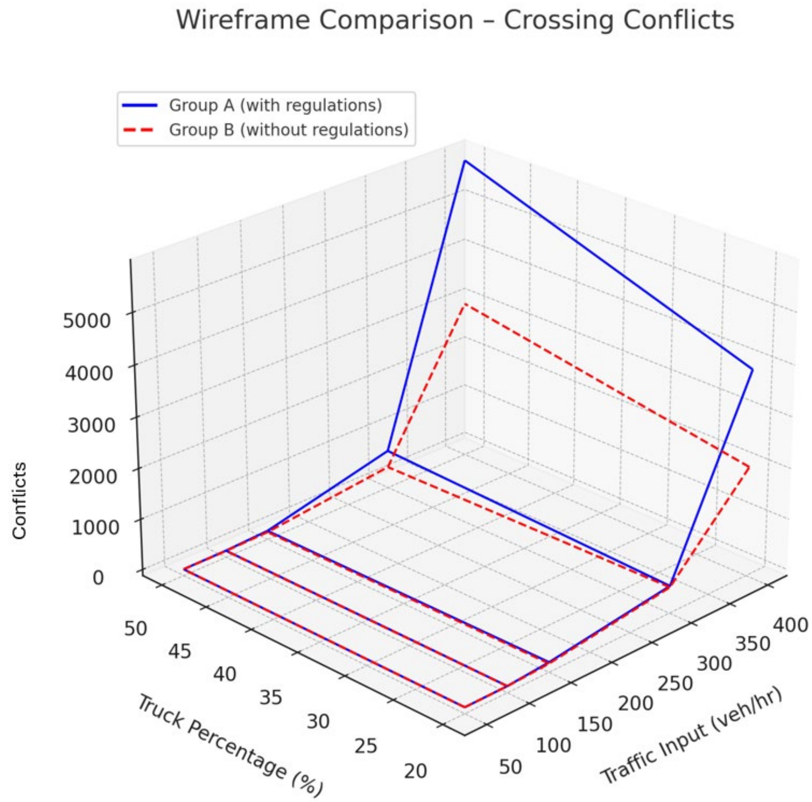

Figure 40: 3D wireframe comparison of crossing conflicts between Group A and B

As shown in **Figure 40**, crossing conflicts followed a similar trend, with Group B showing lower conflict values compared with Group A. The key factor driving this result is the temporal gap structure created by platoons of different sizes. The long platoons in Group B pass through crossing points as a single coordinated block, followed by a large, predictable gap in traffic. Minor road vehicles typically adjust their behavior by waiting for the platoon to clear and then accepting the large gap that follows, resulting in fewer risky crossing attempts.

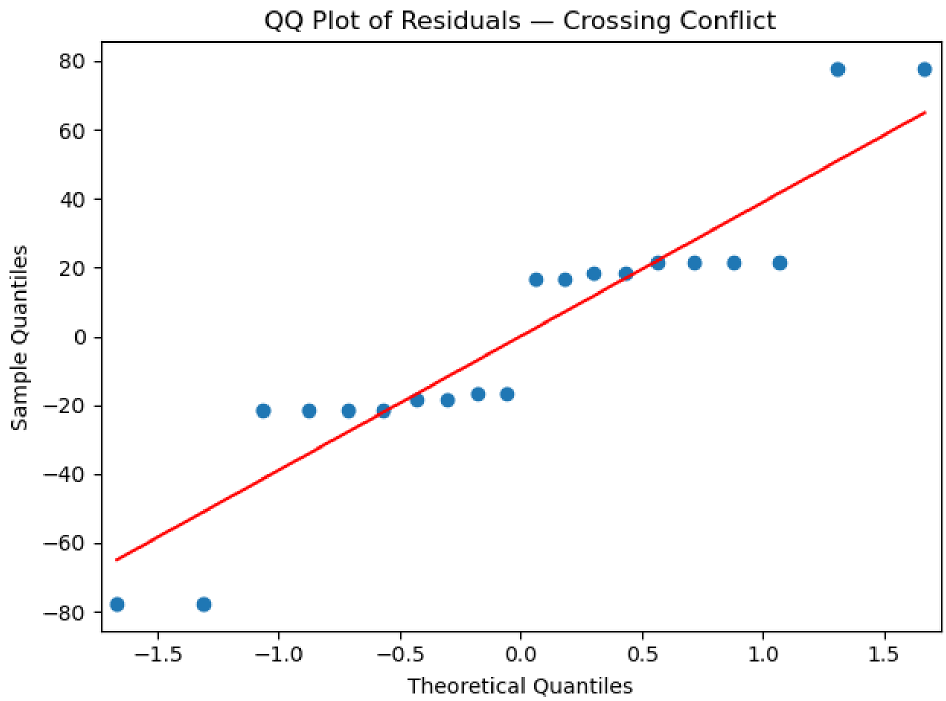

Figure 41: QQ plot of residuals for crossing conflicts

The Shapiro-Wilk test ($p = 0.0332$) indicates mild non-normality, which is visible in the QQ plot (**Figure 41**) as slight deviations in the tails. Despite this, the residual distribution remains approximately linear, supporting the robustness of ANOVA inference.

Table 16: ANOVA Test Results Summary for Crossing Conflicts

Source	**Sum Sq**	**df**	**F-Value**	**P-Value (PR(>F))**
Group	19,908.05	1.0	2.625292	0.180488
Traffic Input	18,165,841.30	4.0	598.886393	0.000008
Truck Percentage	233,928.45	1.0	30.848352	0.005143
Group & Traffic Input	26,579.70	4.0	0.876272	0.549386
Group & Truck Percentage	9,202.05	1.0	1.213482	0.332471
Traffic Input & Truck Percentage	730,010.30	4.0	24.066776	0.004647

The ANOVA results in **Table 16** show that Traffic Input and Truck Percentage both exhibited strong effects ($p < 0.01$), while the Group effect was non-significant ($p = 0.180$). Crossing conflicts are driven primarily by traffic flow dynamics rather than platooning regulations implementation.

4.5.3 Rear End Conflicts

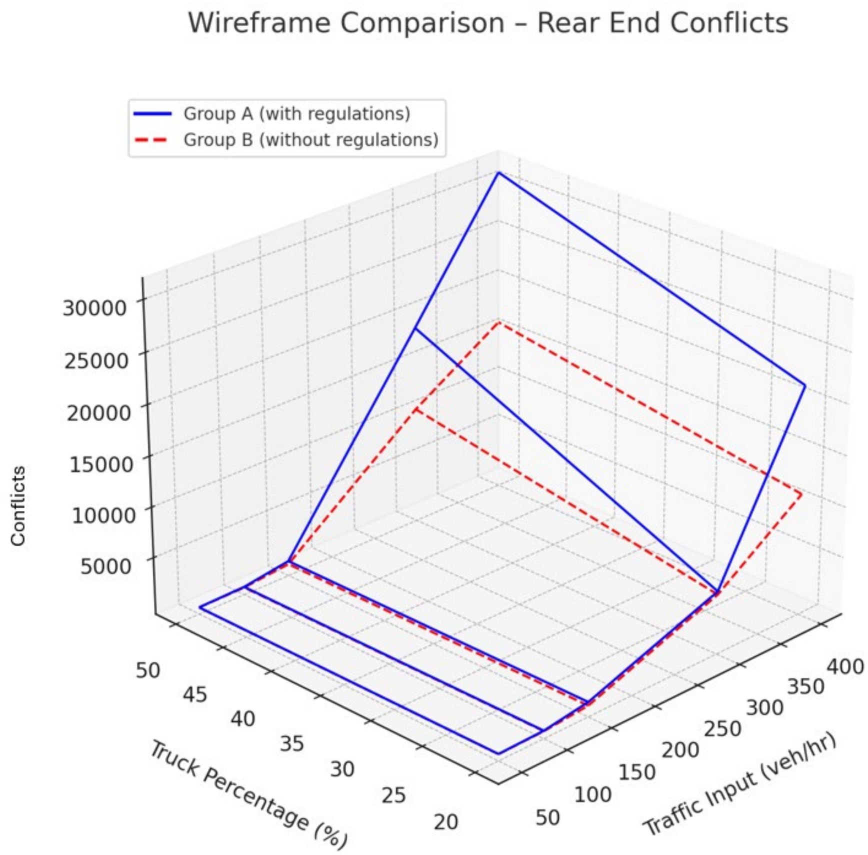

Figure 42: 3D wireframe comparison of rear end conflicts between Group A and B

Figure 42 indicates that rear-end conflicts showed a strong dependence on platoon size, with Group B consistently experiencing fewer incidents than Group A across all traffic conditions. The frequency of rear-end conflicts was substantially higher in Group A, particularly under conditions of high truck percentages and heavy traffic volume. Mechanistically, small two-truck platoons create more interfaces where vehicles must adjust speeds when encountering or catching up to these platoons. Rear-end collisions are more likely as a result of these interactions, which intensify speed differentials and produce braking shockwaves that travel upstream. In contrast, longer platoons formed in group B (without regulations) maintain more stable internal spacing and impose steadier flow conditions on surrounding vehicles. The uniform speed and synchronized behavior of long platoons reduce abrupt decelerations and mitigate the formation of shockwaves, thereby reducing rear-end conflicts.

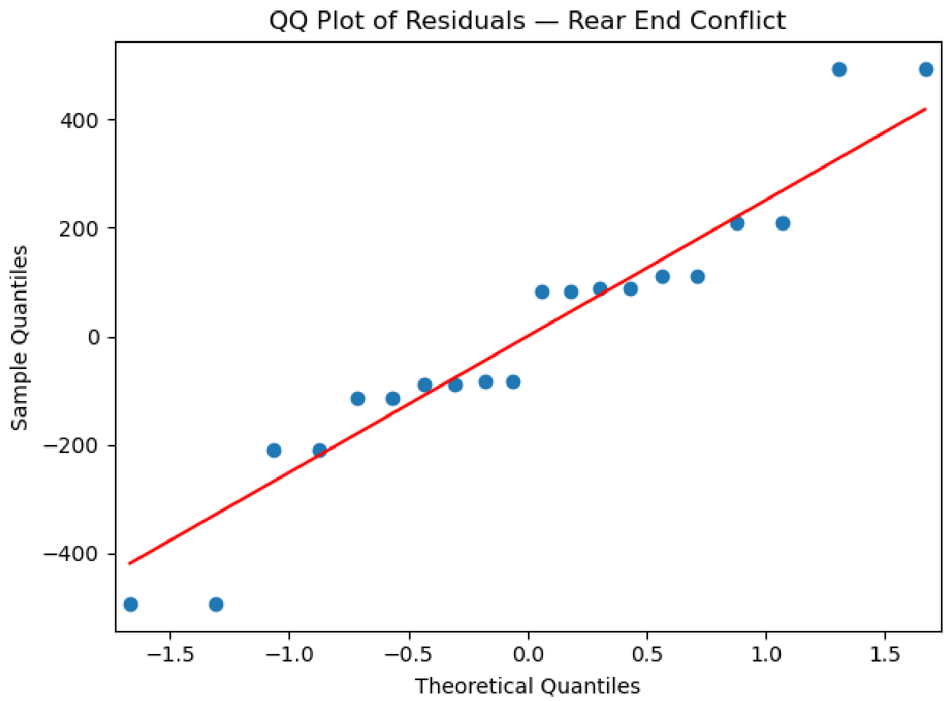

Figure 43: QQ plot of residuals by rear end conflict

The Shapiro-Wilk test ($p = 0.2250$) confirms residual normality, and the QQ plot (**Figure 43**) shows points tightly aligned with the 45° line, suggesting that model assumptions were well satisfied.

Table 17: ANOVA Test Results Summary for Rear End Conflicts

Source	**Sum Sq**	**df**	**F-Value**	**P-Value (PR(>F))**
Group A vs B	4,853,095.0	1.0	15.431436	0.017128
Traffic Input	541,333,800.0	4.0	430.321153	0.000016
Truck Percentage	26,625,090.0	1.0	84.660065	0.000775
Group & Traffic Input	10,249,570.0	4.0	8.147666	0.033238
Group & Truck Percentage	149,299.2	1.0	0.474728	0.528704
Traffic Input & Truck Percentage	41,624,240.0	4.0	33.088256	0.002531

The ANOVA results in **Table 17** show that significant effects were observed for Group ($p = 0.017$), Traffic Input ($p < 0.001$), and Truck Percentage ($p < 0.001$), along with notable Group & Traffic Input ($p = 0.033$) and Traffic Input & Truck Percentage ($p = 0.003$) interactions. Rear-end conflicts are significantly reduced with platooning regulation implementation, especially at higher traffic inputs. This aligns with expectations, as automated following control stabilizes headways and dampens stop-and-go oscillations.

4.5.4 Lane Change Conflicts

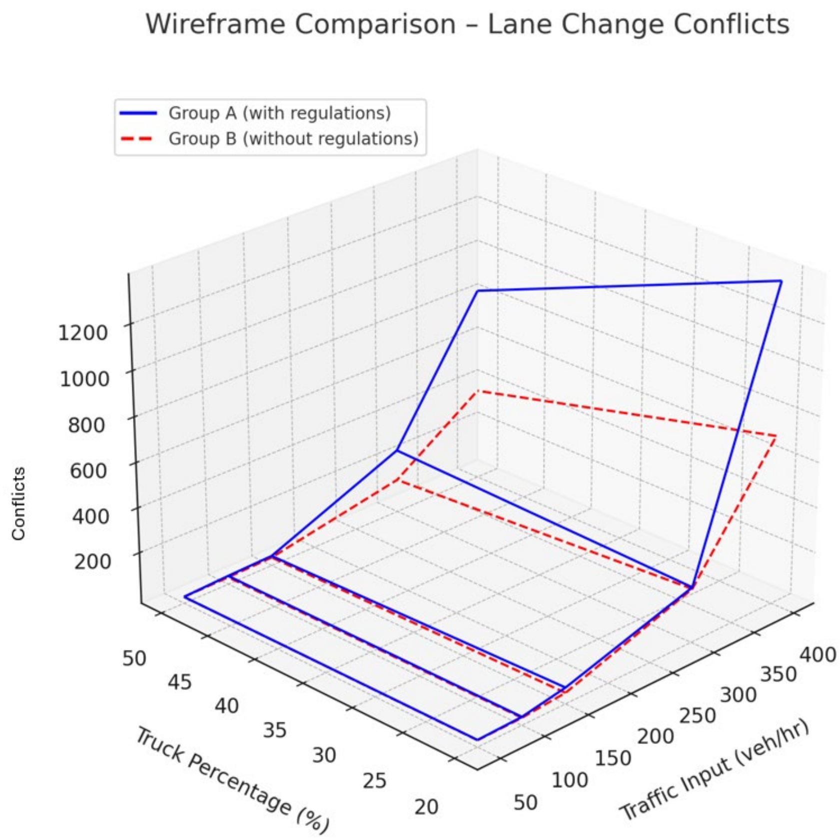

Figure 44: 3D wireframe comparison of lane change conflicts between Group A and B

As shown in **Figure 44**, lane-change conflicts were consistently higher in Group A. The large number of small platoons creates more platoon boundaries where passing and merging attempts occur. Each two-truck platoon introduces two boundaries that vehicles attempt to overtake or merge into, increasing the frequency of lane-changing maneuvers. By contrast, Group B forms fewer but substantially longer platoons. This reduces the number of platoon boundaries and therefore decreases the number of opportunities for lane-changing interactions to occur. In addition, drivers are less likely to attempt overtaking an eight-truck platoon because the required passing distance is considerably longer, making the maneuver more challenging and less attractive. Overall, the reduced frequency of passing events around long platoons explains the lower lane-change conflict rates observed in Group B.

Lane-change conflicts were consistently higher in Group A. The large number of small platoons creates more platoon boundaries where passing and merging attempts occur. Each two-truck platoon introduces two boundaries that vehicles attempt to overtake or merge into, increasing the frequency of lane-changing maneuvers.

By contrast, Group B forms fewer but substantially longer platoons. This reduces the number of platoon boundaries and therefore decreases the number of opportunities for lane-changing interactions to occur. In addition, drivers are less likely to attempt overtaking an eight-truck platoon because the required passing distance is considerably longer, making the maneuver more challenging and less attractive. Overall, the reduced frequency of passing events around long platoons explains the lower lane-change conflict rates observed in Group B.

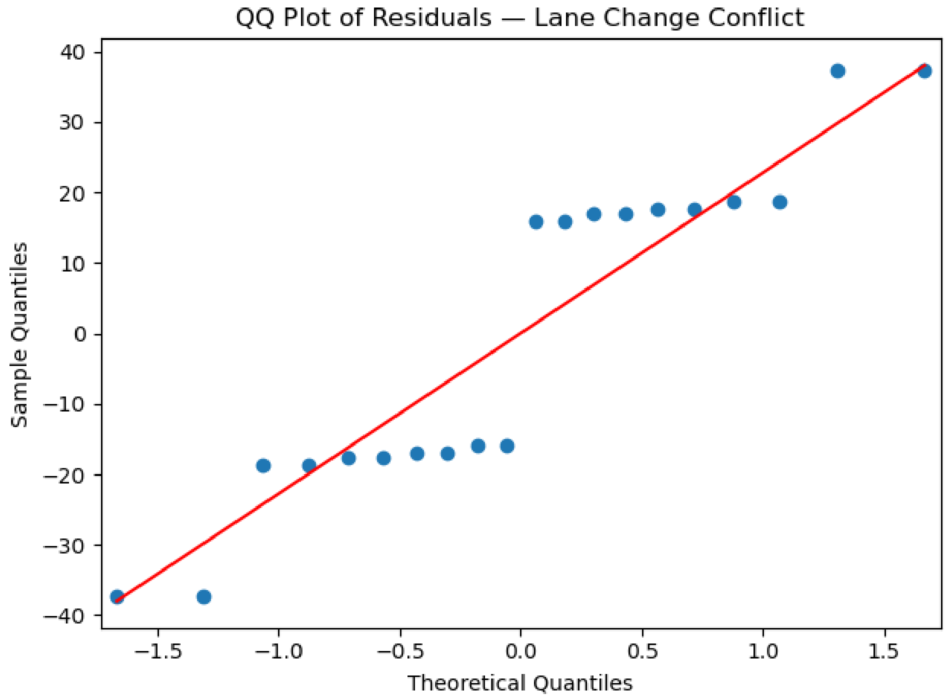

Figure 45: QQ plot of residuals by lane change conflict

The QQ plot (**Figure 45**) reveals moderate skewness and heavier tails, consistent with the Shapiro-Wilk result, suggesting that the variance structure may differ slightly across traffic conditions. However, given the balanced design and relatively low F-ratios, ANOVA remains appropriate for exploratory interpretation.

Table 18: ANOVA Test Results Summary for Lane Change Conflicts

Source	Sum Sq	df	F-Value	P-Value (PR(>F))
Group	1,201.25	1.0	0.463588	0.533326
Traffic Input	907,009.20	4.0	87.508606	0.000380
Truck Percentage	14,098.05	1.0	5.440742	0.080029
Group & Traffic Input	7,705.00	4.0	0.743381	0.609600
Group & Truck Percentage	6,230.45	1.0	2.404465	0.195928
Traffic Input & Truck Percentage	59,940.20	4.0	5.783054	0.058795

The ANOVA results in **Table 18** show that although traffic input remained significant ($p < 0.001$), Group had no effect ($p = 0.533$). Interactions were all non-significant. Lane change conflicts are primarily influenced by flow intensity. This may reflect that platooning constrains lane changes but does not eliminate lane-change-induced turbulence.

In summary, the combined results suggest that truck platooning implementation meaningfully influences rear-end and total conflict types, the categories most directly associated with longitudinal vehicle control. However, crossing and lane-change conflicts remain largely governed by exogenous traffic factors and driver behavioral variability. These findings highlight that, from a surrogate safety perspective, permitting longer platoons may be advantageous on rural highways if roadway geometry, traffic regulations, and communication systems can support their safe operation.

4.6 Section Conclusion

This part of the project evaluates the operational and safety impacts of truck platooning on U.S. Highway 287 in Wyoming, a rural corridor with limited overtaking opportunities. Using high-resolution microsimulation and conflict-based safety analysis, the research assessed the effects of roadway geometry, traffic demand, truck percentages, and platoon size regulations. Two configurations were tested: Group A (maximum of two trucks on undivided segments) and Group B (up to eight trucks). The findings offer practical guidance for evidence-based freight and CAV policies, demonstrating that successful platooning requires a context-dependent approach balancing mobility and safety.

Roadway geometry is the primary determinant of traffic performance. Multilane divided segments consistently supported higher speeds (5–6 mph greater) and significantly lower delays (150–160 seconds less) than two-lane undivided segments, highlighting the critical role of overtaking opportunities and directional separation. On undivided segments where overtaking is restricted, long platoons act as moving bottlenecks. Under these conditions, shorter two-truck platoons (Group A) slightly but significantly improved mobility by reducing queues and delays compared with eight-truck platoons (Group B). Furthermore, increased traffic inputs (exceeding 150 vehicles/hour) and higher truck percentages (from 20% to 50%) severely exacerbated mobility penalties on undivided highways. Ultimately, long platoons are viable on divided highways, whereas shorter platoons are necessary on undivided segments to maintain flow quality.

The safety analysis revealed substantial differences based on platoon size regulations. Shorter platoons (Group A) generated a higher number of total and rear-end conflicts, especially under heavy traffic and high truck percentages. Numerous small platoons create more boundaries and speed variability, which increases interactions with human-driven vehicles and leads to more frequent braking events. Conversely, longer platoons (Group B) operate as stable, synchronized units that smooth surrounding traffic flow and mitigate shockwaves, effectively reducing longitudinal conflict risk. Lateral conflicts (crossing and lane-changing) were primarily driven by overall traffic demand rather than platoon regulations. Therefore, while longer platoons enhance longitudinal safety under heavy traffic, this benefit must be carefully weighed against their operational drawbacks on constrained rural segments.

Despite its rigorous design, this part of the project has two primary limitations. First, the absence of active truck platoon operations in Wyoming prevented the calibration and validation of the simulation using real-world observed behaviors, traffic interactions, and safety outcomes. Second, the simulations relied on idealized weather assumptions and did not account for severe weather conditions typical of Wyoming, such as snow, fog, and strong winds, which significantly impact real-world traffic operations and safety.

To advance truck platooning research and deployment, future efforts should transition from fixed restrictions to real-time, V2X-enabled (V2V and V2I) dynamic platoon management. This approach would allow for variable lengths, adaptive gap-opening, and cooperative multi-step overtaking. Furthermore, simulation models must be expanded to test platoons under stress conditions like higher volumes, steep grades, and adverse weather, while incorporating mixed-fleet dynamics and varied human driver compliance. Moving forward, these advanced modeling efforts must be empirically calibrated and validated using real-world data from WYDOT connected vehicle testbeds. Analysis should then be expanded statewide to fully evaluate Wyoming's infrastructure readiness. Finally, these technical evaluations should be paired with comprehensive cost-benefit and policy analyses to quantify the trade-offs between fuel efficiency, safety, and traffic delay, helping formulate practical and operationally relevant regulatory recommendations.

5. GAP OPENING CONTROL FOR TRUCK PLATOONS TO FACILITATE OVERTAKING ON TWO-LANE HIGHWAYS

This section has been published as the paper “Gap Opening Control to Facilitate Human-Driven Vehicle Overtaking of Connected and Automated Vehicle Platoons on Two-Lane Highways” 2025 IEEE 3rd International Conference on Mobility, Operations, Services and Technologies (MOST), DOI: 10.1109/MOST65065.2025.00017. Slight modifications were applied to ensure consistency in this report.

5.1 Introduction

Despite the advantages and benefits from the strategy of implementing truck platoons on highways, connected and automated vehicle (CAV) platooning introduces new challenges, particularly regarding its safe integration into mixed traffic environments shared with human-driven vehicles (HDVs) (*13*, *18*, *22*, *73*, *74*, *80*, *81*). One of the most pressing concerns is that HDVs often struggle to navigate around these closely spaced convoys. Safety risks are heightened in situations where overtaking maneuvers are necessary (*26*, *81*). The limited gaps within the platoon can obstruct a clear path for human drivers. These risks are amplified on two-lane undivided highways, where passing vehicles must share the same lane with opposing traffic, making overtaking maneuvers both complex and hazardous (*22*, *74*, *97*, *117*, *118*).

The safety implications of overtaking platoons on two-lane highways bring the need for adaptive strategies to accommodate HDVs. A key aspect of this challenge is to determine when and how the platoon should dynamically adjust its formation to create a sufficient gap for overtaking. Failure to provide adequate space could lead to incomplete overtaking and collisions with oncoming traffic. Conversely, if the platoon splits unnecessarily, it may compromise the efficiency benefits of platooning, undermining its primary advantage of reduced aerodynamic drag.

Guided step-by-step overtaking is a potential solution to address the safety challenges in HDVs overtaking of CAV platoons (*124*, *125*). In guided step-by-step overtaking, the passing vehicle overtakes part of the platoon in each step and overtakes the entire platoon with multiple steps. In each step, the passing vehicle provides a message of where in the platoon is safe to merge into to avoid collision with oncoming traffic. The message can be provided using indicator or message sign displays on platoon vehicles or transmitted directly onto the passing vehicle’s in-vehicle driver assistance devices (*68*, *97*, *126*, *127*).

There are two major control tasks in guided overtaking of platoons: (1) determine a suitable gap in the platoon for the passing vehicle to merge into; and (2) control the gap’s follower vehicle to open the gap to a length that can safely accommodate the passing vehicle in a timely and smooth manner. Prior studies have focused on either task but not integrating both. Existing research on merge gap identification has focused on modeling and incorporating the passing vehicle’s driving behavior in the overtaking platoon scenarios, formulating the problem from the passing vehicle’s perspective, and developing algorithms to solve for optimal passing vehicle movements to complete the step-by-step overtaking (*124*, *125*). While providing a driver assistance solution for the overtaking platoon problem is significant progress, to truly guarantee safety and efficiency of step-by-step overtaking, more work can be done from the platoon’s perspective. An advantage to developing a platoon vehicle control solution for the overtaking problem is that platoon vehicles are already equipped with CAV technologies, which provide the necessary platform and resources for implementation of sophisticated control algorithms. Additionally, existing gap opening controller designs are available and are developed based on the CACC framework, although mostly for handling cut-in or on-ramp merging scenarios (*128–134*). They can be easily adapted to handle step-by-step overtaking once we incorporate scenario-specific setup parameters and constraints in the control decision process. Our controller design considers constraints such as the variability in HDV behavior, real-time adjustments to opposing traffic dynamics, and the need to optimize platoon stability during gap opening.

This chapter's objective is to address the technical challenges in accommodating HDVs in overtaking CAV platoons by developing a platoon control strategy to identify the optimal gap in a platoon to open in order to facilitate safe and efficient overtaking, as well as the optimal time to start the gap opening maneuver. This chapter extends existing gap opening controller designs from ramp merging applications in (*131*, *132*) to the overtaking context, incorporating scenario-specific dynamics and restrictions. The strategy consists of a set of algorithms that determine the key parameters for gap opening (i.e., gap location, start and end times) based on real-time dynamics of passing and opposing vehicles and the platoon vehicles, ensuring that the maneuver can be completed efficiently and accurately without compromising safety. We focus on the partial overtaking scenario, where the platoon temporarily adjusts to open a gap for a single vehicle. We aim to provide a robust solution for this basic and more general problem so it can be further expanded to resolve more complex problems of step-by-step and multi-passing-vehicle step-by-step overtaking of platoons on two-lane undivided highways.

This chapter is followed by the formulation of a research problem in Section 5.2. Section 5.3 introduces the details of control strategy design, including algorithms for determining optimal gaps to open and optimal gap opening start time. Section 5.4 presents simulation results and discusses the performance and potential further improvements of the control strategy. Section 5.5 concludes the chapter and provides recommendations on applications.

5.2 Problem Statement

Overtaking a platoon involves critical challenges, including ensuring safe interactions of the passing human-driven vehicle (HDV) with opposing traffic and the control reliability of a vehicle platoon when opening a gap to accommodate the passing vehicle. Therefore, a robust strategy is needed for guiding the passing vehicle during overtaking of a platoon and simultaneously providing a safe space for the vehicle to merge into the platoon.

Assumptions used in this chapter of the report are:

1) Only the platooned vehicles are CAVs with CACC capabilities, and all other vehicles are HDVs without any active data sharing with the platoon vehicles. All vehicle kinematics of the HDV are assumed to be detected by the platoon vehicles and used in the CAV platoon's control decision making. The CAV platoon provides guidance messaging to the passing HDV, which is assumed to follow the guidance when overtaking.

2) The scenario of overtaking on a two-lane undivided highway has a similar merging maneuver with the on-ramp scenario, but the constraints considered in selection of merging gap are related to the movement of vehicles in the opposing direction and not static geometric constraints.

3) Considering that a passing vehicle starts its overtaking maneuver near the tail of a platoon, the platoon can start guiding the passing vehicle when it is still following the tail.

Therefore, in circumstances where the passing vehicle has a clearance to overtake multiple platoon vehicles, the spatial and temporal clearances should allow us to optimize the control strategy to maximize accuracy and reliability.

Variables used throughout this section and their definitions are listed in **Table 19**.

Table 19: List of Variables and Definitions

Variable	Definition
$a_i(t)$	Acceleration of i-th platoon vehicle
$d_i(t)$	Gap between i-th and $(i-1)$-th platoon vehicles
$d_{r,i}(t)$	Desired gap between i-th and $(i-1)$-th platoon vehicles
$e_{1,i}$, $e_{2,i}$, and $e_{3,i}$	Gap, speed, and acceleration errors of i-th platoon vehicle
e_{pred}	Vehicle trajectory prediction error
$\Upsilon_i(t)$	Gap opening term of i-th platoon vehicle
Υ_{ini} and Υ_{end}	Initial and final gap increase
$J_{error,k}$	Gap opening controller error of the k-th platoon vehicle
k	ID of the platoon vehicle to be primarily controlled to open gap between itself and its preceding vehicle
k_p and k_d	Control gain parameters
L_i	Summation of platoon vehicle's length, standstill distance, and following gap
λ	Polynomial fitting weight decay parameter
n	Platoon size (total number of vehicles in the platoon)
$q_p(t)$ and $q_p^*(t)$	Position and predicted position of passing vehicle
$q_0(t)$ and $q_0^*(t)$	Position and predicted position of opposing vehicle
$q_t(t)$ and $q_t^*(t)$	Position and predicted position of platoon head (front bumper of 1st platoon vehicle)
Q_p, Q_0 and Q_t	Sets of passing, opposing, and platoon vehicle position data
$t_{current}$	Current time
t_{end}	Time to complete merge of passing vehicle, also time to complete gap opening
t_{start}	Time to start gap opening
τ	Platoon vehicle driveline dynamics parameter
u_i	Control input of i-th platoon vehicle
$v_i(t)$	Speed of i-th platoon vehicle
w_i	Weights of the i-th data point of polynomial fitting

Guided step-by-step overtaking of a platoon is an operation for a situation where a passing vehicle attempts to overtake a multi-vehicle platoon on a two-lane undivided highway but cannot complete it in one step due to restrictions from opposing traffic. The step-by-step operation allows the passing vehicle to overtake part of the platoon (i.e., m out of n vehicles, where n is the size of the platoon and $m < n$) in one step and complete overtaking the entire platoon (of n vehicles) in multiple steps. In each step, the passing vehicle is guided by messages sent by the platoon indicating when it is safe to start passing and where it is safe to merge. Each step is a basic scenario of "single vehicle overtaking part of a platoon," as shown in **Figure 46**. To safely accommodate the passing vehicle in each basic scenario, the platoon tracks and predicts all vehicle trajectories to determine the gap position as well as the start and end times for gap opening. Since the control strategy operates iteratively in real time, the trajectory predictions and outputs are updated at each time step.

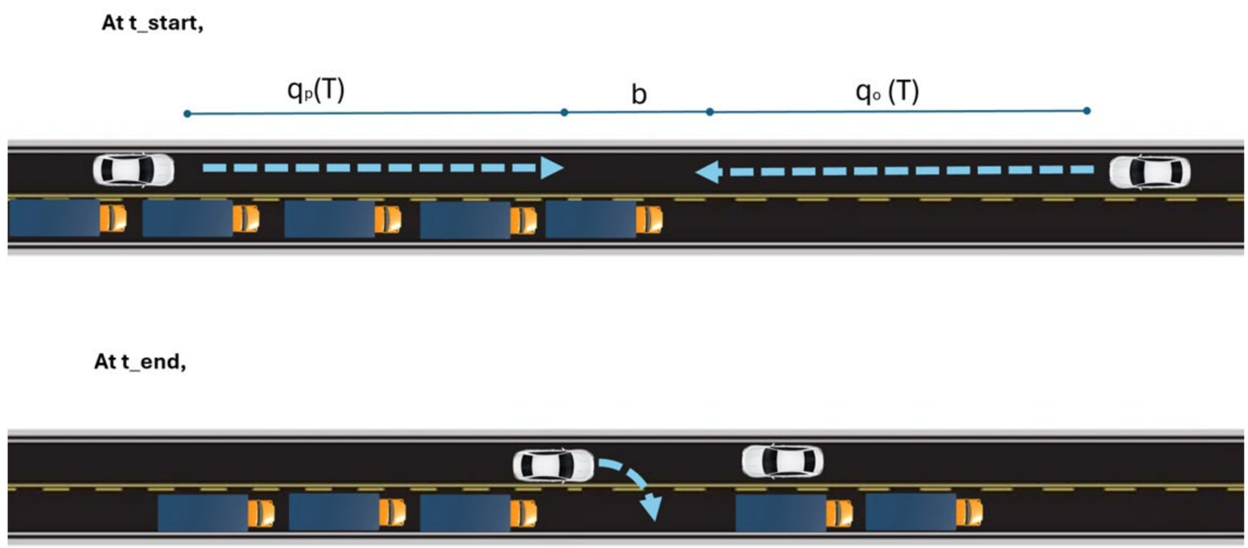

Figure 46: Illustration of the "single vehicle overtaking part of a platoon" scenario and the gap opening problem. Parameters in the figure: t_{start} and tend are time points to start and end the gap opening process; $q_p(T)$ and $q_0(T)$ are the distances covered by passing and opposing vehicles by time T, respectively and b is the safety buffer distance between the two vehicles.

5.2.1 Identifying the Gap

Identifying the gap is the first important task of the opening strategy. We define sets as:

$$Q_p = \{q_p(t) \,|0 \le t \le t_{current}\} \quad [5\text{-}1]$$

$$Q_0 = \{q_0(t) \,|0 \le t \le t_{current}\} \quad [5\text{-}2]$$

$$Q_t = \{q_t(t) \,|0 \le t \le t_{current}\} \quad [5\text{-}3]$$

Representing real-time position data of the passing, opposing, and platoon vehicles. Predictions of positions at a future time point $T > t_{current}$ can be obtained at each $t_{current}$ and are denoted by $q_p^*(T)$, $q_0^*(T)$ and $q_t^*(T)$. We assume that to avoid collision, the passing vehicle needs to complete merging back into its original lane and still is away from the opposing vehicle by a certain distance, b. Therefore, by the end of the scenario described, we have a relationship of $q_0^*(T) - q_0^*(T) - b = 0$. Using the relationship, we can determine if the passing vehicle can complete overtaking the entire platoon or if a gap needs to be opened in the platoon to safely accommodate the passing vehicle.

5.2.2 Opening the Gap

In **Figure 47**, we can see the variables in maintaining a platoon's inter-vehicle following gap. The gap is between two adjacent vehicles, a preceding vehicle $(i - 1)$ and a follower vehicle i.

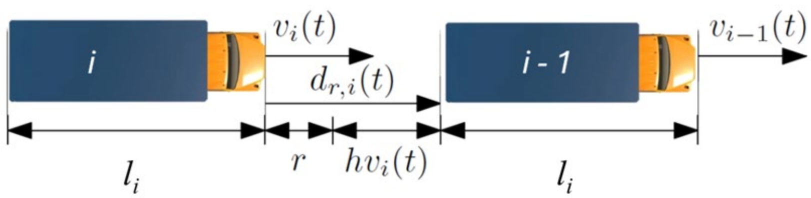

Figure 47: Following gap between two adjacent platoon vehicles and relevant variables. Parameter in the figure: l_i and l_{i-1} are lengths of the follower and preceding vehicles, v_i and v_{i-1} are their speeds, $d_{r,i}(t)$ is the desired following gap, r and h are standstill distance and tie gap, respectively. These terms were adapted from (131).

A CAV platoon using CACC keeps a constant time gap h as short as 0.3–0.5 seconds. The actual gap is the sum of a constant standstill distance r and the multiplication of constant time gap and vehicle speed $hv_i(t)$. To open the gap, we must add an extra distance upon the existing following gap. We can achieve that by setting up a function of desired following gap $d_{r,i}(t)$, which consists of $r + hv_i(t)$ and a term for additional gap length, γ(t), and increasing γ(t) over time, until the gap is large enough to safely accommodate the passing vehicle. The desired gap size can be predetermined based on platoon speed and a typical time gap that is comfortable for human drivers (e.g., 2–3 seconds).

5.2.3 Optimizing the Process

As mentioned in the assumptions, the gap opening process can be optimized to ensure maximum control accuracy and reliability. The potential parameters for implementing gap opening control are the gap location and gap opening start and end times. The gap location is denoted by k, representing the gap between the $(k - 1)$-th and k-th platoon vehicles. The start and end times are denoted by t_{start} and t_{end}. Given that the gap selection process will determine k and t_{end}, we identify a trade-off, with respect to t_{start}, between the gap selection accuracy, gap opening control reliability, and platoon string stability. With the trade-off identified, we can add an optimization component to the control strategy to determine the optimal t_{start}, as shown in **Figure 48**. The cost function is formulated as:

$$min_{t_{start}} - \alpha t_{start} + \beta J_{error,k}(t_{start}) + \theta J_{ss}(t_{start}) \qquad [5\text{-}4]$$

to reflect the trade-off, where $J_{error,k}(t_{start})$ and $J_{ss}(t_{start})$ are the error generated by controlling the k-th platoon vehicle for gap opening and the error generated by k-th vehicle's follower vehicles for assessing string stability; the parameters α, β, and θ are weights on the three cost terms. By solving the optimization problem, we can obtain a t_{start} that minimizes the overall cost.

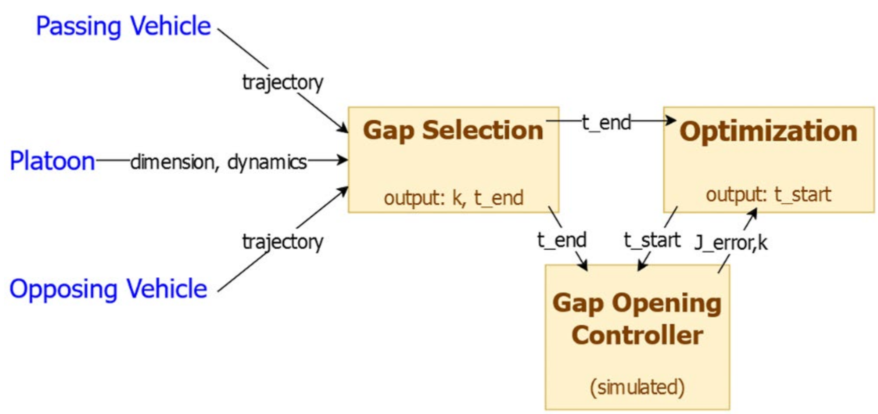

Figure 48: The gap opening decision-making process. Arrows indicate data flows

5.3 Control Strategy

This sub-chapter presents details of the platoon gap opening control strategy designed for the scenario of a single vehicle overtaking part of the platoon. The control strategy is explained in three different sections: Gap Selection, Gap Opening, and Optimal Start Time for Gap Opening. At the end of this subsection, we will talk briefly about the control strategy as a whole.

5.3.1 Gap Selection

In this subchapter, we are going to discuss real-time merge gap identification; first we are going to work from the point where, as assumed, the platoon is equipped with sensors that track the passing and opposing vehicles' positions in real time. The positions are used in predicting passing and opposing vehicles' trajectories, which are fitted as fifth-degree polynomials, as what has been implemented in prior research for modeling vehicle longitudinal trajectories (*135*, *136*). Higher-degree polynomials are not used to reduce risk of overfitting. The polynomials are:

$$q_p^*(t) = \alpha_1 t^5 + \alpha_2 t^4 + \alpha_3 t^3 + \alpha_4 t^2 + \alpha_5 t + \alpha_6 \quad [5\text{-}5]$$

$$q_0^*(t) = \beta_1 t^5 + \beta_2 t^4 + \beta_3 t^3 + \beta_4 t^2 + \beta_5 t + \beta_6 \quad [5\text{-}6]$$

where α_1 ... α_6 and β_1 ... β_6 are coefficients of the passing and opposing vehicle polynomials, respectively.

The polynomials are fitted in real-time using the exponentially weighted least squares method. The objective function for the polynomial fitting is to minimize the weighted least squares error:

$$J_{poly} = \sum_{i=1}^{n} w_i (q(t_i) - q^*(t_i))^2 \quad [5\text{-}7]$$

where n is the total number of data points; w_i is the weight of the i-th data point defined as $w_i = e^{-\lambda(tcurrent-ti)}$, with λ a weight decay parameter controlling how quickly older data points lose importance, and t_{current} the current time; and $q(t_i)$ and $q^*(t_i)$ are the true and polynomial-estimated vehicle position of the i-th data point (i.e., time point t_i).

For the passing vehicle to safely complete an overtaking or partial overtaking, we need to make sure that the passing vehicle safely returns to its original lane before the opposing vehicle reaches the same position. So, the positions of the two vehicles have the following relationship at the time point t_{end}:

$$q_o(t_{end}) - q_p(t_{end}) = b \qquad [5\text{-}8]$$

where $q_o(t_{end})$ and $q_p(t_{end})$ are the positions of opposing and passing vehicles at time point t_{end}, and b is a safety buffer distance, which can be preset as a constant.

We can use the predicted passing and opposing vehicle trajectories and the above relationship to solve for the time t_{end}, which would be the time the passing vehicle should complete the merging into a gap in the platoon or in front of the platoon head.

From time point 0 to time point t_{end}, the platoon is also assumed to be able to track its own moving trajectory and predict the platoon head position at time t_{end}, $q_t^* t_{end}$. Assuming that if vehicles in the platoon are the same length, we can then identify the k-th vehicle, which is the follower vehicle of the merge gap for the passing vehicle to avoid collision with opposing traffic:

$$k = \left(\frac{q_t^*(t_{end}) - q_p^*(t_{end})}{L_i}\right) + 1 \qquad [5\text{-}9]$$

Where $L_i = l_i + r + hv_i$ is the “footprint” of a platoon vehicle. It is the sum of each platoon vehicle’s length, l_i, standstill distance, r, and following gap, hv_i, determined by the platoon’s constant time gap following policy, h, and the vehicle’s speed v_i. If $k \leq 1$, the passing vehicle can safely overtake the entire platoon.

Pseudo code of the gap selection algorithm is presented in **Algorithm 5-1**. The algorithm takes inputs of the current time $t_{current}$, step size Δt related to sensor sampling rate $\frac{1}{\Delta t}$ in Hz, sets of passing and opposing vehicle positions:

$$Q_p = \{q_p(t) | 0 \leq t \leq t_{current}\} \qquad [5\text{-}10]$$

$$Q_o = \{q_o(t) | 0 \leq t \leq t_{current}\} \qquad [5\text{-}11]$$

That are functions of platoon position $q_t^*(t)$, which is assumed to be readily available for the platoon controller, passing opposing safety buffer b, exponential weight decay parameter λ for polynomial fitting, and platoon vehicle’s footprint L_{i}.

The outputs are the gap identifier k and the gap opening and passing vehicle merge end time t_{end}. **Algorithm 5-1** consists of major steps, including fitting the passing and opposing vehicle polynomials, solving for t_{end}, and calculating k.

Next, we will discuss the complexity that **Algorithm 5-1** can adopt, the terms that it is based on, and how it is developed. The relevant inputs affecting complexity are s and the sets of Q_p and Q_o, the size of which can all be represented by: $s + 1 = |t_{current}/\Delta t| + 1$, with step size Δt. The operation to check if $t_{data} < 6$ has a complexity of $O(1)$. The polynomial fitting steps involve fitting a polynomial function of degree d, and the complexity is typically $O(d^3)$, where $d = 5$ under the current setup, and $d < s$. Assume that m is the number of iterations required for solving the equation $q_o^*(t_{end}) - q_p^*(t_{end}) - b = 0$ for t_{end}, then the process costs $O(m)$. Evaluating polynomial values $q_o^*(t_{end})$ and $q_p^*(t_{end})$ have a complexity of $O(d)$, and the final calculations of $q_t^*(t_{end})$, k, and others have a complexity of $O(1)$. Therefore, the overall complexity is primarily determined by polynomial fitting ($O(d)$), equation solving ($O(m)$), and processing the dataset ($O(s+1)$). We can expect that $d < s+1$ and $m < s+1$, thus the complexity of **Algorithm 5-1** is $O(s+1)$, where s is dependent of Δt determined by sensor sampling rate in Hz. For a sampling rate of 1 Hz (1 sample per second, i.e., $\Delta t = 1\ s$), the complexity would be $O(t_{current} + 1)$. Since $t_{current} + 1 \leq t_{end}$, the final complexity is $O(t_{end})$.

Algorithm 5-1. Gap Selection

Input: $t_{current}, \Delta t,\ Q_p,\ Q_0,\ q_t^*(t),\ b,\ \lambda,\ L_i$
Output: Predicted gap k and merge time t_{end} for the current time $t_{current}$
$s \leftarrow \lfloor t_{current}/\Delta t \rfloor$
if $s + 1 < 6$ **then**
Return None, None ⇒ Not enough data for fitting
end if
Fit polynomial $q_p^*(t)$ with ($Q_p[0{:}s], \lambda$)
Fit polynomial $q_o^*(t)$ with ($Q_o[0{:}s], \lambda$)
Solve for t_{end} form $q_o^*(t_{end}) - q_p^*(t_{end}) - b = 0$
if $q_t^*(t_{end}) > q_p^*(t_{end})$ **then**
$k \leftarrow \left\lceil \left(q_o^*(t_{end}) - q_p^*(t_{end}) \right) / L_i \right\rceil$
else
$k \leftarrow 1$
end if
return k, t_{end}

We now move on to the accuracy of gap selection. We can state that at each time point, $t < t_{end}$, **Algorithm 5-1** iterates once to identify the merge gap, k, and time to complete the merge, t_{end}. We noted that as ($t_{end} - t$) reduces, meaning that t is moving closer and closer to t_{end}, the accuracy of gap prediction improves, thus we formulate the following subroutine as a small proposition:

At time t, if we determine the gap to open and start the opening maneuver, we will base our decision on the passing and opposing vehicle polynomials fitted at time t and their corresponding predictions of t_{end} and $q_p(t_{end})$. The prediction error can be expressed as:

$$e_{pred} = \sum_{t_i=t}^{t_{end}} \left(q_p(t_i) - q_p^*(t_i)\right)^2, t \leq t_{end} \qquad [5\text{-}12]$$

where $q_p(t_i)$ and $q_p^*(t_i)$ are the true and predicted positions of passing vehicle at time point t_i.

As t moves closer to t_{end}, the number of time points between t and t_{end} reduces, so the number of terms in the error summation reduces, thus, the prediction error decreases. This analysis shows that the later the gap is selected before time t_{end}, the more accurate the selection will be.

5.3.2 Gap Opening

First, we need to discuss the vehicle model and controllers: The vehicle dynamics, error dynamics, and control law designs are adopted from (*131*, *132*, *136*), for a CACC-based vehicle platoon gap opening to handle on-ramp merging scenarios.

The vehicle dynamics are modeled as follows:

$$\dot{q}_i(t) = v_i(t) \quad [5\text{-}13a]$$

$$\dot{d}_i(t) = v_{i-1}(t) - v_i(t) \quad [5\text{-}13b]$$

$$\dot{v}_i(t) = a_i(t) \quad [5\text{-}13c]$$

$$\dot{a}_i(t) = \frac{1}{\tau}u_i(t) - \frac{1}{\tau}a_i(t) \quad [5\text{-}13d]$$

The desired inter-vehicle following gap based on the constant time gap policy is:

$$d_{r,i}(t) = r + hv_i(t) + \gamma_i(t) \quad [5\text{-}14]$$

where $\gamma_i(t)$ is a term of increased gap, which is adjusted by the gap opening controller.

The error is defined as $e_1 = d_i - d_{r,i}$. The error states are $[e_{1,i}\ \ e_{2,i}\ \ e_{3,i}] = [e_i,\ \dot{e}_i,\ \ddot{e}_i]$ The error dynamics of the controller are:

$$e_{1,i} = d_i - d_{r,i} \quad [5\text{-}15a]$$

$$e_{2,i} = v_{i-1} - v_i - \dot{\gamma} - ha_i \quad [5\text{-}15b]$$

$$e_{3,i} = a_{i-1} - a_i\left(1 - \frac{h}{\tau}\right) - \ddot{\gamma} - \frac{h}{\tau}u_i \quad [5\text{-}15c]$$

$$\dot{e}_{3,i} = -\frac{1}{\tau}e_{3,i} + \frac{1}{\tau}u_{i-1} - \frac{1}{\tau}\xi_i \quad [5\text{-}15d]$$

Where $\xi_i = h_i\dot{u}_i + u_i + \ddot{\gamma}_i + \tau\dddot{\gamma}_i$. By designing the function as: $\xi_i = k_p e_{1,i} + k_d e_{2,i} + u_{i-1}$, with control parameters k_p and k_d, the control law is derived as:

$$\dot{u}_i = \frac{1}{h}\left(k_p e_{1,i} + k_d e_{2,i} + u_{i-1} - u_i\ddot{\gamma}_i - \tau\dddot{\gamma}_i\right) \quad [5\text{-}16]$$

Here, it is important to underscore the gap opening term, which will be represented as γ. The γ trajectory is modeled as a fifth-degree polynomial to ensure C^2 continuity, so that the third derivative, $\dddot{\gamma}$, can be obtained at all times (*131*). For this particular section, coefficients in the γ function are preset or calculated based on specific constraints of the vehicle overtaking platoon scenario.

$$\gamma(t) = c_1 + c_2 t + c_3 t^2 + c_4 t^3 + c_5 t^4 + c_6 t^5 \qquad [5\text{-}17]$$

The coefficients (c) are:

$$c_1 = \gamma_{ini},\ c_2 = \dot{\gamma}_{ini},\ c_3 = 0.5\ddot{\gamma}_{ini}, \qquad [5\text{-}18a, b, c]$$

$$c_4 = \frac{20(\gamma_{end}-\gamma_{ini})-3T(4\dot{\gamma}_{ini}+T\ddot{\gamma}_{ini})}{2T^3} \qquad [5\text{-}18d]$$

$$c_5 = \frac{-30(\gamma_{end}-\gamma_{ini})-T(16\dot{\gamma}_{ini}+3T\ddot{\gamma}_{ini})}{2T^4} \qquad [5\text{-}18e]$$

$$c_6 = \frac{12(\gamma_{end}-\gamma_{ini})-T(6\dot{\gamma}_{ini}+T\ddot{\gamma}_{ini})}{2T^5} \qquad [5\text{-}18f]$$

where $T = t_{end} - t_{start}$ is the amount of time between the start and end of the gap opening process.

The controller is designed to reach γ_{end} at time t_{end}, so that the preceding (($k-1$)-th) and follower (k-th) vehicles should be able to accommodate the passing vehicle in between. For gap opening, the initial γ value is set to γ_{ini}= 0. The final γ value, γ_{end}, is preset based on the length of passing vehicle and typical following gaps that human drivers feel comfortable with (e.g., 2–3 seconds).

The gap opening end time, t_{end}, is determined by **Algorithm 5-1** based on vehicle trajectories in the overtaking process, and t_{start} will be determined by solving the optimization problem of balancing the trade-off between gap selection accuracy, control error, and platoon string stability.

The next step is the controller error and string stability: The gap opening controller follows a feed-forward design and increases the gap between the k-th and ($k-1$)-th platoon vehicles by slowing down the follower, k. As the maneuver tries to follow a desired gap-increase trajectory, the induced errors between the actual and desired trajectories should be assessed.

Over the period between the start and end times of the gap opening maneuver, t_{start} and t_{end}, the controller error can be measured as a root mean squared error (RMSE):

$$J_{error,k}(t_{start}) = \sqrt{\frac{\int_{t_{start}}^{t_{end}} \sum_{i=1}^{3} e_{i,k}^2(t)dt}{t_{end}-t_{start}}} \qquad [5\text{-}19]$$

where k indicates the k-th vehicle in the platoon, which is the primarily controlled vehicle to achieve gap opening.

As the k-th vehicle reduces speed to open its following gap, the platoon vehicles following the k-th vehicle (i.e., the $(k+1)$ th, $(k+2)$-th, ..., and n-th vehicles) are disturbed. Following the CACC control dynamics, the follower vehicles will need to adjust their speed along with the k-th vehicle. Considering potential error propagation, we want to make sure that the gap opening process does not cause a significant disturbance and the platoon stays string stable. String stability can be quantified by measuring the amplification of velocity errors between consecutive vehicles and the propagation of position or gap errors over time. For simplicity, we can measure the sum of follower vehicles' control errors as follows and ensure the gap opening process minimizes it.

$$J_{ss}(t_{start}) = \sum_{j=k+1}^{n} \sqrt{\frac{\int_{t_{start}}^{t_{end}} \sum_{i=1}^{3} e_{i,j}^2(t)dt}{t_{end}-t_{start}}} \qquad [5\text{-}20]$$

Instead of having an increasing $\gamma(t)$ in the desired following gap and error dynamics, the follower vehicles use regular CACC error dynamics as the model adopted from (*136*), with $\gamma(t) = 0$, aiming to keep a following gap of $d_{r,i} = r + hv_i$ with their corresponding preceding vehicles. The control law is instead $\dot{u}_i = \left(k_p e_{1,i} + k_d e_{2,i} + u_{i-1} - u_i\right)/h$.

5.3.3 Optimal Start Time for Gap Opening

We need to state the optimal start time for gap opening in different stages: formulation of optimization problem, complexity of **Algorithm 5-2**.

Formulation of optimization problem: At each current time point, $t_{current}$, during the overtaking process, before the passing vehicle reaches the gap determined by **Algorithm 5-1** as the safe merge gap, we need to decide on a time point, denoted by t_{start}, to start the gap opening maneuver. The value of t_{start} affects the accuracy of gap selection as well as the controller error and platoon string stability; we formulate the following optimization problem to determine the optimal t_{start}.

$$\min_{t_{start}} -\alpha t_{start} + \beta J_{error,k}(t_{start}) + \theta J_{ss}(t_{start}) \qquad [5\text{-}21a]$$

$$\text{s.t. } t_{current} < t_{start} < t_{end} \qquad [5\text{-}21b]$$

The α, β, and θ parameters are weights on corresponding parts of the objective function that represent gap selection accuracy, gap opening controller error, and control error related to string stability, respectively. The optimization problem is solved concurrently with the gap selection algorithm and a simulation of the gap opening controller. The gap selection algorithm provides real-time estimation of t_{end}, and the controller simulation provides estimations on errors and string stability effects. To solve the optimization problem, sequential quadratic programming (SQP) is used to handle the dynamic constraints.

Pseudo code of the optimization process to determine optimal t_{start} is shown in **Algorithm 5-2**. At each time step, **Algorithm 5-2** runs concurrently with **Algorithm 5-1**. **Algorithm 5-2** takes inputs of the current time $t_{current}$, gap opening end time tend determined by **Algorithm 5-1**, platoon following time gap h, standstill distance r, vehicle driveline parameter τ, weights objective function terms α, β, and θ, final gap increase γ_{end}, k-th platoon vehicle initial state $[q_k d_k v_k a_k u_k]$, and control parameters k_p and k_d. The output is optimal gap opening start time $t_{start\_optimal}$. The primary steps in **Algorithm 5-2** are those of solving the optimization problem using sequential least squares programming (SLSQP).

Algorithm 5-2. Optimal T_{start}

Input: $t_{current}$, t_{end}, h, r, τ, α, β, θ, γ_{end}, initial state $[q_k d_k v_k a_k u_k]$, parameters k_p, k_d

Output: Optimal start time $t_{start\_optimal}$.

if t_{end} != None **AND** $t_{current} < t_{end}$ **then**

Define constraints:

$$t_{current} < t_{start} < t_{end}$$

Define objective function:

$$J(t_{start}) = -\alpha t_{start} + \beta J_{error,k}(t_{start}) + \theta J_{ss}(t_{start})$$

where J_{error}: integrated error based on system dynamics.

Solve optimization problem using SLSQP:

Minimize $J(t_{start})$ subject to constraints.

Obtain optimal t_{start}: $t_{start\_optimal}$

if $t_{current} \geq t_{start\_optimal}$ then

  return None

end if

else

  return None

end if

return $t_{start\_optimal}$

Complexity of Algorithm 5-2: The key variables or components affecting complexity of **Algorithm 5-2** are t_{end}, $J_{error}(t_{start})$, $J_{ss}(t_{start})$, and the SLSQP algorithm. The initialization of $t_{start\_initial}$ has a complexity of $O(1)$. The objective function involves three terms: (1) a linear term of $-\alpha t_{start}$ with complexity of $O(1)$; (2) an error term of $J_{error}(t_{start})$ with its complexity depending on the evaluation of system dynamics, which we can denote as C_{error}; and an string stability error term of $J_{error}(t_{start})$, with a complexity depending on $(n - k)C_{error}$, where n is the total number of platoon vehicles, k is the gap opening platoon vehicle, and $(n - k)$ is the number of follower vehicles behind k. Based on the system dynamics, $C_{error} = O((t_{end} - t_{start})/\Delta t)$, with step size Δt related to the sensor sampling rate in Hz. The complexity of the SLSQP algorithm is related to the number of iterations required by the optimizer, m, and the cost of evaluating Jt_{start} in each iteration, C_{eval}. Thus, the SLSQP complexity is $O(m \cdot C_{eval})$. We assume that:

$$C_{eval} = (n - k + 1) \cdot C_{error} = O((n - k + 1) \cdot (t_{end} - t_{start})/\Delta t) \qquad [5\text{-}22]$$

then the overall complexity of Algorithm 2 is:

$O(m \cdot (n - k + 1) \cdot (t_{end} - t_{start})/\Delta t)$

[5-23]

For a sampling rate of 1 Hz (i.e., Δt = 1 s) and assuming $t_{current}$ = 0, m = 1, and k = 1, the complexity is $O(n \cdot t_{end})$, related to the size of platoon and passing vehicle merge time.

5.3.4 Control Strategy as a Whole

The gap opening control strategy as a whole determines k, t_{end}, and t_{start} iteratively in real time, from when a passing vehicle starts to overtake the platoon until t_{start}, during which **Algorithm 5-1** and **Algorithm 5-2** are called at each time point. The process is presented as pseudo code in **Algorithm 5-3**. The algorithm takes all inputs needed for Algorithms 5-1 and 5-2, and generates outputs of k, t_{end}, and t_{start} optimal. **Algorithm 5-3** runs iteratively until $t_{current} \geq t_{start_{optimal}}$, and the gap opening controller will start executing the actual gap opening maneuver between the k-th and $(k - 1)$-th platoon vehicles.

The complexity of **Algorithm 5-3** is analyzed as follows. The whole loop iterates when $t_{current} \geq t_{end}$ so the number of iterations $N = t_{end} - t_{current}$. **Algorithm 5-1** and **Algorithm 5-2** have complexity of $O(t_{current}/\Delta t)$ and $O(m \cdot (n - k + 1) \cdot (t_{end} - t_{current})/\Delta t)$, respectively, and are called in each iteration. Therefore, the overall complexity of **Algorithm 5-3** is $O(N \cdot (t_{current} + m \cdot (n - k + 1) \cdot (t_{end} - t_{current}))/\Delta t)$. For $\Delta t = 1\,s$, and assuming $m = 1$ and $k = 1$, the overall complexity would be about $O(n \cdot t_{end}^2)$.

Algorithm 5-3. Gap Opening Decision

Input:
For GapSelection: $t_{current}, \Delta t, Q_p, Q_o, q_t^*(t), b, \lambda, L_i$
For OptimalTstart: $t_{current}, t_{end}, h, r, \tau, \alpha, \beta, \theta, \gamma_{end}, [q_k, d_k, v_k, a_k, u_k], k_p, k_d$
Output: $k, t_{end}, t_{start_{optimal}}$
Initialize: $t_{current} \leftarrow 0;\ t_{end} \leftarrow 1; k \leftarrow 1$
While $t_{current} < t_{end}$ **do**
$k, t_{end} \leftarrow$ GapSelection $\left(t_{current}, \Delta t,\ Q_p, Q_o, q_t^*(t)\right), b, \lambda, L_i)$
$t_{start_{optimal}} \leftarrow$ OptimalStart $t_{end}, h, r, \tau, \alpha, \beta, \theta, \gamma_{end}, [q_k, d_k, v_k, a_k, u_k], k_p, k_d$
Increment $t_{current} \leftarrow t_{current} + 1$
end while
return $k, t_{end}, t_{start_{optimal}}$

5.4 Simulation

5.4.1 Simulation Setup

We present a numerical simulation to show how the gap opening control strategy works. In the simulation scenario, a vehicle following a platoon of $n = 5$ vehicles on a two-lane undivided highway starts to overtake the platoon. The parameters used to initiate the simulation are listed in **Table 20**. In this simulation, the following assumptions are made to simplify the scenario and provide a clear illustration of the results: (1) the platoon moves at a constant speed; (2) the passing and opposing vehicles maintain constant acceleration and deceleration, respectively; and (3) the buffer distance between the passing and opposing vehicles is set to 0 m.

Table 20: Parameters Used in the Simulation Setup

Parameter	Definition
Platoon head initial position	$q_t(0) = 200\ m$
Platoon size	$n = 5\ vehs$
Platoon vehicle length	$L_i = 15\ m$
Platoon time gap	$h = 0.75\ s$
Platoon standstill distance	$r = 5\ m$
Platoon speed	$v_t(t) = 20\ m/s$
Platoon head trajectory	$q_t(t) = q_t(0) + v_t(0)t$
Passing vehicle initial position	$q_p(0) = 0\ m$
Passing vehicle initial speed	$v_p(0) = 22\ m/s$
Passing vehicle acceleration	$a_p(t) = 0.05\ m/s^2$
Passing vehicle trajectory	$q_p(t) = q_p(0) + v_p(0)t + 0.5a_p(t)t^2$
Opposing vehicle initial position	$q_o(0) = 2{,}000\ m$
Opposing vehicle initial speed	$v_o(0) = 20\ m/s$
Opposing vehicle deceleration	$a_o(t) = -0.03\ m/s^2$
Opposing vehicle trajectory	$q_o(0) = q_0(0) - v_o(0)t - 0.5a_o(t)t^2$
Passing-opposing buffer	$b = 0\ m$
Polynomial fitting wight decay parameter	$\lambda = 0.1$
Driveline dynamics parameter	$\tau = 0.1$; Source: (*131*)
Control gain parameters	$k_p = 0.2$; $k_d = 0.7$; Source: (*131*)
Initial and final gap increase	$\gamma_{ini} = 0\ m$; $\gamma_{end} = 65\ m$
Optimization objective weights	$\alpha = 0.05;\ \beta = 0.50;\ \theta = 0.45$

5.4.2 Results

Figure 49 shows the time-position diagram that indicates the trajectories of platoon vehicles as well as the passing and opposing vehicles. As we set $b = 0$, the intersecting point between the passing and opposing vehicle trajectories is where—in time and position—the passing vehicle needs to completely merge into the platoon to avoid collision with the opposing vehicle. The gap-selection **Algorithm 5-1** predicts the vehicle trajectories at every time step and the intersecting point, and generates the outputs, t_{end} and k, which are the time to complete merge and the gap (between the k-th and ($k - 1$)-th platoon vehicles) to use for the merge, respectively. In the simulation, **Algorithm 5-1**'s prediction of t_{end} = 47.09 s stabilized from $t_{current}$ = 5 s, and the predicted gap location is k = 3 (i.e., between the 3rd and 2nd platoon vehicles). The k-th vehicle then has two followers, $k + 1$ and $k + 2$.

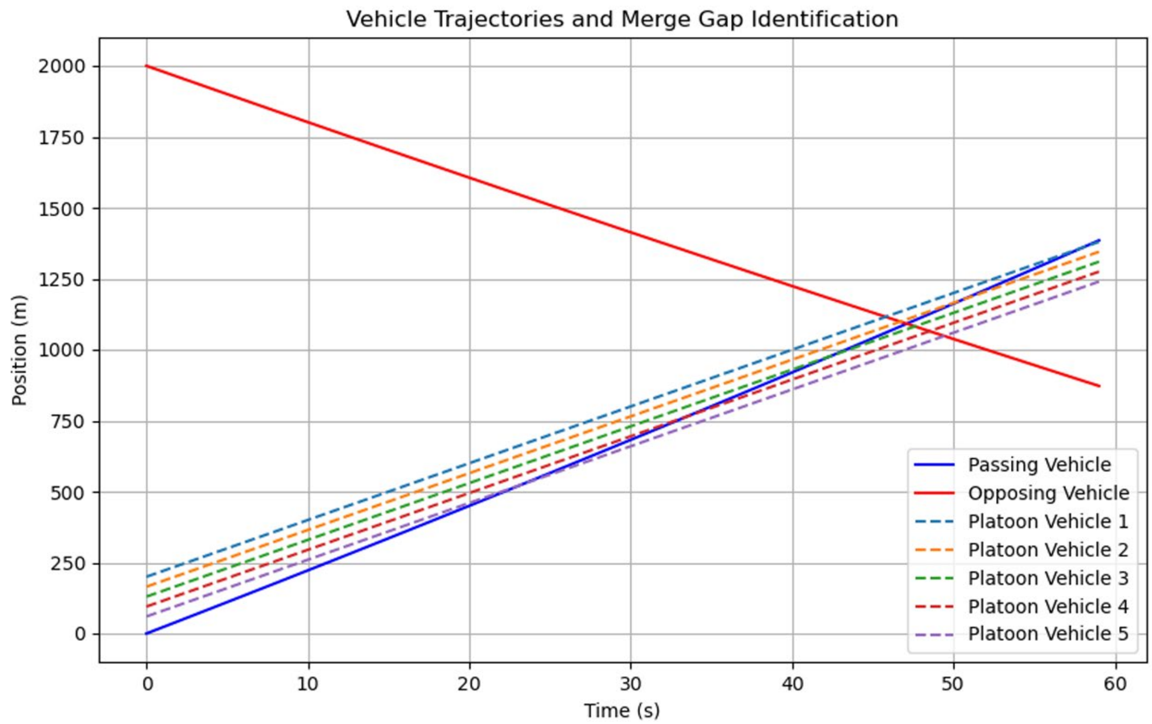

Figure 49: Simulated vehicle trajectories and merge gap

While **Algorithm 5-1** is predicting t_{end} and k at every time step, **Algorithm 5-2** determines the optimal t_{start}. **Figure 50** presents the optimal t_{start} at every time step until the 16th second. The results were based on unstable trajectory prediction for $t_{current}$ = 0 to 5 s, and the optimal t_{start} stayed at 16.12 s afterwards. Therefore, the controller should start opening the gap at $t_{current}$ = 16.12 s.

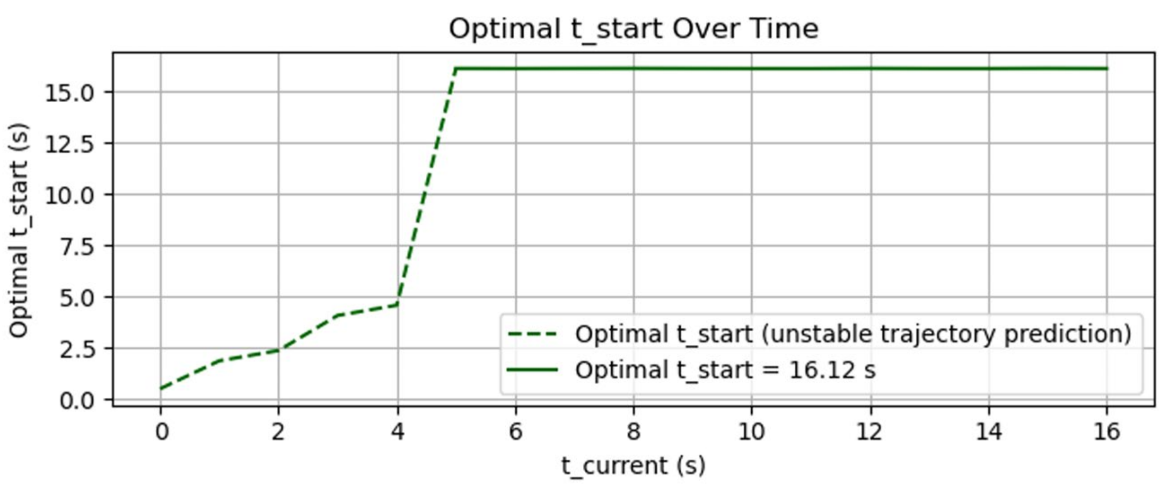

Figure 50: Optimal t_{start} determined at each time point

The optimal t_{start} is determined based on the cost function and constraints (Equations 5-21 a and b) to balance the trade-off between gap prediction accuracy and gap opening control and platoon string stability errors. **Figure 51** shows the simulated controller dynamics for t_{start} = 16.12 s and t_{end} = 47.09 s. We observe that the simulated "actual" gap trajectory closely follows the desired trajectory; the acceleration of the follower (k-th platoon vehicle) also closely follows the control input, leading to a smooth change in its speed and achieves the goal of gap opening within the 30.97 seconds between t_{start} and t_{end}. The $(k + 1)$-th and $(k + 2)$-th vehicles adjusted their speeds and accelerations following the k-th vehicle and maintained their following gap well without a large deviation from 20 m. The following disturbance dissipates quickly after t_{end}, which is observed from the velocity and acceleration/control dynamics plots.

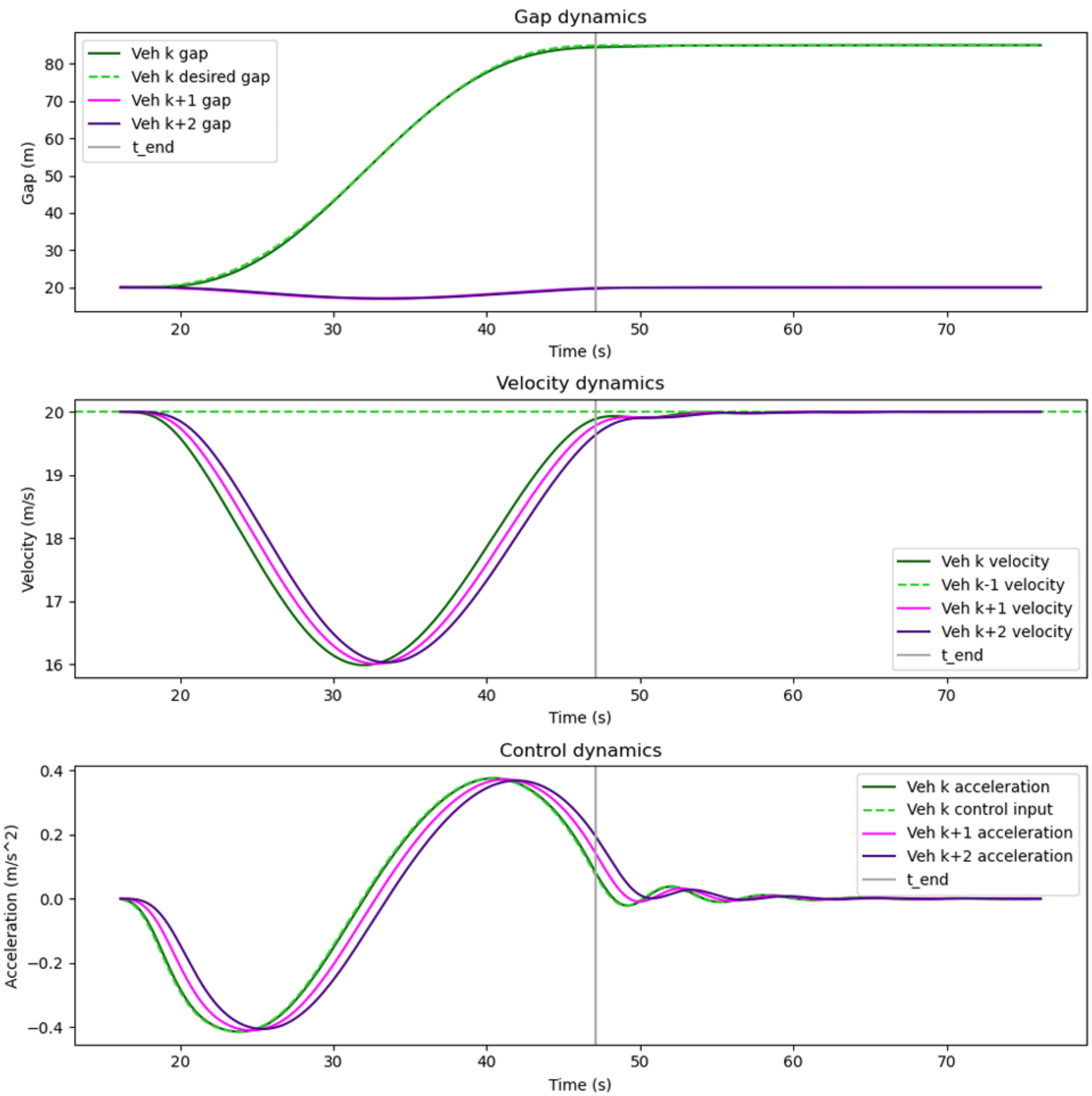

Figure 51: Gap, velocity, and acceleration/control dynamics, with optimal t_{start} = 16.12 s and t_{end} = 47.09 s

To verify that t_{start} = 16.12 s is the optimal start time of the gap opening maneuver given a determined t_{end}, we compare the controller dynamics and error results from using t_{start} = 16.12 s with those from using t_{start} = 20 s, 25 s, and 30 s. The comparison is shown in **Figure 52**, from which we observe that the controller error $J_{error,k}$ increased from 0.44 to 0.73, 1.90, and 44.35 as t_{start} increases. The string stability related error J_{ss} increased from 0.0000 to 0.0001, 0.0004, and 0.0180. The increased errors can also be observed from the vehicle gap, velocity, and acceleration/control dynamics. As we use errors in all three dynamic measures in the calculation of $J_{error,k}$ and J_{ss}, the significant change in gap dynamics from an early start to a late one primarily contributes to the change in those errors, which can be viewed in the side-by-side comparison of the gap dynamics plots. We also observe increased oscillations in the vehicle's velocity and acceleration with delayed t_{start}. These simulation results show again that as t_{start} moves closer to t_{end}, the controller will start struggling to fully open the gap and maintain string stability within the more limited amount of time.

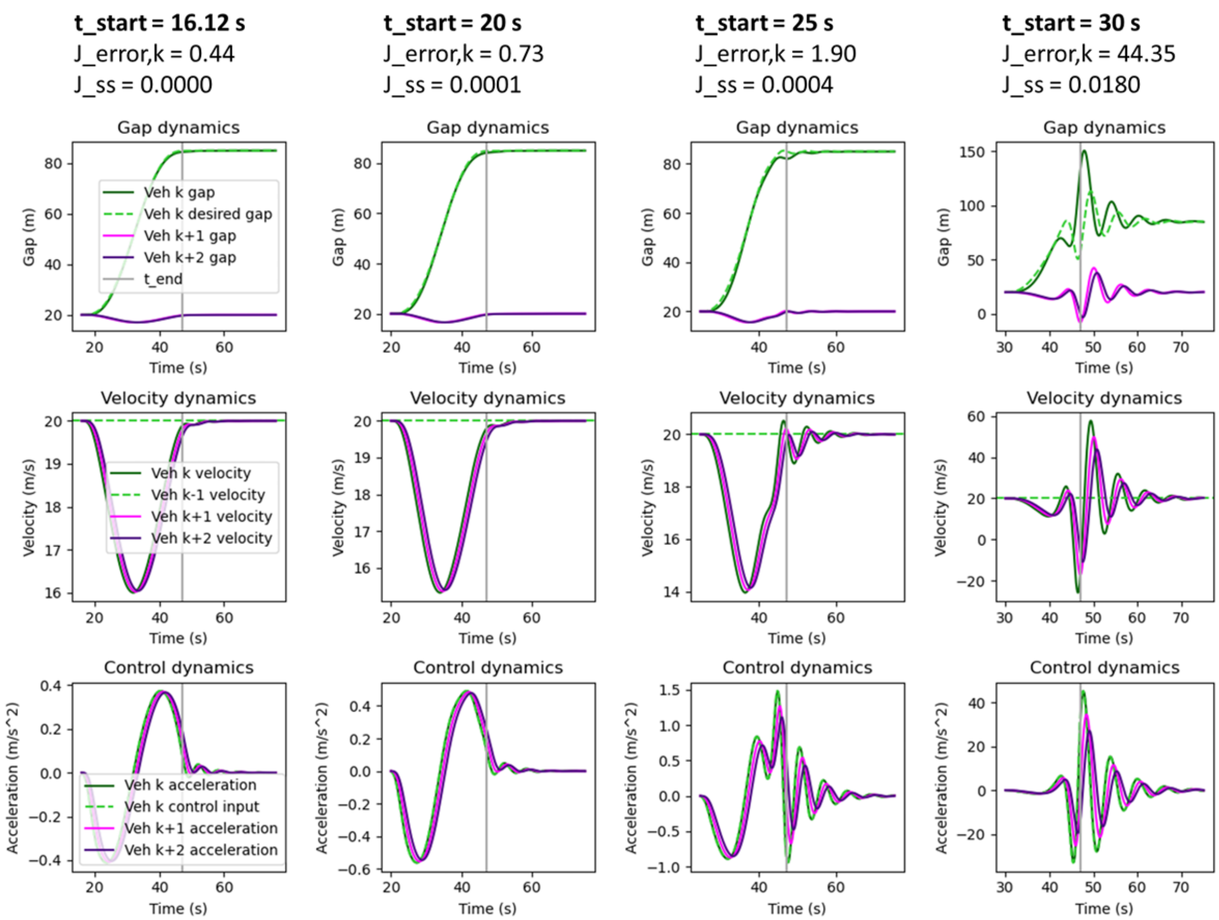

Figure 52: Comparison of vehicle dynamics and gap opening controller and string stability errors with different t_{start} and the same t_{end} = 47.09 s

5.4.3 Discussion

As shown by the simulation results, the proposed algorithms successfully provided suggestions of optimal gap location and start and end times for gap opening based on predicted passing and opposing vehicle trajectories. The amount of time between the t_{start} and t_{end} determined by the algorithms is enough for the gap opening controller to smoothly conduct the maneuver, with minimal control error and impact on string stability.

There are some challenges the proposed **Algorithm 5-1** and **Algorithm 5-2** face and could be further addressed in future work:

1) Fitting a 5th degree polynomial of the position-time trajectories of passing and opposing vehicles is only one method of tracking and predicting the vehicles' movements. Predictions based on those polynomials may not be accurate if adversarial movements such as frequent acceleration changes occur. We used an exponentially decayed weighting method to address the issue, but techniques such as incorporating physical models or Kalman filter into polynomial fitting will be tested in future studies.

2) To determine the optimal start time t_{start}, the objective function can incorporate other types of costs such as energy consumption and emission-related costs. We only considered the gap prediction inaccuracy and gap opening control and string stability error costs because we found a significant trade-off relationship with regard to t_{start} between those costs. To incorporate other costs, the relationship between the newly introduced costs and existing ones needs to be investigated.

3) For simplicity, the proposed algorithms use the same t_{end} as the end time of both the passing vehicle merge and platoon gap opening maneuvers. For a more sophisticated decision process, the gap opening maneuver can be restricted to complete just before the start of the passing vehicle's merging maneuver. To achieve that, the algorithms need to incorporate prediction of the passing vehicle's lateral movement. Polynomial fitting techniques similar to what is used for longitudinal trajectory prediction may be investigated to examine feasibility for lateral trajectory prediction.

5.5 Section Conclusion

The proposed control strategy for guided step-by-step overtaking of CAV platoons on two-lane undivided highways demonstrates its effectiveness in addressing the safety and efficiency challenges posed by mixed traffic environments. Through simulation, the gap-selection algorithm successfully identified the optimal location and duration for gap opening to ensure that passing vehicles could merge safely into the platoon. The optimization algorithm determined optimal timing for initiating the gap opening maneuver, balancing the trade-off between gap prediction accuracy, controller performance, and platoon string stability. The results confirm the feasibility of implementing the proposed solution in CAV platooning systems to ensure safe integration with HDVs. In addition to the promising performance of the proposed control strategy, we also identify directions for future improvement. Enhancing trajectory prediction accuracy through advanced methods such as incorporating physical models or Kalman filtering could mitigate errors in adversarial traffic conditions. Expanding the cost function for optimal start time to include considerations like energy efficiency and emissions would further refine the system's effectiveness and sustainability. Additionally, separating the end times of the gap opening and merging maneuvers by integrating lateral movement predictions could optimize maneuver coordination and reduce unnecessary delays. By addressing these challenges, future research can build upon the foundational framework established in this part of the project to develop more comprehensive and adaptive solutions for safe and efficient CAV platooning in diverse traffic environments.

6. CONCLUSIONS AND RECOMMENDATIONS

6.1 Discussion of Findings

The findings of this research highlight a fundamental tension between the operational efficiencies of automated truck platoons and the geometric limitations of rural, two-lane undivided highways. The analytical overtaking models demonstrated that as platoon length increases, the time and distance required for a human-driven vehicle (HDV) to safely complete a passing maneuver scale linearly, effectively transforming long convoys into hazardous rolling blockades. On divided multilane highways, the microsimulation confirmed that these large platoons operate seamlessly, maintaining high speeds and low delays because passing vehicles can easily utilize adjacent lanes. However, on undivided segments, the available sight distance is severely restricted by oncoming traffic, horizontal curves, and crest vertical curves. Under these conditions, an unregulated eight-truck platoon forces human drivers to accept significantly higher collision risks or face severe, cascading delays, underscoring that existing static infrastructure policies are entirely inadequate for mixed-autonomy freight operations.

While the implementation of dynamic platooning rules proved highly effective at resolving these macroscopic mobility issues, the simulation revealed a paradoxical microscopic safety challenge. By actively restricting platoon sizes to a maximum of two trucks on constrained segments, the system successfully restored network fluidity and drastically reduced overall travel delays. Yet, breaking large convoys into numerous smaller platoons inadvertently multiplied the number of platoon boundaries across the corridor. The surrogate safety analysis exposed that this fragmentation generates localized traffic friction, leading to a measurable increase in rear-end and lane-change conflicts as human drivers attempt to weave between the segmented convoys. Conversely, longer platoons were shown to act as stable, synchronized units that smooth surrounding traffic and dampen longitudinal shockwaves, presenting a complex trade-off between network capacity and localized collision risk.

These conflicting dynamics demonstrate that passive regulation alone cannot safely integrate automated platoons into human-driven traffic on two-lane roads; active, cooperative vehicle control is required. The exploration of the CACC-based gap-opening control strategy provides a robust technological resolution to the friction observed in the simulation. By enabling a platoon to actively predict an approaching human driver's trajectory and dynamically open an internal gap, the system can safely harbor passing vehicles for guided, step-by-step overtaking. This cooperative approach balances the competing demands identified throughout the study: it allows freight operators to maintain the aerodynamic and string-stability benefits of longer platoons while actively mitigating the severe safety hazards and mobility constraints imposed on everyday drivers traversing rural highway networks.

6.2 Conclusions

The progression from analytical modeling to active control development in this project highlights that integrating truck platooning on two-lane undivided highways requires a fundamental shift from static legislation to dynamic, cooperative systems. Analytical overtaking models confirmed that long truck platoons exponentially increase the time and distance required for HDVs to complete a passing maneuver. On two-lane undivided highways, unregulated large platoons act as dangerous moving bottlenecks that severely elevate collision risks and constrain the entire traffic corridor. However, the stochastic algorithm developed to dictate platooning rules proved highly effective at mitigating these mobility risks. By actively restricting platoon lengths based on immediate horizontal or vertical curvature and opposing traffic flow, the dynamic rules successfully prevented severe upstream delays and restored macroscopic traffic fluidity.

While mandating smaller platoons improves overall travel times on undivided roads, the microscopic simulation-based evaluation demonstrated a critical operational trade-off. The increased frequency of segmented platoon boundaries introduces significant localized friction, and surrogate safety analysis revealed that this fragmentation slightly elevates lane-change and rear-end conflicts among eager HDV drivers attempting to navigate between the smaller convoys. To address these limitations, the development of an active gap-opening control algorithm effectively neutralizes the localized conflicts observed in the simulation. Utilizing cooperative adaptive cruise control to sense approaching HDVs and proactively split the platoon provides safe, temporary harbors for passing vehicles, enabling guided, step-by-step overtaking. By cooperating with macroscopic dynamic rules, this flexible gap control presents a holistic pathway to successfully deploy automated truck platoons on two-lane highways while fully maintaining the string stability of platoons and the safety of all road users.

6.3 Recommendations for Implementation and Future Research

To ensure the safe and highly efficient deployment of truck platooning technologies, infrastructure owner-operators and policymakers must adopt synchronized, adaptive management strategies. Implementing the frameworks established in this research offers several distinct advantages for state and local transportation authorities, primarily through proactive risk management. By relying on surrogate safety measures to strictly quantify safety risks prior to crash occurrences, agencies can confidently integrate heavy automated freight without jeopardizing the safety of human drivers. Furthermore, dynamic platooning rules allow agencies to maximize the throughput and economic benefits of existing rural corridors. This context-aware approach reduces or delays the immediate need for costly physical capacity expansions, such as adding passing lanes or widening roads, by substituting physical infrastructure with digital traffic management, ensuring freight efficiency is not needlessly throttled where the roadway can safely accommodate it.

Transitioning these findings into real-world practice requires a strategic, phased approach centered on deploying digital infrastructure and mandating adaptive vehicle behaviors. State transportation agencies should begin deploying roadside units and V2I communication networks along critical freight corridors to establish geofenced zones where maximum platoon sizes and speeds dynamically adjust to local geometries. In conjunction with these limits, state policies should require that platooning systems deployed on undivided roadways integrate active, cooperative gap-opening algorithms to recognize HDV overtaking attempts and proactively yield space. These frameworks must then be empirically calibrated through controlled field testing via small-scale pilot programs on representative rural corridors to gather real-world kinematic data. Finally, future research must prioritize enhancing the robustness of the underlying control algorithms by incorporating physical models or Kalman filtering to better anticipate erratic HDV cut-ins, alongside aggressive testing under adverse weather scenarios like snow and fog to validate the system before widespread commercial rollout.

7. REFERENCES

1. Franke, U., F. Bottiger, Z. Zomotor, and D. Seeberger. "Truck Platooning in Mixed Traffic. Presented at the Proceedings of the Intelligent Vehicles '95." Symposium, 1995.
2. Schakel, W. J., B. van Arem, and B. D. Netten. "Effects of Cooperative Adaptive Cruise Control on Traffic Flow Stability." Presented at the 2010 13th International IEEE Conference on Intelligent Transportation Systems - (ITSC 2010), 2010.
3. Lammert, M. P., A. Duran, J. Diez, K. Burton, and A. Nicholson. "Effect of Platooning on Fuel Consumption of Class 8 Vehicles Over a Range of Speeds, Following Distances, and Mass." *SAE International Journal of Commercial Vehicles*, Vol. 7, No. 2, 2014, pp. 626–639. https://doi.org/10.4271/2014-01-2438.
4. McAuliffe, B., M. Lammert, X.-Y. Lu, S. Shladover, M.-D. Surcel, and A. Kailas. "Influences on Energy Savings of Heavy Trucks Using Cooperative Adaptive Cruise Control." Presented at the WCX World Congress Experience, 2018.
5. Lammert, M. P., B. McAuliffe, P. Smith, A. Raeesi, M. Hoffman, and D. Bevly. "Impact of Lateral Alignment on the Energy Savings of a Truck Platoon." Presented at the WCX SAE World Congress Experience, 2020.
6. Neubauer, M., and W. Schildorfer. "Towards Truck Platooning Deployment Requirements." In *Energy-Efficient and Semi-automated Truck Platooning* (A. Schirrer, A. L. Gratzer, S. Thormann, S. Jakubek, M. Neubauer, and W. Schildorfer, eds.), Springer International Publishing, Cham, pp. 21–39.
7. Tsugawa, S., S. Jeschke, and S. E. Shladover. "A Review of Truck Platooning Projects for Energy Savings." *IEEE Transactions on Intelligent Vehicles*, Vol. 1, No. 1, 2016, pp. 68–77. https://doi.org/10.1109/TIV.2016.2577499.
8. McAuliffe, B., M. Croken, M. Ahmadi-Baloutaki, and A. Raeesi. *Fuel-Economy Testing of a Three-Vehicle Truck Platooning System*. Publication LTR-AL-2017-0008. National Research Council Canada, 2017.
9. McAuliffe, B., and M. Ahmadi-Baloutaki. "A Wind-Tunnel Investigation of the Influence of Separation Distance, Lateral Stagger, and Trailer Configuration on the Drag-Reduction Potential of a Two-Truck Platoon." *SAE International Journal of Commercial Vehicles*, Vol. 11, 2018, pp. 125–150. https://doi.org/10.4271/02-11-02-0011.
10. McAuliffe, B., A. Raeesi, M. Lammert, P. Smith, M. Hoffman, and D. Bevly. *Impact of Mixed Traffic on the Energy Savings of a Truck Platoon*. Publication NREL/CP-5400-78218. National Renewable Energy Laboratory, 2020, pp. 1472–1496.
11. Talebpour, A., and H. S. Mahmassani. "Influence of Connected and Autonomous Vehicles on Traffic Flow Stability and Throughput." *Transportation Research Part C: Emerging Technologies*, Vol. 71, 2016, pp. 143–163. https://doi.org/10.1016/j.trc.2016.07.007.
12. Calvert, S. C., W. J. Schakel, and B. van Arem. "Evaluation and Modelling of the Traffic Flow Effects of Truck Platooning." *Transportation Research Part C: Emerging Technologies*, Vol. 105, 2019, pp. 1–22. https://doi.org/10.1016/j.trc.2019.05.019.
13. Wang, M., S. van Maarseveen, R. Happee, O. Tool, and B. van Arem. "Benefits and Risks of Truck Platooning on Freeway Operations Near Entrance Ramp." *Transportation Research Record*, Vol. 2673, No. 8, 2019, pp. 588–602. https://doi.org/10.1177/0361198119842821.
14. Zhao, C., L. Li, J. Li, K. Li, and Z. Li. "The Impact of Truck Platoons on the Traffic Dynamics Around Off-Ramp Regions." *IEEE Access*, Vol. 9, 2021, pp. 57010–57019. https://doi.org/10.1109/ACCESS.2021.3072070.
15. Lee, S., C. Oh, and S. Hong. "Exploring Lane Change Safety Issues for Manually Driven Vehicles in Vehicle Platooning Environments." *IET Intelligent Transport Systems*, Vol. 12, No. 9, 2018, pp. 1142–1147. https://doi.org/10.1049/iet-its.2018.5167.
16. Gouy, M., K. Wiedemann, A. Stevens, G. Brunett, and N. Reed. "Driving next to Automated Vehicle Platoons: How Do Short Time Headways Influence Non-Platoon Drivers' Longitudinal

Control?" *Transportation Research Part F: Traffic Psychology and Behaviour*, Vol. 27, 2014, pp. 264–273. https://doi.org/10.1016/j.trf.2014.03.003.

17. Spasovic, L. N., D. Bensenski, J. Lee, and New Jersey Institute of Technology. *Impact Assessments of Automated Truck Platooning on Highway Traffic Flow and Adjacent Drivers*. Publication CAIT-UTC-NC53. 2019.
18. Faber, T., S. Sharma, M. Snelder, G. Klunder, L. Tavasszy, and H. van Lint. "Evaluating Traffic Efficiency and Safety by Varying Truck Platoon Characteristics in a Critical Traffic Situation." *Transportation Research Record*, Vol. 2674, No. 10, 2020, pp. 525–547. https://doi.org/10.1177/0361198120935443.
19. The Simon Law Firm, P.C. State Minimum Distance Requirement for Trucks Legality of Platooning. The Simon Law Firm, P.C., Dec, 2019.
20. Asare, S., J. Chang, and B. L. Staples. *Truck Platooning Early Deployment – Independent Evaluation: Requirements for Performance Measures*. Publication FHWA-JPO-19-773. US Department of Transportation, 2019, p. 39.
21. Bergenhem, C., M. Majdandzic, and S. Ursing. "Concepts and Risk Analysis for a Cooperative and Automated Highway Platooning System." Cham, 2020.
22. Haq, M. T., A. Farid, and K. Ksaibati. "Estimating Passing Sight Distances for Overtaking Truck Platoons–Calibration and Validation Using VISSIM." *International Journal of Transportation Science and Technology*, 2021.
23. Caltrans. "Longer Combination Vehicles." https://dot.ca.gov/programs/traffic-operations/legal-truck-access/exemption-lcv. Accessed Sept. 12, 2023.
24. Mitchell, D. "Heavy Vehicle Productivity Trends and Road Freight Regulation in Australia." 2010.
25. Barton, R. A., and J. Morrall. "Study of Long Combination Vehicles on Two-Lane Highways." *Transportation Research Record*, Vol. 1613, No. 1, 1998, pp. 43–49. https://doi.org/10.3141/1613-06.
26. Hanley, P. F., and D. J. Forkenbrock. "Safety of Passing Longer Combination Vehicles on Two-Lane Highways." *Transportation Research Part A: Policy and Practice*, Vol. 39, No. 1, 2005, pp. 1–15. https://doi.org/10.1016/j.tra.2004.09.001.
27. USGAO. *Truck Safety - The Safety of Longer Combination Vehicles Is Unknown*. US General Accounting Office, 1992.
28. USGAO. *Longer Combination Trucks - Potential Infrastructure Impacts, Productivity Benefits, and Safety Concerns*. US General Accounting Office, 1994.
29. Van Valkenburg, G. W., and H. L. Michael. "Criteria for No-Passing Zones." *Highway Research Record*, No. 366, 1971.
30. Gericke, O. F., and C. M. Walton. "Effect of Increased Truck Size and Weight on Rural Highway Geometric Design (and Redesign) Principles and Practices." *Transportation Research Record*, Vol. 806, 1981.
31. Wilson, T., and W. Best. "Driving Strategies in Overtaking." *Accident Analysis & Prevention*, Vol. 14, No. 3, 1982, pp. 179–185. https://doi.org/10.1016/0001-4575(82)90026-4.
32. Fancher, P. S. "Sight Distance Problems Related to LargeTrucks." *Transportation Research Record*, Vol. 1052, 1986.
33. Glennon, J. C. "New and Improved Model of Passing Sight Distance on Two-Lane Highways." *Transportation Research Record*, Vol. 1195, 1988, pp. 132–137.
34. Rilett, L. R., B. G. Hutchinson, and M. Whitney. "Mechanics of the Passing Maneuver and the Impact of Large Trucks." *Transportation Research Part A: General*, Vol. 24, No. 2, 1990, pp. 121–128. https://doi.org/10.1016/0191-2607(90)90019-3.
35. Hassan, Y., S. M. Easa, and A. O. A. El Halim. "Passing Sight Distance on Two-Lane Highways: Review and Revision." *Transportation Research Part A: Policy and Practice*, Vol. 30, No. 6, 1996, pp. 453–467. https://doi.org/10.1016/0965-8564(95)00032-1.

36. Harwood, D. W., D. K. Gilmore, K. R. Richard, J. M. Dunn, and C. Sun. *Passing Sight Distance Criteria*. Publication NCHRP Report 605. Transportation Research Board, Washington, D.C., 2008, p. 23278.
37. Wang, Y., and M. P. Cartmell. "New Model for Passing Sight Distance on Two-Lane Highways." *Journal of Transportation Engineering*, Vol. 124, No. 6, 1998, pp. 536–545. https://doi.org/10.1061/(ASCE)0733-947X(1998)124:6(536).
38. AASHTO. *A Policy on Geometric Design of Highways and Streets*. American Association of State Highway and Transportation Officials, 2018.
39. Tang, T. Q., H. J. Huang, S. C. Wong, and X. Y. Xu. "A New Overtaking Model and Numerical Tests." *Physica A: Statistical Mechanics and its Applications*, Vol. 376, 2007, pp. 649–657. https://doi.org/10.1016/j.physa.2006.10.044.
40. Sledge, N. H., and K. M. Marshek. "Comparison of Ideal Vehicle Lane-Change Trajectories." *SAE Transactions*, Vol. 106, 1997, pp. 2004–2027.
41. Zheng, H., J. Zhou, Q. Shao, and Y. Wang. "Investigation of a Longitudinal and Lateral Lane-Changing Motion Planning Model for Intelligent Vehicles in Dynamical Driving Environments." *IEEE Access*, Vol. 7, 2019, pp. 44783–44802. https://doi.org/10.1109/ACCESS.2019.2909273.
42. Do, Q. H., H. Tehrani, S. Mita, M. Egawa, K. Muto, and K. Yoneda. "Human Drivers Based Active-Passive Model for Automated Lane Change." *IEEE Intelligent Transportation Systems Magazine*, Vol. 9, No. 1, 2017, pp. 42–56. https://doi.org/10.1109/MITS.2016.2613913.
43. Papadimitriou, I., and M. Tomizuka. "Fast Lane Changing Computations Using Polynomials." In *Proceedings of the 2003 American Control Conference, 2003.*, No. 1, 2003, pp. 48–53 vol.1.
44. Yao, W., H. Zhao, F. Davoine, and H. Zha. "Learning Lane Change Trajectories from On-Road Driving Data." Presented at the 2012 IEEE Intelligent Vehicles Symposium, 2012.
45. Yao, W., H. Zhao, P. Bonnifait, and H. Zha. "Lane Change Trajectory Prediction by Using Recorded Human Driving Data." Presented at the 2013 IEEE Intelligent Vehicles Symposium (IV), 2013.
46. Jenkins, J. M., and L. R. Rilett. "Application of Distributed Traffic Simulation for Passing Behavior Study." *Transportation Research Record*, Vol. 1899, No. 1, 2004, pp. 11–18. https://doi.org/10.3141/1899-02.
47. Jenkins, J. M., and L. R. Rilett. "Classifying Passing Maneuvers: A Behavioral Approach." *Transportation Research Record*, Vol. 1937, No. 1, 2005, pp. 14–21. https://doi.org/10.1177/0361198105193700103.
48. Farah, H., and T. Toledo. "Passing Behavior on Two-Lane Highways." *Transportation Research Part F: Traffic Psychology and Behaviour*, Vol. 13, No. 6, 2010, pp. 355–364. https://doi.org/10.1016/j.trf.2010.07.003.
49. Vlahogianni, E. I. "Modeling Duration of Overtaking in Two Lane Highways." *Transportation Research Part F: Traffic Psychology and Behaviour*, Vol. 20, 2013, pp. 135–146. https://doi.org/10.1016/j.trf.2013.07.003.
50. Figueira, A. C., and A. P. C. Larocca. "Analysis of the Factors Influencing Overtaking in Two-Lane Highways: A Driving Simulator Study." *Transportation Research Part F: Traffic Psychology and Behaviour*, Vol. 69, 2020, pp. 38–48. https://doi.org/10.1016/j.trf.2020.01.006.
51. Branzi, V., M. Meocci, L. Domenichini, and M. Calcinai. "A Combined Simulation Approach to Evaluate Overtaking Behaviour on Two-Lane Two-Way Rural Roads." *Journal of Advanced Transportation*, Vol. 2021, 2021, p. e9973138. https://doi.org/10.1155/2021/9973138.
52. Zhang, J., D. Geng, F. Guo, Z. Yang, and J. Shi. "Research On Influencing Factors of Overtaking Behavior Based On Six-Degrees-Of-Freedom Driving Simulator." Presented at the 2021 4th International Symposium on Traffic Transportation and Civil Architecture (ISTTCA), 2021.
53. Hill, J. D., and L. N. Boyle. "Driver Stress as Influenced by Driving Maneuvers and Roadway Conditions." *Transportation Research Part F: Traffic Psychology and Behaviour*, Vol. 10, No. 3, 2007, pp. 177–186. https://doi.org/10.1016/j.trf.2006.09.002.

54. Gordon, D. A., and T. M. Mast. "Drivers' Judgments in Overtaking and Passing." *Human Factors*, Vol. 12, No. 3, 1970, pp. 341–346. https://doi.org/10.1177/001872087001200310.
55. Mahajan, V., C. Katrakazas, and C. Antoniou. "Crash Risk Estimation Due to Lane Changing: A Data-Driven Approach Using Naturalistic Data." *IEEE Transactions on Intelligent Transportation Systems*, Vol. 23, No. 4, 2022, pp. 3756–3765. https://doi.org/10.1109/TITS.2020.3042097.
56. Zhang, R., Q. Bao, K. Brijs, E. Hermans, and Y. Shen. "Identification and Comparative Safety Analysis of Overtaking Patterns on Two-Lane Highways: A Simulator Study with Novice Drivers." *Transportation Research Record*, 2022, p. 03611981221100240. https://doi.org/10.1177/03611981221100240.
57. Sen, B., J. D. Smith, W. G. Najm, and John A. Volpe. National Transportation Systems Center (U.S.). *Analysis of Lane Change Crashes*. Publication HS-809 571. National Highway Traffic Safety Administration, 2003.
58. Nodine, E., A. Lam, M. Yanagisawa, W. Najm, and John A. Volpe. National Transportation Systems Center (U.S.). *Naturalistic Study of Truck Following Behavior*. Publication DOT-VNTSC-FHWA-16-06. United States Department of Transportation, 2016.
59. Lu, X.-Y., and S. E. Shladover. "Automated Truck Platoon Control and Field Test." In *Road Vehicle Automation* (G. Meyer and S. Beiker, eds.), Springer International Publishing, Cham, pp. 247–261.
60. Duret, A., M. Wang, and A. Ladino. "A Hierarchical Approach for Splitting Truck Platoons near Network Discontinuities." *Transportation Research Part B: Methodological*, Vol. 132, 2020, pp. 285–302. https://doi.org/10.1016/j.trb.2019.04.006.
61. Hegeman, G., K. Brookhuis, and S. Hoogendoorn. "Opportunities of Advanced Driver Assistance Systems towards Overtaking." *European Journal of Transport and Infrastructure Research*, Vol. 5, No. 4, 2005. https://doi.org/10.18757/ejtir.2005.5.4.4408.
62. Hegeman, G. Assisted Overtaking: An Assessment of Overtaking on Two-Lane Rural Roads. 2008.
63. Toledo-Moreo, R. A. "Cooperative Overtaking Assistance System." 2009.
64. Hohm, A., and H. Winner. "Assessment of Adequate Overtaking Margin (AOM) for an Overtaking Assistance System." Presented at the 2010 IEEE Intelligent Vehicles Symposium, 2010.
65. Olaverri-Monreal, C., P. Gomes, R. Fernandes, F. Vieira, and M. Ferreira. "The See-Through System: A VANET-Enabled Assistant for Overtaking Maneuvers." Presented at the 2010 IEEE Intelligent Vehicles Symposium, 2010.
66. Belyaev, E., A. Vinel, K. Egiazarian, and Y. Koucheryavy. "Power Control in See-Through Overtaking Assistance System." *IEEE Communications Letters*, Vol. 17, No. 3, 2013, pp. 612–615. https://doi.org/10.1109/LCOMM.2013.012213.122362.
67. Chiang, H.-H., Y.-L. Chen, B.-F. Wu, and T.-T. Lee. "Embedded Driver-Assistance System Using Multiple Sensors for Safe Overtaking Maneuver." *IEEE Systems Journal*, Vol. 8, No. 3, 2014, pp. 681–698. https://doi.org/10.1109/JSYST.2012.2212636.
68. Fu, R., W. Liu, H. Zhang, X. Liu, and W. Yuan. "Adopting an HMI for Overtaking Assistance - Impact of Distance Display, Advice, and Guidance Information on Driver Gaze and Performance." *Accident Analysis & Prevention*, Vol. 191, 2023, p. 107204. https://doi.org/10.1016/j.aap.2023.107204.
69. Shladover, S. E. "Introduction to Truck Platooning." Oct. 2017.
70. Janssen, R., H. Zwijnenberg, I. Blankers, and J. de Kruijff. *Truck Platooning: Driving the Future of Transportation*. TNO: Netherlands Organization for Applied Scientific Research, 2015.
71. Caltagirone, L., S. Torabi, and M. Wahde. "Truck Platooning Based on Lead Vehicle Speed Profile Optimization and Artificial Physics." 2015.
72. Chen, D., S. Ahn, M. Chitturi, and D. Noyce. "Truck Platooning on Uphill Grades under Cooperative Adaptive Cruise Control (CACC)." *Transportation Research Part C: Emerging Technologies*, Vol. 94, 2018, pp. 50–66. https://doi.org/10.1016/j.trc.2017.08.025.
73. Nowakowski, C., S. E. Shladover, X.-Y. Lu, D. Thompson, and A. Kailas. *Cooperative Adaptive Cruise Control (CACC) For Truck Platooning: Operational Concept Alternatives*. UC Berkeley: California Partners for Advanced Transportation Technology, 2015.

74. (Fred) Song, Y. "Integrated Overtaking Model and Safety Analysis for Truck Platooning Requirements on Two-Lane Undivided Highways." *Transportation Research Record: Journal of the Transportation Research Board*, Vol. 2678, No. 8, 2024, pp. 745–760. https://doi.org/10.1177/03611981231220635.
75. Smith, P., J. Ward, J. Pierce, D. Bevly, and R. Daily. "Experimental Results and Analysis of a Longitudinal Controlled Cooperative Adaptive Cruise Control (CACC) Truck Platoon." 2019.
76. Xiaoxiang, M., T. Zhimin, and C. Feng. "A Reliability-Based Approach to Evaluate the Lateral Safety of Truck Platoon under Extreme Weather Conditions." *Accident Analysis & Prevention*, Vol. 174, 2022, p. 106775.
77. Yang, D., A. Kuijpers, G. Dane, and T. van der Sande. "Impacts of large-scale truck platooning on Dutch highways." *Transportation Research Procedia*, Vol. 37, 2019, pp. 425–432.
78. Taylor, A. H., M. J. Droege, G. M. Shaver, J. A. Sandoval, S. Erlien, and J. Kuszmaul. "Capturing the Impact of Speed, Grade, and Traffic on Class 8 Truck Platooning." *IEEE Transactions on Vehicular Technology*, Vol. 69, 2020, pp. 10506–10518.
79. Wu, W., and X. Ma. "Evaluation of the Risk of Truck Platoon under Crosswind Regarding the Lateral Displacement on Horizontal Curves." *Journal of Advanced Transportation*, Vol. 2023, 2023, p. e4771818.
80. Axelsson, J. "Safety in Vehicle Platooning: A Systematic Literature Review." *IEEE Transactions on Intelligent Transportation Systems*, Vol. 18, 2017, pp. 1033–1045.
81. van Nunen, E., F. Esposto, A. K. Saberi, and J.-P. Paardekooper. "Evaluation of Safety Indicators for Truck Platooning." 2017.
82. Sarkar, A., J. Engstrom, and R. Hanowski. *Analysis of Car Cut-Ins Between Trucks Based on Existing Naturalistic Driving Data*. Publication 22-UI-102. Virginia Tech Transportation Institute, 2022.
83. FHWA. Variable Speed Limits. Federal Highway Administration, 2024.
84. Katz, B., J. Ma, H. Rigdon, K. Sykes, Z. Huang, K. Raboy, and J. Chu. *Synthesis of Variable Speed Limit Signs*. Publication FHWA-HOP-17-003. United States. Federal Highway Administration, 2017.
85. Jeong, H., S. Park, S. Park, H. Cho, and I. Yun. "Study on the Selection of Sections Applicable to Truck Platooning in the Expressway Network." *Sustainability*, Vol. 12, No. 19, 2020, p. 8058.
86. Log, M. M., M. H. R. Eitrheim, K. Pitera, T. Tørset, and T. Levin. "Operational and Infrastructure Readiness for Semi-Automated Truck Platoons on Rural Roads: Article." *Proceedings from the Annual Transport Conference at Aalborg University*, Vol. 30, 2023, pp. 96–114.
87. Al-Kaisy, A. "Two-Lane Highways: Indispensable Rural Mobility." *Encyclopedia*, Vol. 2, No. 1, 2022, pp. 625–631.
88. FHWA. *The Magnitude and Severity of Passing Accidents on Two-Lane Rural Roads*. Publication HSIS Summary Report FHWA-RD-94-068. Federal Highway Administration, 1994.
89. Zhang, G., and S. Zhou. *Enhancing Vehicle Sensing for Traffic Safety and Mobility Performance Improvements Using Roadside LiDAR Sensor Data*. Publication INE/CSET 24.06. University of Hawaii, 2024.
90. Ma, Y., C. Ma, C. Lv, S. Zhang, Y. Tian, T. Zhao, C. Du, and J. Wu. "Vehicle Trajectory Prediction in Expressway Merging Areas Based on Self-Supervised Mechanism." *Journal of Transportation Engineering, Part A: Systems*, Vol. 150, 2024, p. 04024013.
91. Zhang, Q., N. Bhattarai, H. Chen, H. Xu, and H. Liu. "Vehicle Trajectory Tracking Using Adaptive Kalman Filter from Roadside Lidar." *Journal of Transportation Engineering, Part A: Systems*, Vol. 149, 2023, p. 04023043.
92. Zhang, K., L. Zhao, C. Dong, L. Wu, and L. Zheng. "AI-TP: Attention-Based Interaction-Aware Trajectory Prediction for Autonomous Driving." *IEEE Transactions on Intelligent Vehicles*, Vol. 8, 2023, pp. 73–83.

93. Ding, Z., and H. Zhao. "Incorporating Driving Knowledge in Deep Learning Based Vehicle Trajectory Prediction: A Survey." *IEEE Transactions on Intelligent Vehicles*, Vol. 8, 2023, pp. 3996–4015.
94. Zhao, C., A. Song, Y. Du, and B. Yang. "TrajGAT: A Map-Embedded Graph Attention Network for Real-Time Vehicle Trajectory Imputation of Roadside Perception." *Transportation Research Part C: Emerging Technologies*, Vol. 142, 2022, p. 103787.
95. Song, X., R. Pi, C. Lv, J. Wu, H. Zhang, H. Zheng, J. Jiang, and H. He. "Augmented Multiple Vehicles' Trajectories Extraction Under Occlusions With Roadside LiDAR Data." *IEEE Sensors Journal*, Vol. 21, 2021, pp. 21921–21930.
96. Deo, N., and M. M. Trivedi. "Multi-Modal Trajectory Prediction of Surrounding Vehicles with Maneuver Based LSTMs." 2018.
97. Garcia, A., and D. Pastor-Serrano. "Determination of Minimum Horizontal Curve Radius for Safe Stopping Sight Distance of Vehicles Overpassing Truck Platoons." *Computer-Aided Civil and Infrastructure Engineering*, Vol. 37, No. 5, 2022, pp. 539–557. https://doi.org/10.1111/mice.12758.
98. Ma, Y., Y. Zheng, J. Cheng, and S. Easa. "Real-Time Visualization Method for Estimating 3D Highway Sight Distance Using LiDAR Data." *Journal of Transportation Engineering, Part A: Systems*, Vol. 145, 2019, p. 04019006.
99. Amiridis, K., B. Psarianos, and N. Stamatiadis. "Generic Methodology for 3-D Available Sight Distance Calculation." 2016.
100. Amiridis, K., and B. Psarianos. "Calculation of the Available 3-D Sight Distance by Modeling the Roadway as a 3-D B-Spline Surface." Vol. 2, 2016.
101. Ismail, K., and T. Sayed. "New Algorithm for Calculating 3D Available Sight Distance." *Journal of Transportation Engineering*, Vol. 133, 2007, pp. 572–581.
102. Lu, X.-Y., and S. E. Shladover. "Review of Variable Speed Limits and Advisories: Theory, Algorithms, and Practice." *Transportation Research Record*, Vol. 2423, No. 1, 2014, pp. 15–23. https://doi.org/10.3141/2423-03.
103. Yu, R., and M. Abdel-Aty. "An Optimal Variable Speed Limits System to Ameliorate Traffic Safety Risk." *Transportation Research Part C: Emerging Technologies*, Vol. 46, 2014, pp. 235–246. https://doi.org/10.1016/j.trc.2014.05.016.
104. Grumert, E., X. Ma, and A. Tapani. "Analysis of a Cooperative Variable Speed Limit System Using Microscopic Traffic Simulation." *Transportation Research Part C: Emerging Technologies*, Vol. 52, 2015, pp. 173–186. https://doi.org/10.1016/j.trc.2014.11.004.
105. Brown, L. D., T. T. Cai, and A. DasGupta. "Interval Estimation for a Binomial Proportion." *Statistical Science*, Vol. 16, 2001, pp. 101–133.
106. Devore, J. L. *Probability and Statistics for Engineering and the Sciences*. Cengage Learning, Boston, MA, USA, 2012.
107. Wallis, S. "Binomial Confidence Intervals and Contingency Tests: Mathematical Fundamentals and the Evaluation of Alternative Methods." *Journal of Quantitative Linguistics*, Vol. 20, 2013, pp. 178–208.
108. Boyd, S., and L. Vandenberghe. *Convex Optimization*. Cambridge University Press, 2004.
109. Nemirovski, A., A. Juditsky, G. Lan, and A. Shapiro. "Robust Stochastic Approximation Approach to Stochastic Programming." *SIAM Journal on Optimization*, Vol. 19, No. 4, 2009, pp. 1574–1609.
110. Bar-Gera, H., and D. Shinar. "The Tendency of Drivers to Pass Other Vehicles." *Transportation Research Part F: Traffic Psychology and Behaviour*, Vol. 8, 2005, pp. 429–439.
111. Kwon, J., P. Varaiya, and A. Skabardonis. "Estimation of Truck Traffic Volume from Single Loop Detectors with Lane-to-Lane Speed Correlation." *Transportation Research Record: Journal of the Transportation Research Board*, Vol. 1856, 2003, pp. 106–117.
112. Llorca, C., A. T. Moreno, and A. Garcia. "Modelling Vehicles Acceleration during Overtaking Manoeuvres." *IET Intelligent Transport Systems*, Vol. 10, No. 3, 2016, pp. 206–215.
113. Song, Y. "Deciding Truck Platooning Operational Rules With Stochastic Approximation for Vehicle Safe Overtaking on Two-Lane Undivided Highways." *IEEE Transactions on Intelligent*

Transportation Systems, Vol. 26, No. 5, 2025, pp. 6201–6215. https://doi.org/10.1109/TITS.2025.3553841.
114. Group, P. *PTV Vissim 2024 User Manual*. PTV Group, Karlsruhe, Germany, 2024.
115. Lin, Z., F. Chen, İ. Öztürk, and N. Merat. "Overtaking Automated Truck Platoons: Effects of Platoon Organisations and Traffic Situation on Driving Behaviours of Nearby Manual Vehicle Drivers." *Transportation Research Part F: Traffic Psychology and Behaviour*, Vol. 109, 2025, pp. 1208–1228. https://doi.org/10.1016/j.trf.2025.01.026.
116. Song, Y. F., Z. T. Soe, and R. Freyre. "Gap Opening Control to Facilitate Human-Driven Vehicle Overtaking of Connected and Automated Vehicle Platoons on Two-Lane Highways." Presented at the 2025 IEEE 3rd International Conference on Mobility, Operations, Services and Technologies (MOST), Newark, DE, USA, 2025.
117. Branzi, V., M. Meocci, L. Domenichini, and M. Calcinai. "A Combined Simulation Approach to Evaluate Overtaking Behaviour on Two-Lane Two-Way Rural Roads." *Journal of Advanced Transportation*, Vol. 2021, 2021, pp. 1–18. https://doi.org/10.1155/2021/9973138.
118. Zhang, R., B. Qiong, K. Brijs, E. Hermans, Q. Qu, and Y. Shen. "Overtaking Maneuvers on Two-Lane Highways under the Microscope: Exploration of a Multidimensional Framework for the Analysis of Safety, Comfort and Efficiency Using Simulator Data." *Accident Analysis & Prevention*, Vol. 202, 2024, p. 107613. https://doi.org/10.1016/j.aap.2024.107613.
119. Sharifiilierdy, S. "Evaluating the Impact of Automated Truck Platooning on Urban Freeway Traffic Flow: A Microsimulation Study on the I-10 Freeway in Los Angeles County." California State Polytechnic University, Pomona, Apr 05, 2024.
120. Ahmed, T., A. Ali, Y. Huang, and P. Lu. "Evaluating the Impact of Human-Driven and Autonomous Vehicles in Adverse Weather Conditions Using a Verkehr in Städten—SIMulationsmodell (VISSIM) and Surrogate Safety Assessment Model (SSAM)." *Electronics*, Vol. 14, No. 10, 2025, p. 2046. https://doi.org/10.3390/electronics14102046.
121. Douglas Gettman and Linda Head. *Surrogate Safety Assessment Model and Validation: Final Report*. Publication FHWA-HRT-08-051. Federal Highway Administration (FHWA), U.S. Department of Transportation, Washington, D.C., 2008.
122. Cohen, J. *Statistical Power Analysis for the Behavioral Sciences*. Psychology Press, New York, NY, 2009.
123. Federal Highway Administration (FHWA). *Surrogate Safety Assessment Model (SSAM): Software User's Manual*. Publication FHWA-HRT-08-049. U.S. Department of Transportation, Federal Highway Administration, Washington, D.C., 2008.
124. Chen, J., W. ShangGuan, B. Cai, M. Bhat, and Y. Du. "Intelligent Platoon Operating Slot Optimization Method Based on Drivers' Overtaking Behavior." Presented at the 2019 IEEE Intelligent Transportation Systems Conference (ITSC), 2019.
125. Chen, J., M. Bhat, S. Jiang, and D. Zhao. "Advanced Driver Assistance Strategies for a Single-Vehicle Overtaking a Platoon on the Two-Lane Two-Way Road." *IEEE Access*, Vol. 8, 2020, pp. 77285–77297. https://doi.org/10.1109/ACCESS.2020.2989082.
126. Chao, S.-F., S. M. Roldan, M. Jannat, M. Arnold, and Inc. Leidos. *Human Factors Issues Related to Truck Platooning Operations*. Publication FHWA-HRT-24-065. 2024.
127. Walch, M., M. Woide, K. Mühl, M. Baumann, and M. Weber. "Cooperative Overtaking: Overcoming Automated Vehicles' Obstructed Sensor Range via Driver Help." 2019.
128. Milanes, V., S. E. Shladover, J. Spring, C. Nowakowski, H. Kawazoe, and M. Nakamura. "Cooperative Adaptive Cruise Control in Real Traffic Situations." *IEEE Transactions on Intelligent Transportation Systems*, Vol. 15, No. 1, 2014, pp. 296–305. https://doi.org/10.1109/TITS.2013.2278494.
129. Milanés, V., and S. E. Shladover. "Handling Cut-In Vehicles in Strings of Cooperative Adaptive Cruise Control Vehicles." *Journal of Intelligent Transportation Systems*, Vol. 20, No. 2, 2016, pp. 178–191. https://doi.org/10.1080/15472450.2015.1016023.

130. Bang, S., and S. Ahn. "Control of Connected and Autonomous Vehicles with Cut-in Movement Using Spring Mass Damper System." *Transportation Research Record*, Vol. 2672, No. 20, 2018, pp. 133–143. https://doi.org/10.1177/0361198118796927.
131. Scholte, W. J., P. W. A. Zegelaar, and H. Nijmeijer. "Gap Opening Controller Design to Accommodate Merges in Cooperative Autonomous Platoons *." *IFAC-PapersOnLine*, Vol. 53, No. 2, 2020, pp. 15294–15299. https://doi.org/10.1016/j.ifacol.2020.12.2327.
132. Scholte, W. J., P. W. A. Zegelaar, and H. Nijmeijer. "A Control Strategy for Merging a Single Vehicle into a Platoon at Highway On-Ramps." *Transportation Research Part C: Emerging Technologies*, Vol. 136, 2022, p. 103511. https://doi.org/10.1016/j.trc.2021.103511.
133. Lu, Y., L. Huang, J. Yao, and R. Su. "Intention Prediction-Based Control for Vehicle Platoon to Handle Driver Cut-In." *IEEE Transactions on Intelligent Transportation Systems*, Vol. 24, No. 5, 2023, pp. 5489–5501. https://doi.org/10.1109/TITS.2023.3239606.
134. Song, L., X. Ma, E. Hashemi, and H. Wang. "A Defensive Motion Framework for Autonomous Platoon to Handle Cut-in Maneuvers." Presented at the 2023 IEEE 26th International Conference on Intelligent Transportation Systems (ITSC), 2023.
135. Kou, Y., and C. Ma. "Dual-Objective Intelligent Vehicle Lane Changing Trajectory Planning Based on Polynomial Optimization." *Physica A: Statistical Mechanics and its Applications*, Vol. 617, 2023, p. 128665. https://doi.org/10.1016/j.physa.2023.128665.
136. Ploeg, J., B. T. M. Scheepers, E. Van Nunen, N. Van De Wouw, and H. Nijmeijer. "Design and Experimental Evaluation of Cooperative Adaptive Cruise Control." Presented at the 2011 14th International IEEE Conference on Intelligent Transportation Systems - (ITSC 2011), 2011.

8. APPENDICES

8.1 ASD/PSD Models and Assumed Parameter Values Used in Simulation

Overtaking safety is primarily determined by the comparison of ASD and PSD. Based on the model framework, ASD is restricted by traffic flow, horizontal and vertical curves, and truck platoon following gap. PSD is affected by truck platoon operating speed and total length, which are further affected by posted speed limit and roadway uphill grade. Additionally, PSD is also related to the operational parameters of surrounding vehicles related to overtaking. This Appendix section provides modeling details of ASD and PSD related parameters used in simulation.

8.1.1 ASD

1) Traffic Flow: An overtaking vehicle needs to take a gap in the opposing traffic to complete the maneuver. Therefore, available gaps in the opposing traffic limits the ASD. In our simulation, we assume that the opposing vehicles arrive following a Poisson process. We pre-set a probability, p, of seeing a gap greater than or equal to the one calculated, then the time gap is:

$$t_{Ogap} = \frac{3600\ln(p)}{q} \quad [8\text{-}1]$$

where t_{Ogap} is the time gap in opposing traffic in seconds; is the assumed probability of seeing a gap larger than or equal to what is calculated; and q is the mean flow rate of opposing traffic in vehicles per hour.

The space gap is then the ASD restricted by traffic flow which is calculated as:

$$ASD_1 = v_O t_{Ogap} \quad [8\text{-}2]$$

where ASD_1 is the ASD restricted by traffic flow in meters; v_O is the average speed of opposing vehicles in m/s. Note that in a real-time traffic management application of the algorithm, feed of updated traffic conditions can be used to estimate the available gaps in traffic stream.

2) Horizontal Curves: When overtaking takes place on a horizontal curve, the truck platoon obstructs the sightline of the overtaking vehicle driver, restricting the ASD. The horizontal curve ASD model we used is based on a model developed by Garcia and Pastor-Serrano, which also considers the increase in ASD due to truck platoon's inter-truck following gap (*97*). **Figure 53** illustrates the restricted ASD on horizontal curves, with the platoon following gap considered. The calculation process is detailed as follows.

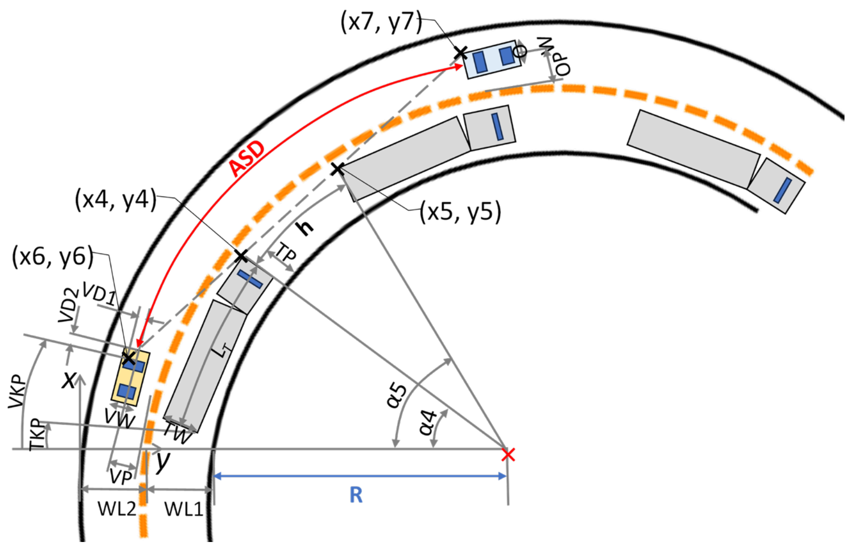

Figure 53 Variables for assessing ASD on horizontal curves, adapted from (97).

The angle between the curve's starting point and the trailing truck's front bumper is calculated as the summation of two angles. One angle is between the curve's starting point and rear bumper of the trailing truck, and the other is between the rear bumper and front bumper of the trailing truck.

$$\alpha_4 = \frac{200\text{TKP}}{\pi(R+\text{WL}_1+\text{WL}_2)} + \frac{200L_T}{\pi(R+\text{TP})} \qquad [8\text{-}3]$$

where α_4 is the angle between curve starting point and trailing truck's front bumper in gradians; TKP is the distance between curve starting point and trailing truck's rear bumper in meters; R is the curve radius in meters; WL_1 and WL_2 are the widths, in meters, of the right and left lane, respectively; L_T is length of the truck in meters; and TP is the distance between right edge of the right lane and center axis of the truck in meters.

The position of trailing truck's front left corner is calculated by solving the following pair of equations.

$$\begin{cases} x_4^2 + [y_4 - (R + \text{WL}_1 + \text{WL}_2)]^2 = \left(R + \text{WL}_1 + \text{TP} + \frac{\text{TW}}{2}\right)^2 \\ y_4 = R + WL_1 + WL_2 - \tan\left[\frac{(100-\alpha_4)\pi}{200}\right] x_4 \end{cases} \qquad [8\text{-}4]$$

where (x_4, y_4) is the position of trailing truck's front left corner; TW is width of the truck in meters.

The angle between curve starting point and rear left corner of the preceding truck is calculated as:

$$\alpha_5 = \frac{200\text{TKP}}{\pi(R+\text{WL}_1+\text{WL}_2)} + \frac{200L_T+h}{\pi(R+\text{TP})} \qquad [8\text{-}5]$$

where α_5 is the angle between curve starting point and rear left corner of the preceding truck; *h* is the following gap between the trailing and preceding trucks in meters.

The position of preceding truck's rear left corner, (x_5,y_5), is calculated by solving the following pair of equations:

$$\begin{cases} x_5^2 + [y_5 - (R + WL_1 + WL_2)]^2 = \left(R + TP + \frac{TW}{2}\right)^2 \\ y_5 = R + WL_1 + WL_2 - \tan\left[\frac{(100-\alpha_5)\pi}{200}\right] x_5 \end{cases} \quad [8\text{-}6]$$

Truck platoon's inter-truck following gap contributes to the ASD when the overtaking vehicle driver's sight line aligns with the straight line going through (x_4,y_4) and (x_5,y_5). The driver's position (x_6,y_6) can be calculated by solving the following pair of equations.

$$\begin{cases} \frac{x_6 - x_4}{x_5 - x_4} = \frac{y_6 - y_4}{y_5 - y_4} \\ x_6^2 + [y_6 - (R + \mathrm{WL}_1 + \mathrm{WL}_2)]^2 = (R + \mathrm{WL}_1 + \mathrm{VP} + \mathrm{VD}_1)^2 \end{cases} \quad [8\text{-}7]$$

where (x_6,y_6) is the overtaking vehicle driver's position; VP is the distance between the center lane line and center axis of the overtaking vehicle; and VD_1 is the distance between driver's position and center axis of the vehicle.

The farthest point where the overtaking driver can see an opposing vehicle is on the straight line passing through (x_4,y_4), (x_5,y_5), and (x_6,y_6). This point is the front right corner of the opposing vehicle and is calculated by solving the following pair of equations.

$$\begin{cases} \frac{x_7 - x_4}{x_5 - x_4} = \frac{y_7 - y_4}{y_5 - y_4} \\ x_7^2 + [y_7 - (R + \mathrm{WL}_1 + \mathrm{WL}_2)]^2 = \left(R + \mathrm{WL}_1 + \mathrm{VP} + \frac{\mathrm{OW}}{2}\right)^2 \end{cases} \quad [8\text{-}8]$$

where (x_7,y_7) is the position of opposing vehicle's front right corner; OW is the width of opposing vehicle.

ASD is the arc length between the overtaking vehicle's front bumper and the opposing vehicle's front bumper, which is calculated as:

$$ASD_2 = \frac{\pi(R + WL_1 + VP)(\beta - \alpha)}{200} - VD_2 \quad [8\text{-}9]$$

$$\alpha = \tan^{-1}\left(\frac{x_6}{R + WL_1 + WL_2 - y_6}\right)\frac{200}{\pi} \quad [8\text{-}10]$$

$$\beta = \tan^{-1}\left(\frac{x_7}{R + WL_1 + WL_2 - y_7}\right)\frac{200}{\pi} \quad [8\text{-}11]$$

where ASD_2 is the horizontal curve restricted ASD; α is the angle between curve starting point and the overtaking vehicle driver's position; β is the angle between curve starting point and the opposing vehicle's front bumper; VD_2 is the distance between overtaking vehicle's front bumper and driver's position.

3) Crest Vertical Curves: Crest vertical curves on a two-lane highway also restrict driver's sight distance in overtaking, as shown in **Figure 54**. The AASHTO Green Book provides models relating the sight distance, crest vertical curve length, and grade difference.

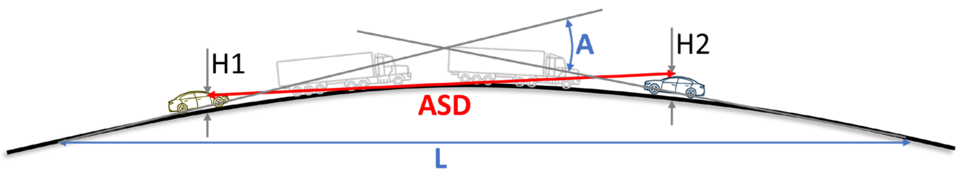

Figure 54 Variables for assessing ASD on crest vertical curves.

Based on the AASHTO model, we use the following equations to calculate the vertical curve restricted ASD (*38*).

$$ASD_3 = \begin{cases} ASD_{3a}, if\ ASD_{3a} > L \\ ASD_{3b}, if\ ASD_{3b} < L \end{cases} \quad [8\text{-}12]$$

$$ASD_{3a} = \frac{L}{2} + \frac{100\left(\sqrt{H_1}+\sqrt{H_2}\right)^2}{A} \quad [8\text{-}13]$$

$$ASD_{3b} = \sqrt{\frac{200\left(\sqrt{H_1}+\sqrt{H_2}\right)^2 L}{A}} \quad [8\text{-}14]$$

where ASD_3 is the crest vertical curve restricted ASD; *L* is the vertical curve length in meters; *A* is the grade difference in percentage; H_1 and H_2 are the heights of overtaking vehicle driver's eyes and the opposing vehicle in meters, respectively, and are both given a value of 1.07. ASD_{3a} is the restricted sight distance if it is larger than the curve length; and ASD_{3b} is the restricted sight distance if it is smaller than the curve length.

After calculating the three types of restricted sight distances, ASD_1, ASD_2, ASD_3, we can then determine the ASD to be the minimum of the three considering traffic and roadway geometric conditions.

$$ASD = \min\left(ASD_1, ASD_2, ASD_3\right) \quad [8\text{-}15]$$

8.1.2 PSD

1) The Overtaking Process: We model the overtaking process into three stages and consider dynamics involved in vehicle lane changing (*74*). The three stages are the lane change stage, overtake stage, and back-to-lane stage, as illustrated in **Figure 55**. Variables related to the process are also shown in the figure.

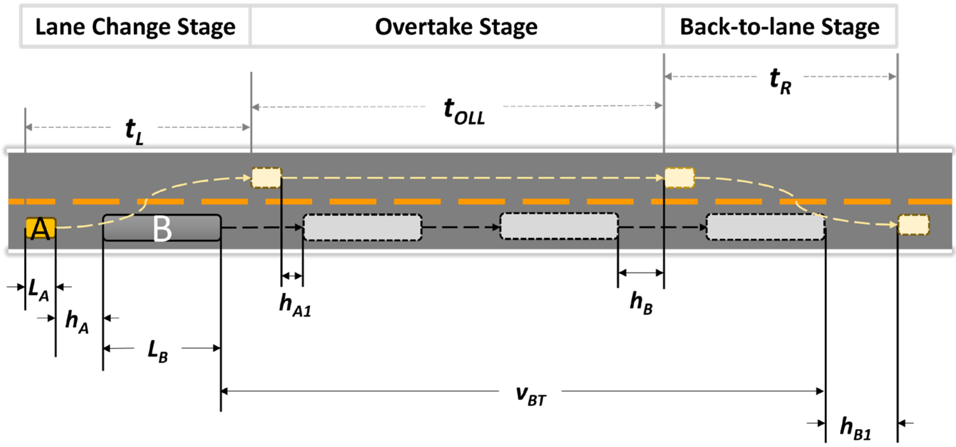

Figure 55 Three stages of overtaking and related variables.

The PSD for overtaking on two-lane highways consists of three parts, the distance needed to be traveled by the overtaking vehicle A to finish the overtake, S_A, the distance traveled by a potential opposing vehicle during the same period, S_O, plus a safety buffer distance, h_O:

$$PSD = S_A + S_0 + h_0 \quad [8\text{-}16]$$

To calculate PSD, we first calculate the time needed to finish the overtake. With overtaking time, it is then easy to calculate the distances. We use a "uniform acceleration until a final speed" (UAFS) model to describe the overtaking vehicle's acceleration [65]. Time to complete the lane change stage is then calculated as:

$$t_L = \frac{-v_{A0} + \sqrt{v_{A0}^2 - 2a_x x_{eL}}}{a_x} \quad [8\text{-}17]$$

where t_L is the time to complete lane change in seconds; v_{A0} is the initial speed of overtaking vehicle in m/s; a_x is the longitudinal acceleration of overtaking vehicle in m/s^2; and x_{eL} is the longitudinal displacement of overtaking vehicle in lane change stage in meters.

Time to complete the overtake stage consists of two parts. The first part allows the overtaking vehicle to continue accelerating after completing the lane change to its desired maximum speed for overtake. The second part is to finish the overtake stage by reaching a desired gap between the front of truck platoon B and the rear bumper of overtaking vehicle A.

$$t_{OLL} = t_1 + t_2 \quad [8\text{-}18]$$

where t_{OLL} is the time to complete overtake stage in seconds; t_1 is the time to complete the first part of overtake stage; and t_2 is the time to complete the second part.

$$t_1 = \frac{v_{Amax} - v_{A1}}{a_x} \quad [8\text{-}19]$$

$$v_{A1} = v_{A0} + a_x t_L \quad [8\text{-}20]$$

where v_{Amax} is the desired final overtaking speed in m/s; v_{A1} is the longitudinal speed of overtaking vehicle at the end of lane change stage in m/s.

$$t_2 = \frac{(v_B - v_{A1} - 0.5a_x)t_1 + h_{A1} + h_B + L_A + L_B}{v_{A2} - v_B} \quad [8\text{-}21]$$

$$v_{A2} = v_{Amax} \quad [8\text{-}22]$$

$$h_{A1} = v_B t_L + h_A - x_{eL} \quad [8\text{-}23]$$

where v_B is the speed of truck platoon in m/s; v_{A2} is the speed of overtaking vehicle at the end of overtake stage in m/s, and is assumed to be equal to v_{Amax}; h_{A1} is the gap between the front bumper of overtaking vehicle and rear bumper of truck platoon at the end of lane change stage in meters; h_B is the desired gap between the rear bumper of overtaking vehicle and front bumper of truck platoon at the end of overtake stage in meters; L_A is the length of overtaking vehicle in meters; and L_B is the length of truck platoon in meters.

Time to complete the return-to-lane stage is calculated as:

$$t_R = \frac{x_{eR}}{v_{A2}} \quad [8\text{-}24]$$

where t_R is the time to complete return-to-lane stage in seconds; x_{eR} is the longitudinal displacement in return-to-lane stage in meters.

The total time needed for the overtaking process is:

$$T = t_L + t_{OLL} + t_R = t_L + (t_1 + t_2) + t_R \quad [8\text{-}25]$$

PSD is calculated as:

$$PSD = S_A + S_O + h_O = (h_A + h_B + L_A + L_B + v_{A2}t_R - v_B t_R + v_B T) + v_O T + h_O \quad [8\text{-}26]$$

where h_{B1} is the gap between the front bumper of truck platoon and the rear bumper of overtaking vehicle in meters; v_O is the speed of opposing vehicle in m/s; and the safety buffer h_O is the distance between the front bumpers of overtaking vehicle and opposing vehicle in meters, which can be pre-set to a reasonable positive value (e.g., $h_O = 2.5(v_{Amax} + v_O)$, accounting for a 2.5-s buffer time).

2) Truck Platoon Parameters: Determination of PSD involves truck platooning parameters operating speed, v_B, and platoon length, L_B. Operating speed is restricted by the posted speed limit, v_{lim}, and trucks usually adhere to the limit by driving at a speed close to or under it. A minimum truck operating speed should be set to avoid severe obstruction of traffic. Platoon length is determined by the number of trucks and the inter-truck following gap:

$$L_B = nL_T + (n-1)h \quad [8\text{-}27]$$

where *n* is the number of trucks in platoon; L_T is truck length in meters; and *h* is the following gap in meters.

There is no consensus on how many trucks can fit into a platoon or what the optimal number is for different scenarios. Existing research on platoon interactions with traffic and roadway infrastructure usually arbitrarily sets a number (e.g., 2, 3, 4, or 5) or runs simulation with a series of numbers (e.g., from 2 to 100 in ascending or descending order). There is consensus, however, that there should be at least two trucks to form a viable "platoon." Therefore, our model limits the minimum platoon size to two trucks.

The inter-truck following gap is determined by the capability of the cooperative adaptive cruise control (CACC) technology used by trucks to form platoons. Current technology allows a following time gap as small as 0.3 s. With an operating speed, for instance, of 29 m/s (65 mph), the gap would be 8.7 m (28.5 ft). Ideally, truck platoons would operate with a minimal following gap as much as possible to achieve a better aerodynamic, which saves fuel consumption and reduces emissions. However, roadway geometry restricts the inter-truck following gap from going toward such a small number. Our model considers uphill grade to be the major roadway geometric restriction on following gap. The relationship between uphill grade and inter-truck following gap is modeled in (*72*).

Considering the impact of uphill grade on truck acceleration, the CACC operational policy requires time headway between consecutive trucks in a platoon to follow this inequality:

$$t_h \geq \frac{f_{\xi_0}(L_T)}{\min\left[\frac{u}{1-\alpha}\left(1-\frac{gG}{100a_m}\right),u\right]+\xi_1} \qquad [8\text{-}28]$$

where t_h is the headway between consecutive trucks (i.e., the time difference between the front bumpers of two consecutive trucks passing the same reference location) in seconds; $f_{\xi_0}(L_T)$ is jam spacing in meters, which is a function of truck length, L_T; ξ_1 is the minimum acceptable time gap in seconds; u is free flow speed in m/s; g is the gravity constant (i.e., 9.8 m/s^2); a_m is truck's maximum acceleration rate in m/s^2; α is acceleration capability in fraction of a_m at u, (i.e., $1 \leq \alpha \leq 1$), and a larger α means a more aggressive acceleration; G is uphill grade in percentage.

The spacing between two consecutive trucks in the platoon is the larger of the following two possible values related to platoon operating speed:

$$s = \max\left(v_B t_h, \xi_1 v_B + f_{\xi_0}(L_T)\right) \qquad [8\text{-}29]$$

where s is the inter-truck spacing in meters; v_B is the platoon operating speed.

The inter-truck following gap can then be calculated by subtracting truck length from the spacing: $h = s - L_T$.

8.1.3 Assumed Values Used in Simulation

Assumed values of other parameters used in the simulation are listed in **Table 21**, supplementing the overtaking parameters listed in **Table 5** and **Table 6** in the main text.

Table 21 Other Parameters and Assumed Values

Parameter	Value
Input	
Posted speed limit: v_{lim}	29 m/s
Parameters for ASD Calculation Lane width: WL_1 and WL_2	3.5 m
Truck width: TW	2.6 m
Distance between truck's center axis and inner edge of lane: TP	1.75 m
Overtaking and opposing vehicle width: VW and OW	2.1 m
Distance between overtaking vehicle's center axis and center lane line: VP	1.75 m
Distance between overtaking vehicle's center axis and driver's position: VD_1	0.45 m
Distance between overtaking vehicle's front bumper and driver's position: VD_2	2.2 m
Distance between opposing vehicle's center axis and center lane line: OP	1.75 m
Platoon Parameters Truck length: L_T	22.4 m
Truck's acceleration capability: α	0.2
Truck's maximum acceleration: a_m	3 m/s^2
Jam spacing: $f_{\xi 0}(L_T) = L_T + 5$	27.4 m
Minimum acceptable time gap: ξ_1	0.3 s

CTIPS Center for Transformative Infrastructure Preservation and Sustainability

USDOT Region 8 University Transportation Center

NDSU Dept 2880 • P.O. Box 6050
Fargo, ND 58108-6050

(701)231-7767

ndsu.ugpti@ndsu.edu